

FLOW INDUCED FAILURES OF COPPER DRINKING WATER TUBE

Jeffrey Michael Coyne

Thesis submitted to the Faculty
of the Virginia Polytechnic Institute and State University
in Partial Fulfillment of the requirements for the degree of

Masters of Science
in
Environmental Engineering

Marc Edwards, Chair
Andrea Dietrich
Paolo Scardina

May 5, 2009
Blacksburg, VA

Keywords: Erosion Corrosion, Flow Induced Failure, Copper, Concentration Cell
Corrosion, Cavitation, High Velocity Impingement, Particle Impingement

Flow Induced Failures of Copper Drinking Water Tube
Jeff Coyne

ABSTRACT

Excessive water flow velocities can contribute to rapid failures of copper premise plumbing systems. This is the first fundamental study to scientifically isolate mechanistic impacts from distinct flow induced failure mechanisms that include concentration cell corrosion, cavitation, particle/bubble impingement and high velocity impingement. Concentration cell effects resulting from exposing different copper surfaces to different flow regimes created a strong electrochemical cell that caused rapid corrosion that persisted for periods lasting from hours to days in certain waters. Free chlorine appeared to inhibit this effect in a range of waters. Under typical water chemistries the resulting non-uniform attack diminished, presumably due to formation of a protective scale or rust layer. Consequently, concentration cell corrosion would not be a major contributor to damage from high flow rates in the range of fresh waters investigated.

In experiments using an ultrasonic processor, implosion of vaporous cavitation bubbles against a copper surface caused dramatic pitting, considerable copper weight loss, and, in some cases, the development of pinhole leaks. Changes in water chemistry and the existence of a pre-existing protective scale layer had nearly no mitigating effects on copper cavitation damage. An exponential relationship was found between the initial copper pipe wall thickness and the time necessary to cause a leak via vaporous cavitation. On the basis of this relationship, a Type M tube would be expected to last 23 and 3000 times less than a Type K and L tube, respectively, when facing continual cavitation attack. However, it was not possible to re-create cavitation damage in any practical circumstance that was tested in copper pipes, even though it is strongly believed that cavitation can play a practical role in service failures.

On the basis of the above results, it was hypothesized that brief intervals of cavitation could remove protective scale from portions of the copper pipe surface exposed to high turbulence. In this case, even if minimal damage from cavitation occurred directly, it could allow concentration cell corrosion to become a significant contributor to non-uniform corrosion damage. On the basis of preliminary testing, it appears that this idea has considerable merit. A combination of brief cavitation and waters that create strong concentration cell effects is expected to cause serious damage to copper pipe. These potential synergies are deserving of additional research.

In experiments testing the effect of high velocity jets (17.5 ft/sec) impinging against submerged copper plates perpendicularly and longitudinally, plates in heated sea water were aggressively gouged and penetrated. It is believed that the copper plate damage resulted from a combination of mechanisms including concentration cell corrosion, cavitation implosion, and high velocity impingement.

Impingement of sand on the surface of copper tube created very little damage. This was surprising given prior reports in the literature.

ACKNOWLEDGEMENTS

First and foremost, thanks to my advisor, Dr. Marc Edwards. No matter how busy, he always found time to meet and discuss research. His encouragement, devotion, and endless ability to impart his expertise helped me in understanding the complex material presented in this work.

Thanks also to Dr. Paolo Scardina, whose practical and theoretical expertise greatly improved the quality of work presented herein, and Dr. Andrea Dietrich for support and direction in finishing this thesis.

Thanks also to my family and friends, who always supported me while completing this thesis. And thanks to everyone in the Edwards research group at Virginia Tech who helped create a productive working environment. I've enjoyed every minute of my time working in the group.

Thank you also to the Copper Development Association for their generous funding.

This thesis is dedicated to Dr. G.V. Loganathan, who was a victim in the events on April 16th, 2007 at Virginia Tech. He remains the best teacher I have ever had.

TABLE OF CONTENTS

ABSTRACT.....	ii
ACKNOWLEDGEMENTS.....	iv
TABLE OF CONTENTS.....	v
LIST OF TABLES.....	viii
LIST OF FIGURES.....	ix
AUTHOR'S PREFACE.....	xvi
CHAPTER 1: REVIEW OF CONVENTIONAL EROSION CORROSION AND FLOW INDUCED FAILURE MECHANISMS.....1	
INTRODUCTION.....	1
REVIEW OF CLASSICAL THEORY AND A NEW PROPOSED APPROACH.....1	
Review of Existing Theories.....	1
New Understanding and Approach.....	2
Concentration Cell Corrosion.....	3
Cavitation Bubble Implosion and damage.....	3
Particle Impingement.....	4
High Velocity Water Impingement.....	4
Flow Electrification.....	5
SUMMARY AND RESTATEMENT OF GOALS.....	7
REFERENCES.....	7
CHAPTER 2: BENCH SCALE STUDIES ON CONCENTRATION CELL CORROSION OF COPPER UNDER DIFFERENTIAL FLOW.....11	
INTRODUCTION.....	11

Concentration Cells Formed by Differential Flow.....	11
Differential Flow in Service.....	13
Effect of Design, Installation, and Water Chemistry.....	16
METHODS AND MATERIALS.....	18
Short-term Concentration Cell Tests.....	18
Long Term Concentration Cell Tests.....	21
RESULTS.....	24
Short-term Concentration Cell Tests.....	24
Copper Exposed to High Flow Conditions.....	24
Copper Exposed to Stagnant Water Conditions.....	28
Long Term Concentration Cell Tests.....	28
DISCUSSION.....	35
CONCLUSIONS.....	37
REFERENCES.....	38
CHAPTER 3: BENCH SCALE STUDIES ON CAVITATION IMPLOSION AND PARTICLE IMPINGEMENT AGAINST COPPER SURFACES.....	39
INTRODUCTION.....	39
METHODS AND MATERIALS.....	41
Ultrasonically Induced Cavitation.....	41
Valve Induced Cavitation.....	42
Particle Impingement.....	44
RESULTS.....	46
Ultrasonically Induced Cavitation.....	46

Valve Induced Cavitation.....	57
Particle Impingement.....	61
DISCUSSION.....	63
CONCLUSIONS.....	64
REFERENCES.....	65
 CHAPTER 4: BENCH SCALE STUDIES ON COMBINED FLOW INDUCED FAILURE	
MECHANISMS.....	66
INTRODUCTION.....	66
METHODS AND MATERIALS.....	66
High Velocity Jet Tests.....	66
Cycled Cavitation.....	69
RESULTS.....	72
High Velocity Jet Tests.....	72
Cycled Cavitation.....	82
DISCUSSION.....	85
High Velocity Jet Tests.....	85
Cycled Cavitation.....	87
CONCLUSIONS.....	92
REFERENCES.....	93
CHAPTER 5: SUMMARY OF KEY CONCLUSIONS.....	94
APPENDIX A.....	96
APPENDIX B.....	105

LIST OF TABLES

Table 2-1: Simplified Example of Expected Failure Time among Concentration Cell Reactions Controlled Anodically and Cathodically for New 3/4" Type M Copper Tube.....	17
Table 2-2: Anodic Corrosion Peak Current Density Observed during the Short-term Concentration Cell Testing.....	27
Table 2-3: Corrosion Current Density Observed during the Short-term Concentration Cell Testing.....	29
Table 2-4: Average Current Density of Wires for Various Orientations as Observed in the Long-term Concentration Cell Experiment.....	31
Table 3-1: Cumulative Penetration of Copper Plates after 4 Hours of Cavitation for various Water Qualities.....	54
Table 3-2: Cumulative Weight Loss of Copper Coupons in Valve Cavitation Damage Tests....	58
Table 3-3: Conditions of each Sand Particle Impingement Test.....	62
Table 3-4: Results of Particle Impingement Tests.....	63
Table 4-1: Summary of Visual Results from Longitudinal and Perpendicular Jet Tests.....	79

LIST OF FIGURES

Figure 1-1: Examples of Failures that Have Been Traditionally Classified as Erosion Corrosion or Flow Induced Failures.....	2
Figure 1-2: Pipe from Real Premise Plumbing Exhibiting Cavitation Bubble Implosion Damage.....	5
Figure 1-3: Example Schematic of Flow Electrification within a Copper Pipe (Edwards, et al., 2008).....	6
Figure 2-1: Key Reactions on Anodic and Cathodic Regions of the Pipe Surface Produce Electron Flow through the Metal (Above).....	12
Figure 2-2: Simplified Schematic of Concentration Cell Pitting Corrosion for Anodically Limited Reaction (Nguyen, 2006).....	13
Figure 2-3: Simplified Schematic of Concentration Cell Pitting Corrosion for Cathodically Limited Reaction (Nguyen, 2006).....	14
Figure 2-4: Conceptualization of Macroscopic Differential Flow Patterns that Naturally arise from Different Water use Patterns in Separate Branches of a Premise Plumbing System.....	15
Figure 2-5: Schematic of Localized High Velocity and Turbulence which may form Downstream from an Obstruction.....	15
Figure 2-6: Simplified Schematic of Small Area (1 cm ²) of Pipe Subject to Turbulence and a Large Area (100 cm ²) of Pipe Subject to Low Velocity.....	17
Figure 2-7: Experimental Setup of Short-term Concentration Cell Testing Apparatus - Pit Wires Externally Electrically Connected to the Large Copper Plate (not Shown in Picture).....	19
Figure 2-8: Concentration Cell Testing Apparatus with Copper Wires Exposed to Both High Flow and Stagnant Water Conditions in the Tee Sections.....	20
Figure 2-9: Experimental Setup of Long-term Concentration Cell Testing Apparatus.....	22

Figure 2-10: Copper Wire Sealed in Silicon Tubing.....	23
Figure 2-11: Example of Typical Data Collected with Short-term Concentration Cell Testing Apparatus.....	25
Figure 2-12: Current Density between Insulated Copper Wires Exposed to High Flow and Copper Plates in Stagnant Bulk Water.....	26
Figure 2-13: Average Current Density between Electrically Connected Insulated Copper Wires Exposed to Flow and Copper Plate in Stagnant Bulk Water in the Long-term Experimental Apparatus.....	30
Figure 2-14: Current Density between Electrically Connected Insulated Copper Wires Exposed to Flow and Copper Plate in Stagnant Bulk Water in Heated Salt Water with and without Chlorine in Short-term Tests.....	32
Figure 2-15: Weight Loss of Wires in Long-term Concentration Cell Experiment.....	33
Figure 2-16: Wires used in Long-term Concentration Cell Test.....	35
Figure 2-17: Copper Plates in Stagnant Bulk Water from Long-term Concentration Cell Tests.....	36
Figure 2-18: Cumulative Wire Weight Loss vs. Average Current Density for all Conditions Tested in Long-term Concentration Cell Test.....	37
Figure 3-1: Simplified Schematic of Destructive Capability of Cavitation Bubble.....	40
Figure 3-2: Experimental Setup of Ultrasonic Induced Cavitation Apparatus.....	42
Figure 3-3: Experimental Setup of Valve Cavitation Apparatus.....	43
Figure 3-4: Copper Components Subjected to Flow with Cavitation.....	44
Figure 3-5: Experimental Setup of Particle Entrained Flow Rig.....	45
Figure 3-6: Grain Size Comparison.....	46

Figure 3-7: Copper Specimen after 30 Minutes of Cavitation.....	47
Figure 3-8: Copper Specimen after 124.5 Hours of Continuous Cavitation.....	48
Figure 3-9: Weight Loss of Copper Specimen Subjected to 124.5 Hours of Continuous Cavitation.....	49
Figure 3-10: A) Copper Specimen with Scale Formed in the Pitting Water with 4 mg/L Cl ₂ at pH 8, B) Damage Caused after 2 Hours of Cavitation, and c) Damage Caused after 4 Hours of Cavitation.....	50
Figure 3-11: Cumulative Weight Loss of Sanded vs. Scale Covered Copper Specimen after 4 hours of Cavitation.....	51
Figure 3-12: Cumulative Weight Loss of Copper Plates after 4 Hours of Cavitation under Various Water Conditions.....	52
Figure 3-13: Cumulative Weight Loss of Copper Plates after 4 Hours of Cavitation using the Pitting Water at pH 6 and 2 Common Corrosion Inhibitors.....	53
Figure 3-14: Leak Formed in 0.02” Thick Copper Plate after 6.5 hours of Cavitation.....	54
Figure 3-15: Duration of Cavitation Necessary to Cause leak in Typical ¾” Type M Copper Tube with Intermediate Thicknesses.....	55
Figure 3-16: 0.004” Thick Copper Plate after Cavitation.....	56
Figure 3-17: Copper Pipe from Real Plumbing System.....	57
Figure 3-18: Weight Loss of Copper Components Subjected to Flow with Cavitation Prior to Film Removal.....	59
Figure 3-19: Copper Coupons used in Valve Cavitation Experiment After Film Removal (Flow Directed into the Page).....	60
Figure 3-20: Weight of Film Accumulated on Copper Sections during Test.....	61

Figure 4-1: Simplified Schematic of Experimental Setup of Jet Tests.....	68
Figure 4-2: Experimental Setup of Jet Testing Apparatus.....	69
Figure 4-3: Experimental Setup of Cycled Cavitation Tests.....	71
Figure 4-4: Surface Subjected to Longitudinal Jet in Room Temperature Fresh Water at pH 8 and 4 mg/L Cl ₂	72
Figure 4-5: Surface Subjected to Perpendicular Jet in Room Temperature Fresh Water at pH 8 and 4 mg/L Cl ₂	73
Figure 4-6: Surface Subjected due to Longitudinal Jet in Heated Salt Water.....	74
Figure 4-7: Surface Subjected to Perpendicular Jet in Heated Salt Water.....	75
Figure 4-8: Surface Subjected to Longitudinal Jet in Heated Salt Water.....	76
Figure 4-9: Schematic of High Velocity Streamline Impingement in Perpendicular Jet Test in Heated Salt Water.....	77
Figure 4-10: Schematic of High Velocity Streamline Impingement in Longitudinal Jet Test in Heated Salt Water.....	78
Figure 4-11: Cumulative Penetration for Various Longitudinal and Perpendicular Jet Test Plates in Heated Salt Water.....	80
Figure 4-12: Cumulative Penetration for Various Longitudinal and Perpendicular Jet Test Plates in Room Temperature Fresh Water at pH 8 and 4 mg/L Cl ₂	81
Figure 4-13: Current Density between Insulated Copper Wire Subjected to Periodic Cavitation and Copper Plate in Stagnant Bulk Water at pH 6.....	83
Figure 4-14: Current Density between Insulated Copper Wire Subjected to Periodic Cavitation and Copper Plate in Stagnant Bulk Water at pH 6.....	84

Figure 4-15: Current Density between Insulated Copper Wire with Greater Surface Area Exposed and Copper Plate in Stagnant Bulk Water.....	85
Figure 4-16: Copper Plate Subject to Longitudinal Jet in Heated Pitting Water at pH 6.....	87
Figure 4-17: Current Density for Wires Subjected to Cavitation relative to Plate in Stagnant Bulk Water following Cavitation.....	89
Figure 4-18: Penetration due to Combined Effect of Cavitation and Concentration Cell Corrosion Cycled Cavitation in a Hypothetical Premise Plumbing System.....	90
Figure 4-19: Penetration due to Combined Effect of Cavitation and Concentration Cell Corrosion Cycled Cavitation in a Hypothetical Premise Plumbing System.....	91
Figure 4-20: Current Density between Insulated Copper Wire Subjected to Periodic Cavitation and Copper Plate in Stagnant Bulk Water at pH 8 with 4 mg/L Cl_2	92
Figure A-1: Anodic Current Density vs. Time to Failure for Different Types and Sizes of Copper Pipe.....	96
Figure A-2: Short-term Concentration Cell Testing Apparatus before Installation of Leak.....	97
Figure A-3: Short-term Concentration Cell Testing Apparatus after Installation of Leak.....	98
Figure A-4: Potential Measured between Insulated Copper Wire Recessed from Flow and Copper Plate Submersed in Stagnant Bulk Water in Short-term Test - Without Leak, Potential Varies with Water Velocity (Indicating Electrification) - With Leak Installed, Electrification is Eliminated to Extent Achievable.....	99
Figure A-5: Potential Measured between Insulated Copper Wire Recessed from Flow and Copper Plate Submersed in Stagnant Bulk Water in Long-term Test – Electrification Effect was Determined to be Insignificant.....	100
Figure A-6: Current Density between Insulated Copper Wire Subject to High Flow and Copper Plate in Stagnant Bulk Water. Note: All Tests were Performed at Room Temperature unless otherwise Stated).....	101

Figure A-7: Current Density between Insulated Copper Wire Subject to High Flow and Copper Plate in Stagnant Bulk Water. Note: All Tests were Performed at Room Temperature).102

Figure A-8: Current Density between Insulated Copper Wire Subject to High Flow and Copper Plate in Stagnant Bulk Water. Note: All Tests were Performed at Room Temperature unless otherwise Stated).103

Figure A-9: Current Density between Insulated Copper Wire Subject to High Flow and Copper Plate in Stagnant Bulk Water. (Note: All Tests were Performed at Room Temperature unless otherwise Stated).104

Figure B-1: Experimental Setup of Jet Copper Plate with Copper Joint Edge.105

Figure B-2: Experimental Setup of Copper Plate with Plastic Surface Blockage.106

Figure B-3: Damage due to Longitudinal Jet with Copper Joint Edge in Heated Salt Water (Note: Small Divots in Undamaged Areas are Point Micrometer Indentations).107

Figure B-4: Damage due to Longitudinal Jet with Plastic Surface Blockage in Heated Salt Water (Note: Small Divots in Undamaged Areas are Point Micrometer Indentations).108

Figure B-5: Damage due to Longitudinal Jet in Heated, Water at pH 6 (Note: Small Divots in Undamaged Areas are Point Micrometer Indentations).109

Figure B-6: Damage due to Perpendicular Jet in Heated Fresh Water at pH 6 (Note: Small Divots in Undamaged Areas are Point Micrometer Indentations).110

Figure B-7: Cumulative Penetration for Various Longitudinal and Perpendicular Jet Test Plates in Heated Fresh Water at pH 6.111

Figure B-8: Cumulative Weight Loss for Various Longitudinal and Perpendicular Jet Test Plates in Heated Salt Water.112

Figure B-9: Cumulative Weight Loss for Longitudinal and Perpendicular Jet Test Plates in Heated Fresh Water at pH 6.113

Figure B-10: Cumulative Weight Loss for Longitudinal and Perpendicular Jet Test Plates in
Room Temperature Fresh Water at 4 mg/L Cl₂ at pH 8.....114

AUTHOR'S PREFACE

Chapter 1 presents a brief literature review of the 5 subsets of flow induced failure, as well as background information that served as motivation for this work. Chapters 2 through 4 present laboratory studies performed by the author of this thesis at Virginia Tech. Chapter 5 provides a summary of the key conclusions from this work.

CHAPTER 1: REVIEW OF CONVENTIONAL EROSION CORROSION AND FLOW INDUCED FAILURE MECHANISMS

Jeff Coyne, Marc Edwards, and Paolo Scardina

INTRODUCTION

Metal plumbing materials can corrode and fail from a variety of mechanisms. This work focuses on rapid failures of copper based plumbing materials in potable water systems due to *erosion corrosion*. In classic erosion corrosion the material appears to have been worn away by hydraulic phenomena (Figure 1-1). While this general concept is widely accepted, there has been very little fundamental progress to elucidate actual mechanisms behind classical erosion corrosion.

REVIEW OF CLASSICAL THEORY AND A NEW PROPOSED APPROACH

Review of Existing Theories

Erosion corrosion has been loosely described in the literature as a localized wearing-away of pipe material due to rapidly flowing corrosive liquid (Knutsson et al., 1972) or accelerated attack due to localized high velocity and excessive turbulence (Myers, 2005). While these vague explanations have obvious relevance to the practical circumstance that caused the damage, they do not provide fundamental insights as to the causal factors or solutions.

A specific erosion corrosion mechanism was described by Obrecht and Quill (1960a-f; 1961) and Murakami et al. (2003), who suggested that erosion corrosion mechanistically removes protective surface films (scales) that leaves bare copper metal fully exposed to the full corrosiveness of the bulk water. Bengough and May (1924) believed that high velocity jets impinging against copper specimens not only prevented a protective surface scale from forming but also accelerated the corrosion rate. Furthermore, they speculated that the jets also caused separation of the anodic and cathodic regions of the copper, driving accelerated corrosion reaction via formation of a concentration cell as described later in this work. Lastly, gas bubble cavitation (Obrecht and Quill, 1960f; Myers and Obrecht, 1972; Sakamoto et al., 1995) and solid particles impacting or impinging (Knutsson et al., 1972; Cohen and Lyman, 1972) against the copper pipe surface has also been blamed as a cause of erosion corrosion.

New Understanding and Approach

None of the previous studies actually isolated the specific mechanistic causes of *erosion corrosion* failures. For example, Knutsson et al. (1972) argued that erosion corrosion is abetted by gas bubbles and solid particles entrained in flow, and yet erosion corrosion damage resulting from subsequent tests performed by the authors was attributed only to rapidly flowing liquid and turbulence. No explanation was offered regarding the mechanistic cause of damage.

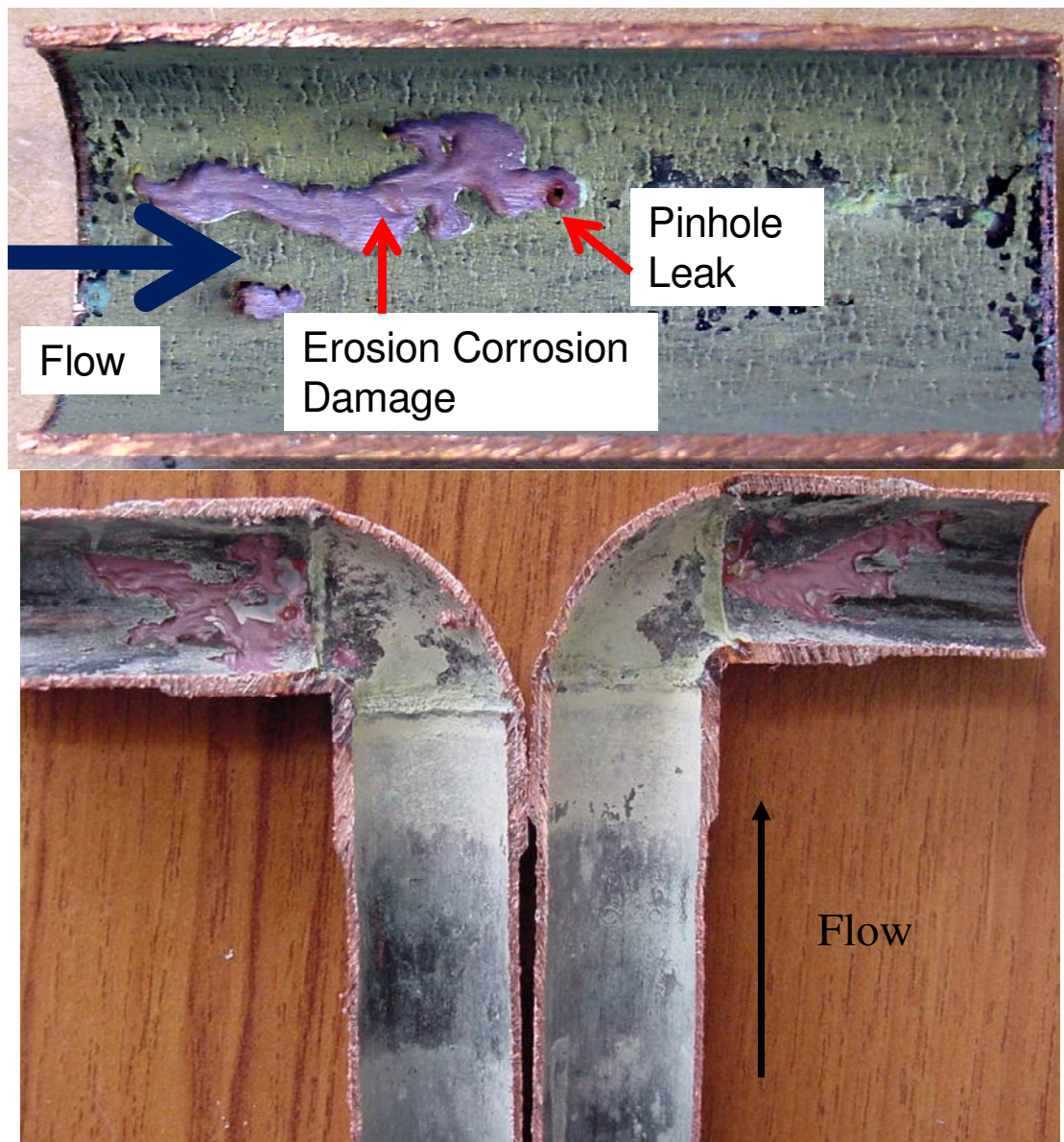


Figure 1-1: Examples of Failures that Have Been Traditionally Classified as Erosion Corrosion or Flow Induced Failures

After reviewing the literature and compiling possible fundamental explanations, it was apparent that even the classical description of such failures was deficient. For instance, accelerated localized corrosion driven by fluid velocity alone had not been proven to physically erode the underlying metal or protective scale. Additionally, some authors argue that erosion corrosion is caused by rapidly flowing liquid, gas bubbles, and suspended particles (Cohen and Lyman, 1972; Knutsson, et al., 1972; Myers and Obrecht, 1972) while some argue it is also caused by a concentration cell phenomenon (Obrecht and Quill, 1960f). Hence, a broader term called *flow induced* failure will be used to describe any failure due to hydraulic phenomena, and this work defines five specific flow induced failure mechanisms including cavitation bubble implosion, particle impingement, high velocity water impingement, and concentration cell corrosion. A fifth mechanism is a recently recognized damage causing phenomenon known as flow electrification, which has been documented in the oil industry but was thought to be negligible for high conductivity potable water systems (Edwards et al., 2007).

Concentration Cell Corrosion

Concentration cells arise due to an electrochemical imbalance created by differing chemical conditions on different sections of copper pipe surfaces. For example, a different level of oxygen at two points of a copper pipe surface (Wood and Fry, 1990) creates a voltage in which the high oxygen area becomes the cathode and the low oxygen area becomes the anode (Obrecht and Quill, 1960f; Bengough and May, 1924). Such a chemical condition can arise from flow patterns concentrating or affecting oxygen or disinfectant levels in distinct sections of pipe.

Cavitation Bubble Implosion and Damage

Cavitation describes the spontaneous formation of bubbles when local hydraulic pressure drops below the gas saturation pressure or below the vapor pressure of water (Novak, 2005). Bubbles consisting of water vapor forming when the localized pressure is below the vapor pressure are highly unstable, and can collapse or implode when the bubble returns to a normal pressure region. The implosion creates a micro-jet of water with pressures sufficient to physically gouge and damage metallic copper (Novak, 2005; During, 1990). Chan and Cheng et al. (2002) suggested that cavitation played a significant role in valve damage in Hong Kong water lines and that copper is highly susceptible to cavitation attack. In addition, recent forensic

evaluations of copper pipe sections revealed a damage pattern consistent with that believed to be cavitation implosion (Figure 1-2).

Particle Impingement

Particle impingement describes the possible mechanical breakdown or wearing-away of pipe material due to particle impact against the plumbing material. Two factors thought to influence this type of damage include impingement angle/velocity and type of material (Benchaita, et al., 1983). Hutchings (1983) found that particles which cause erosion are typically harder than the surface being destroyed and that pipe bends, junctions, and constrictions are at relatively high risk for impingement failure. Actual damage is caused by particles dragging along the inner surface of copper pipe (Hutchings, 1983).

High Velocity Water Impingement

High velocity water impingement is believed to detach copper scale from pipe walls or otherwise alter the type and distribution of scale that forms (Bengough and May, 1924). Landrum (1989) believed that the local velocity of water can be greatly accelerated when it passes by deposits on pipe surfaces. It was stated that velocities can increase from 6 ft/sec (a typical premise plumbing water velocity) to 300 ft/sec just past small flow obstructions like burrs, tubercles or deposits (Landrum, 1989). This substantial increase in velocity and turbulence may be sufficient to detach non-durable copper scale or otherwise prevent pipe scale from forming. Landrum also pointed out that increasing solution velocity makes sustaining protective films more difficult and that copper itself is very sensitive to increasing fluid velocities (1989).



Figure 1-2: Pipe from a Real Premise Plumbing System Exhibiting Possible Cavitation Bubble Implosion Damage

Flow Electrification

Another possible failure mechanism, which has been studied in the oil and gas industry, is known as flow electrification. Once typically thought only to occur in low conductivity liquids such as petroleum, electrification is now believed to contribute to corrosion in potable water systems (Edwards et. al, 2007). Electrification, also termed streaming current or potential, arises when water flows through a conductive (metal) pipe material. The movement of positive ions dissolved in the flowing fluid induces an electrical imbalance as these positive ions flow

past the metallic pipe wall. This flow of positive charges then becomes offset by a necessary and corresponding flow of electrons through the metal piping (Figure 1-3). The source of these corresponding electrons is the active corrosion activity of the metal (i.e. $\text{Cu}^0 \rightarrow \text{Cu}^+ + \text{e}^-$). To simplify, the water flowing through a pipe can accelerate some corrosion activity, in much the same way that static electricity is generated when walking on a carpet.

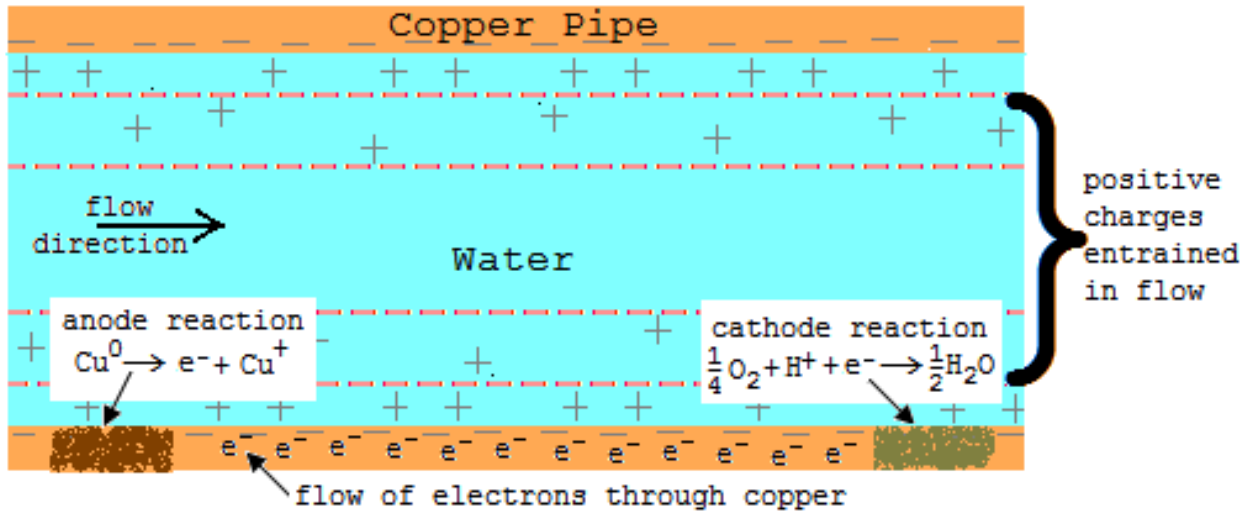


Figure 1-3: Example Schematic of Flow Electrification within a Copper Pipe (Edwards, et al., 2008)

Flow electrification phenomena have been proven to be problematic in the oil industry, where very high voltages from flowing petroleum have actually caused sparks and fires. While potentials induced in potable water premise plumbing systems are far less than those potentials induced in petrochemical pipe flow, it is recognized that this mechanism can accelerate corrosion and induce premature pipe failure. This subject is described in a separate report (Edwards, et al., 2008) and will not be studied purposefully in this work.

SUMMARY AND RESTATEMENT OF GOALS

Damage and failure of copper potable water plumbing can arise mechanistically from fluid flow phenomena. Despite the significance and practical relevance of this type of failure, very little research has attempted to explain mechanistically how or why damage occurs. This work is the first to examine the mechanisms of flow induced failure in practical premise plumbing scenarios by systematically and individually evaluating the propensity of cavitation, particle impingement, high velocity impingement, and concentration cell corrosion to cause copper damage. Additionally, tests were conducted to evaluate the extent of damage from multiple synergistic mechanisms.

While it is understood that some experiments described herein do not test flowing water through actual copper pipe, it is believed that these testing apparatuses sufficiently replicate flow induced damage causing mechanisms, allowing for comparisons to practical plumbing scenarios.

REFERENCES

- Benchaita, M. T., P. Griffith, and E. Rabinowicz. "Erosion of Metallic Plate by Solid Particles Entrained in a Liquid Jet." *Journal of Engineering for Industry*. 105 (1983): 215-222.
- Bengough, Guy D. and R. May. "Seventh Report to the Corrosion Research Committee of the Institute of Metals." *The Journal of the Institute of Metals*. 32 (1924): 90-269.
- Chan, W.M., F.T. Cheng, and W.K. Chow. "Susceptibility of Materials to Cavitation Erosion in Hong Kong." *Journal of the American Water Works Association*. 94.8 (2002):76-84.
- Cohen, Arthur, W. Stuart Lyman. "Service Experience with Copper Plumbing Tube." *Materials Protection and Performance*. 11.2 (1972): 48-53.
- During, E. D. D. Corrosion Atlas. Amsterdam, The Netherlands: Elsevier Science, 1997.

Edwards, Marc, Rebecca Lattyak, Paolo Scardina, Chris Strock. “Flow Electrification and Non-Uniform Copper Corrosion in Potable water Systems.” *Final Draft Report to Copper Development Association*. (August, 2007).

Hutchings, Ian M. “Monograph on the Erosion of Materials by Solid Particle Impact.” *Materials Technology Institute of the Chemical Process Industries*. 10 (1983).

Knutsson, L., E. Mattsson, and B.E. Ramberg. “Erosion in Copper Water Tubing.” *British Corrosion Journal*. 7 (September, 1972).

Landrum, James R. Fundamentals of Designing for Corrosion Control. Houston, Texas: National Association of Corrosion, 1990.

Murakami, Moritoshi, Kazuhiko Sugita, Akihiro Yabuki, and Masanobu Matsumura. “Mechanism of So-called Erosion Corrosion and Flow Velocity Difference Corrosion of Pure Copper.” *Corrosion Engineering*. 52.3 (2003): 155-159.

Myers, James R. “Copper Tube Corrosion in Domestic-Water Systems.” *Heating, Piping and Air Conditioning Engineering*. (June, 2005): 22-31.

Myers, James R., and M.F. Obrecht. “Potable Water Systems: Recognition of Cause Vital to Minimizing Corrosion.” *Materials Protection and Performance*. 11.4 (1972): 41-46.

Novak, Julia Ann (2005). “Cavitation and Bubble Formation in Water Distribution Systems”. Environmental Engineering. Blacksburg, VA. Virginia Polytechnic Institute and State University. **Master of Science**.

Obrecht, M.F., and L. L.Quill. “How Temperature, Treatment, and Velocity of Potable Water Affect Corrosion of Copper and its Alloys in heat exchanges and piping systems.” *Heating, Piping and Air Conditioning*. (January, 1960a): 165-169.

Obrecht, M.F., and L. L. Quill. “How Temperature, Treatment, and Velocity of Potable Water Affect Corrosion of Copper and it as Alloys; Cupro-Nichel, Admiralty Tubes Resist Corrosion Better.” *Heating, Piping and Air Conditioning*. (September, 1960b): 125-133.

Obrecht, M.F., and L. L. Quill. “How Temperature, Treatment, and Velocity of Potable Water Affect Corrosion of Copper and it as Alloys; Different Softened Waters Have Broad Corrosive Effects on Copper Tubing.” *Heating, Piping and Air Conditioning*. (July, 1960c): 115-122.

Obrecht, M.F., and L. L. Quill. “How Temperature, Treatment, and Velocity of Potable Water Affect Corrosion of Copper and it as Alloys; Monitoring System Reveals Effects of Different Operating Conditions.” *Heating, Piping and Air Conditioning*. (April, 1960d): 131-137.

Obrecht, M.F., and L. L. Quill. “How Temperature, Treatment, and Velocity of Potable Water Affect Corrosion of Copper and it as Alloys; Tests Show Effects of Water Quality at Various Temperatures, Velocities.” *Heating, Piping and Air Conditioning*. (May, 1960e): 105-113.

Obrecht, M.F., and L. L. Quill. “How Temperature, Treatment, and Velocity of Potable Water Affect Corrosion of Copper and it as Alloys; What is Corrosion?” *Heating, Piping and Air Conditioning*. (March, 1960f): 109-116.

Obrecht, M.F., and L. L. Quill. “How Temperature, Treatment, and Velocity of Potable Water Affect Corrosion of Copper and it as Alloys.” *Heating, Piping and Air Conditioning*. (April, 1961): 129-134.

Sakamoto, A. T. Yamasaki, and M. Matsumura. “Erosion-corrosion Tests on Copper Alloys for Tap Water use.” *Wear*. (1995): 538-554.

Wood, R. J. K., and S. A. Fry. "Corrosion of Pure Copper in Flowing Seawater Under Cavitating and Noncavitating Flow Conditions". *Transactions of the ASME*. 112 (June, 1990).

CHAPTER 2: BENCH SCALE STUDIES ON CONCENTRATION CELL CORROSION OF COPPER UNDER DIFFERENTIAL FLOW

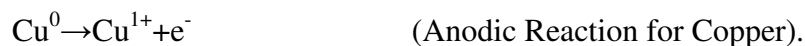
Jeff Coyne, Marc Edwards, and Paolo Scardina

INTRODUCTION

Water flow is linked to non-uniform copper corrosion and service failures through a number of proposed mechanisms. One important mechanism is the formation of an electrochemical concentration cell resulting from differential flow rates (Novak, 2005; Evans, 1937). Dependent on water chemistry and the type of metal, pipe surfaces exposed to a high flow rate can become highly anodic or cathodic relative to areas of the pipe surface exposed to a low flow rate or stagnant conditions. This section reviews the basic electrochemical theory related to this phenomenon, describes practical situations in which differential flow arises in plumbing networks and might contribute to service failures, and establishes the motivation for later experimentation.

Concentration Cells Formed by Differential Flow

A concentration cell can develop whenever different portions of a metallic pipe surface are exposed to differing chemical conditions (Obrecht and Quill, 1960f). The resulting electrochemical imbalance can create an electrochemical potential, separation of anode and cathode, and induce electron flow through the metal. In classic pitting corrosion, electrons are produced at the anode (the active site of the corrosion) (Figure 2-1):



These electrons pass through the pipe to the cathode where they are consumed by reactions usually involving common potable water oxidants like dissolved oxygen or disinfectants:



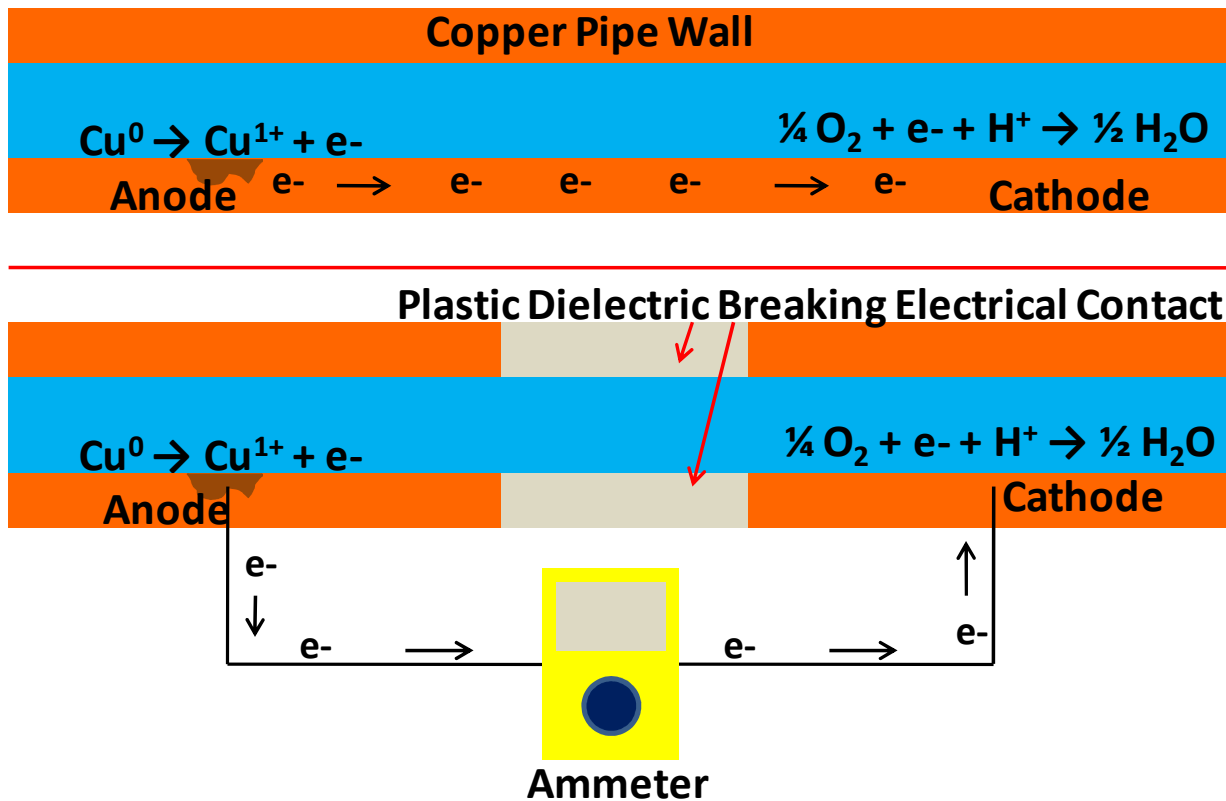


Figure 2-1: Key Reactions on Anodic and Cathodic Regions of the Pipe Surface Produce Electron Flow through the Metal (Above). If the Anodic and Cathodic Regions are not in Electrical Contact, the Resulting Voltage and Current could be Monitored with a Simple Multimeter (Below).

An electrochemical imbalance can be created by differential flow as a result of enhanced transport near the surface of the pipe that is exposed to more turbulence. Specifically, the portion of the surface with higher flow will be exposed to higher concentrations of corrosion reactants (oxidants like O_2 and Cl_2) and lower concentrations of corrosion reaction products (metal cations like Cu^{2+} or Pb^{2+}) than the rest of the pipe (Figure 2- 2). The net result of these imbalances depends on electrochemical kinetics in the specific system. Specifically, if the anodic reaction is rate limiting, the removal of the reaction product such as Cu^{+1} (Wood and Fry, 1990) will have a disproportionate effect, and a local excess of electrons will be created at the surface subject to high flow (Figure 2-2). There will then be a net flow of electrons to the portion of the pipe surface exposed to lower flow where the cathodic reaction will occur (Figure 2-2).

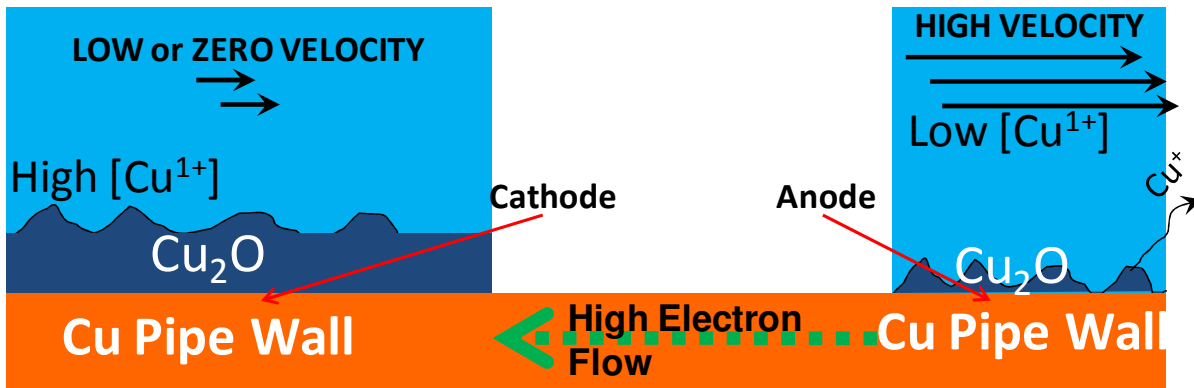


Figure 2-2: Simplified Schematic of Concentration Cell Pitting Corrosion for Anodically Limited Reaction (Nguyen, 2006)

If the cathodic reaction is rate limiting, the higher concentration of oxygen or disinfectant at the surface exposed to high flow (due to the enhanced diffusion of oxygen to the surface (Obrecht and Quill, 1960f)) will have a disproportionate impact (Figure 2-3). This would create a relative deficiency of electrons in the portion of the metal surface exposed to higher flow, and the anodic reaction would then occur at the portion of the pipe surface exposed to lower flow. The direction of flow of electrons through the metal and the location of the anode and cathode would then be reversed from the situation described in Figure 2-2.

Differential Flow in Service

In a premise plumbing potable water system, concentration cells arising from differential flow could develop in a number of situations at either the macro or micro scale. For example, a home may have a section of copper plumbing leading to a kitchen faucet that is frequently used during the day at a typical maximum velocity of 8 ft/sec for washing dishes and preparing food. This branch of the plumbing system could be in electrical contact with other branches that lead to plumbing devices that are less frequently used such as a second bathroom or an outside hose bib (Figure 2-4). These long periods of stagnation in seldom used plumbing fixtures can produce large areas of copper pipe surface that are exposed to relatively high concentrations copper ions. Conversely, the frequent usage of the branch of plumbing leading to a kitchen would have relatively low concentrations of copper corrosion products (i.e. Cu^{+1} and Cu^{+2}) and high levels of oxygen and chlorine in the water versus the less frequently used branch (as copper ions are removed from the system while oxygen and chlorine are introduced to the premise plumbing

from the main during periods of flow). Due to these differing chemical concentrations, entire sections of the plumbing network might therefore become anodic or cathodic to each another.

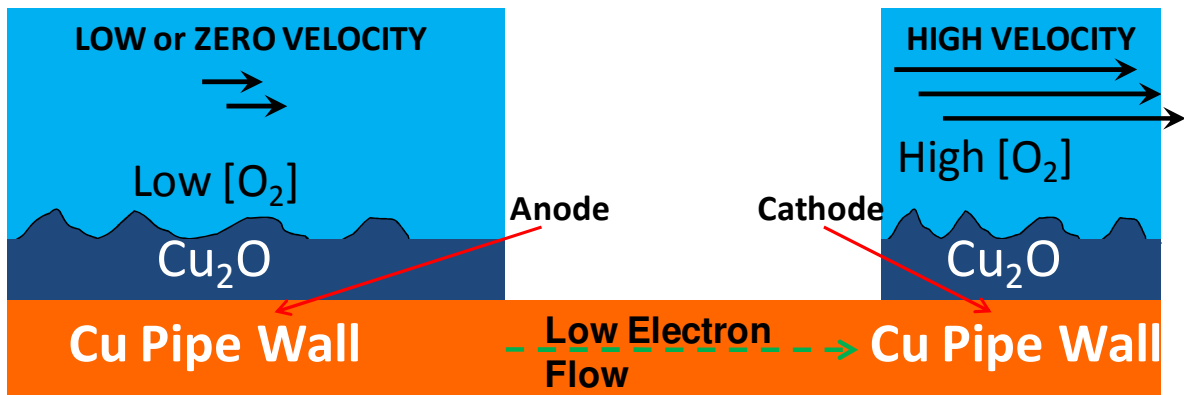


Figure 2-3: Simplified Schematic of Concentration Cell Pitting Corrosion for Cathodically Limited Reaction (Nguyen, 2006)

Differential flow can also develop on surfaces at the microscale (Figure 2-5). For example, if a deposit or burr is present on the inner wall of a copper pipe, the resulting obstruction to flow can create extreme local turbulence and high velocities up to 300 ft/sec (Landrum, 1990) immediately downstream of the obstruction (Figure 2-5). In this type of situation only a very small portion of the overall pipe surface will be exposed to the relatively high turbulent flow, a large portion of the pipe surface is exposed to relatively low flow, and a very small part of the surface (under the deposit) can be exposed to nearly stagnant conditions.

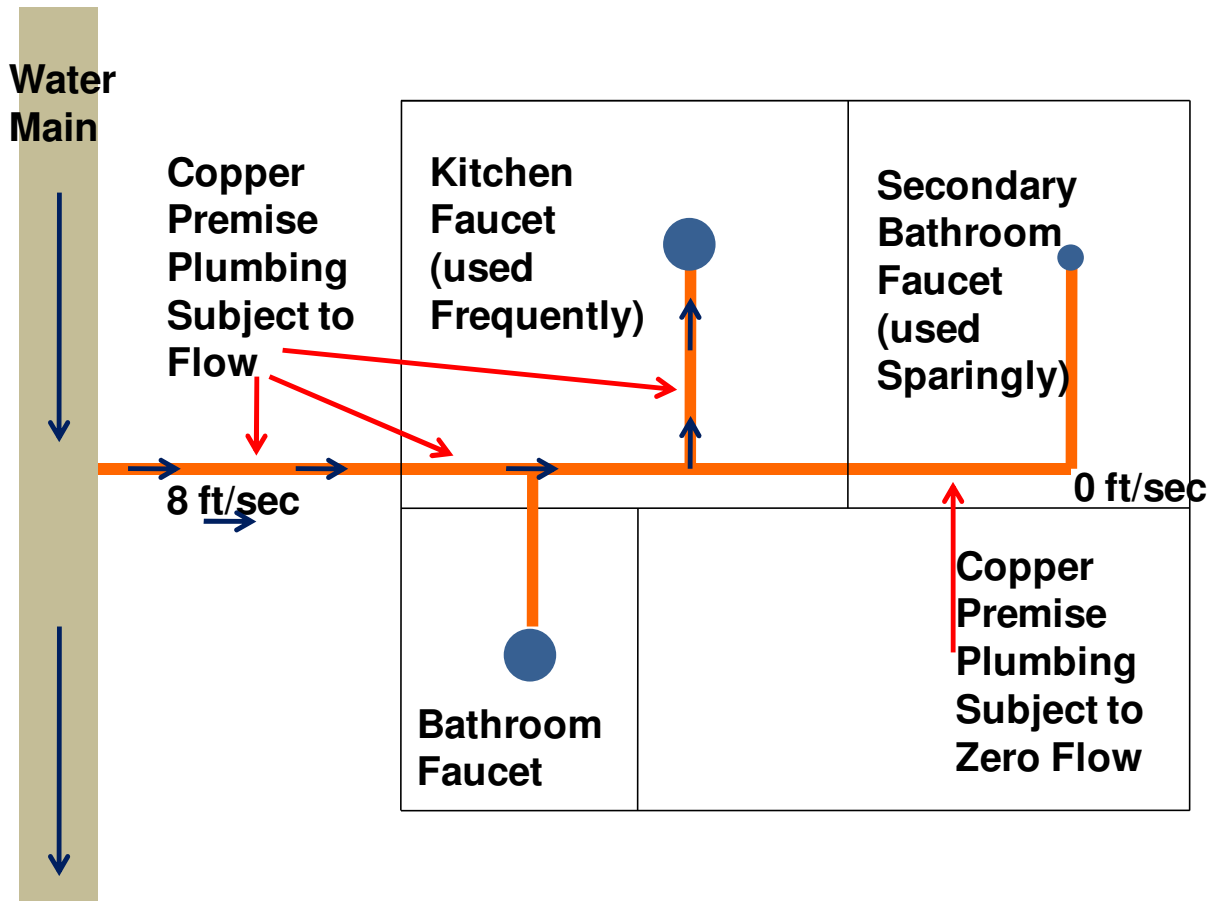


Figure 2-4: Conceptualization of Macroscopic Differential Flow Patterns that Naturally arise from Different Water use Patterns in Separate Branches of a Premise Plumbing System

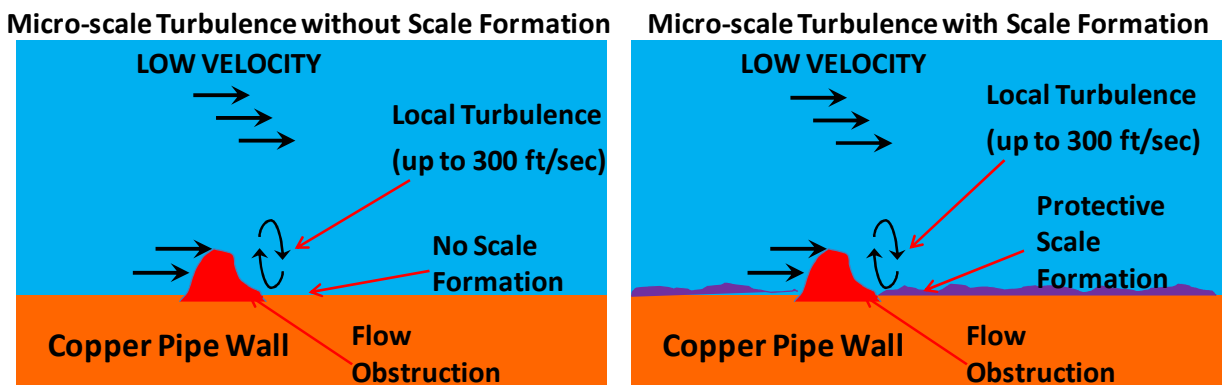


Figure 2-5: Schematic of Localized High Velocity and Turbulence which may form Downstream from an Obstruction (with and without Scale Formation)

Effect of Design, Installation, and Water Chemistry

The ultimate consequences of differential flow are determined by a number of factors. If numerous deposits are formed on the pipe surface or if joints are not deburred during installation, then microscale differential flow cells can occur with high frequency throughout the plumbing system. In other installation scenarios such situations may be rare or nonexistent. Maintaining maximum flows less than 8 ft/sec in cold water systems and 5 ft/sec in hot water systems, as per design recommendations of the Copper Development Association (2006), would also reduce the magnitude of differential flow concentration cells at either the micro or macro scale, when compared to situations that would arise if design velocities were 10, 20 or 30 ft/sec.

Water chemistry also plays a critical role because it controls the type of reactions and scale (i.e., copper rust layers) that form on the metal. As a relatively noble metal, corrosion of copper can be either anodically or cathodically limited depending on the water chemistry (Evans, 1937). As mentioned earlier, in some situations the portion of the surface exposed to the high flow will become anodic and in other situations the portion of surface exposed to high flow will be cathodic (Figure 2-2 and Figure 2-3). But the water chemistry and the overall propensity for pipe failure due to differential flow can be influenced by the type and durability of scale that forms on the copper pipe surfaces at the anode or cathode, as formation of highly durable or protective scales at the anode could protect the surface exposed to flow and mitigate the strength of the concentration cell that is formed.

The chemistry of the water supplied and the mode of operation can also be influential. For example, if the water is operated in a continuous recirculation mode, the concentration of Cu^{+1} and Cu^{+2} reaction products may equilibrate in the bulk water and the concentration of dissolved oxygen and chlorine can become depleted. In such situations, the area of pipe exposed to high flow might not form a strong concentration cell relative to the situation that occurs in fresh water that has not previously contacted the copper surface.

In the vast majority of plumbing installations, water chemistries, and water use patterns that are encountered in premise plumbing, non-uniform corrosion arising from differential flow is of little consequence. It is only in very unusual cases that problems are observed. On the basis of this analysis, rapid failures are expected to occur from this mechanism if non-durable

scale forms on the anodic pipe surface, if the anodic reaction is rate limiting, and if a small area of the pipe surface is subject to very high velocities due to a failure to de-bur or from formation of deposits (Figure 2-5). If all these factors are met, attack at a very small anode is supported by a very large cathode (Figure 2-6), and the attack is perpetuated by a failure to form a protective scale on the part of the surface exposed to high flow (Table 2-1).

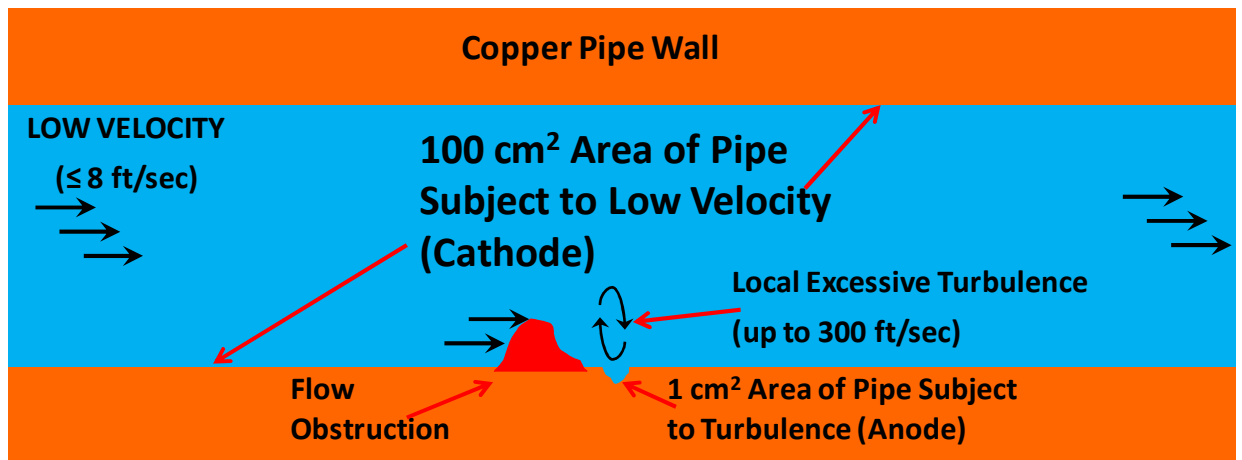


Figure 2-6: Simplified Schematic of Small Area (1 cm²) of Pipe Subject to Turbulence and a Large Area (100 cm²) of Pipe Subject to Low Velocity

Table 2-1: Simplified Example of Expected Failure Time among Concentration Cell Reactions Controlled Anodically and Cathodically for New 3/4" Type M Copper Tube

Rate Limiting Reaction Controlling Concentration Cell:	Measured Electron Flow (Current, μA)	Area of Anodic Portion of Pipe (cm^2)	Current Density ($\mu\text{A}/\text{cm}^2$)	Expected Time to Failure (Yrs)
Anodic Reaction	35	1	35	1
Cathodic Reaction	35	100	0.35	100

If the cathodic reaction is rate limiting, the very small area exposed to high flow becomes the cathode and the anodic attack is distributed over a much greater surface area (Table 2-1). It is therefore believed that water chemistry would control whether a pipe exposed to differential flow would last 100 years or fails in as little as 1 year (Figure A-1).

Unfortunately, at present, there is little to no research on the specific aspects of water chemistry that will determine scale durability or whether copper corrosion will be subject to anodic or cathodic control. Indeed, there have been no systematic investigations into the veracity of the above hypothesis. The goal of this research is to examine fundamental aspects of copper

corrosion arising due to differential flow as a function of water chemistries, and to develop experimental data to refute or support existing theory.

METHODS AND MATERIALS

Two types of experiments were conducted including: 1) Short-term concentration cell tests and 2) Long-term concentration cell tests.

Short-term Concentration Cell Tests

Short-term experiments were designed to examine the effects of concentration cells caused by differential flow between two isolated copper sections in electrical contact through an ammeter (i.e., Figure 2-1). The apparatus consists of a peristaltic pump that recirculated water through a tygon tubing loop with both the intake and discharge submerged at opposite ends of a 25 L reservoir (Figure 2-7). Small diameter tee barb fittings were connected to the tygon tubing at both the suction (or intake) side and the discharge side for the purpose of holding two independent exposed copper wires (Figure 2-8). Two insulated copper wires were placed into each tee fitting (Figure 2-8): one placed out of the flow (subjected to nearly zero velocity) and one placed directly perpendicular to the edge of the flow (allowing longitudinal water flow at a higher velocity across the flat copper surface). At the start of each experiment, all trapped air bubbles/pockets were removed from the section of tubing that held the recessed out of flow copper wire.

The insulated copper wires (14 gauge) that were inserted into the tee (Figure 2-8) were chosen because the size of the wire (about 0.16 cm or 0.06" diameter) approximates the size of many real holes formed in copper tube. Only the tip of the insulated wire (about 0.02 cm²) was exposed to the experimental water. The tip was initially cut flat and sanded smooth at the start of each test to eliminate any initial interference from existing corrosion scales. Each wire was externally electrically connected to a large copper plate submersed in the bulk water (Figure 2-7), which simulates a large portion of premise plumbing subject to stagnant or low flow (Figure 2-4, and Figure 2-5). This copper plate was also sanded prior to each test to ensure uniform starting conditions.

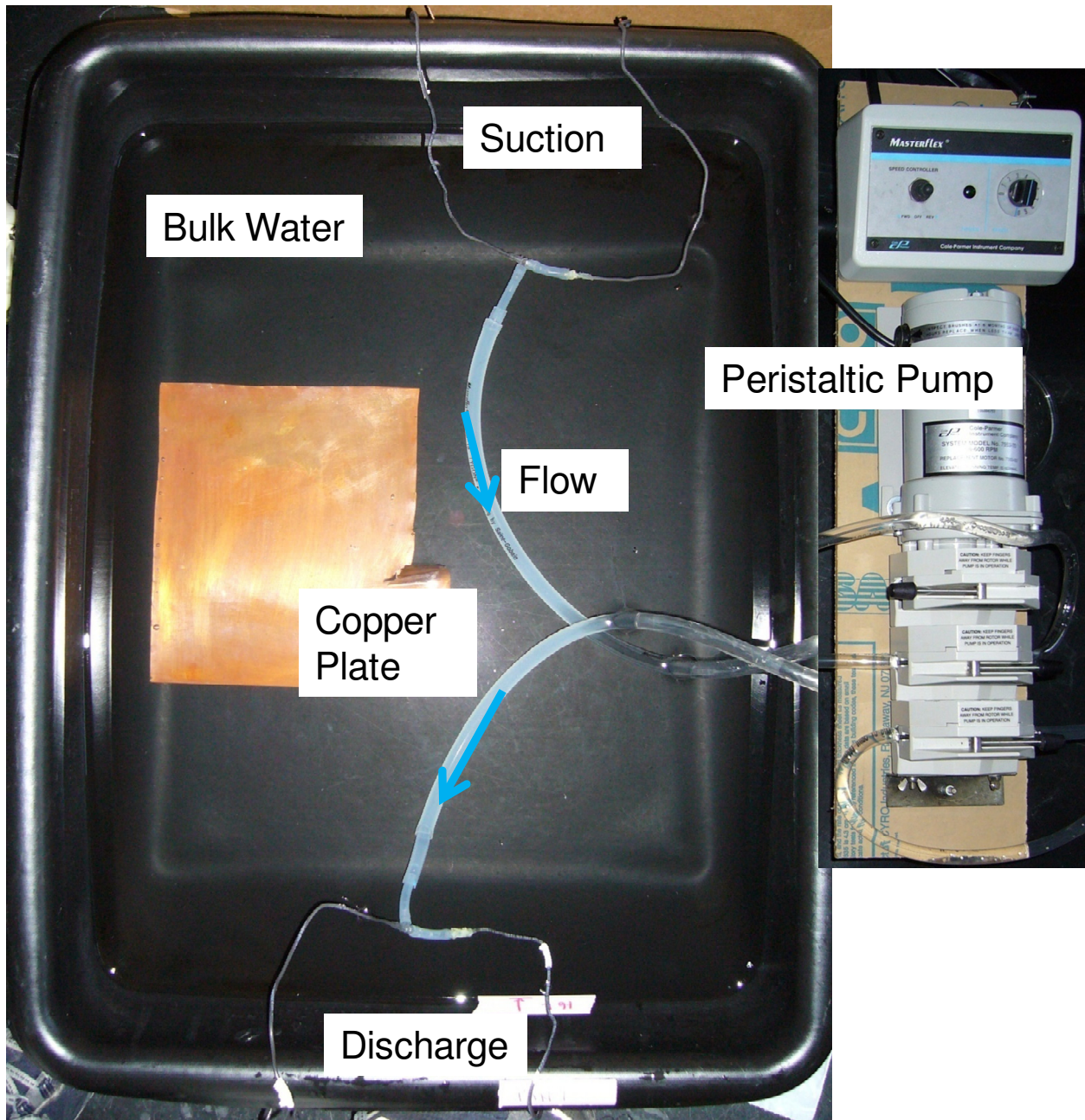


Figure 2-7: Experimental Setup of Short-term Concentration Cell Testing Apparatus - Pit Wires Externally Electrically Connected to the Large Copper Plate (not Shown in Picture)

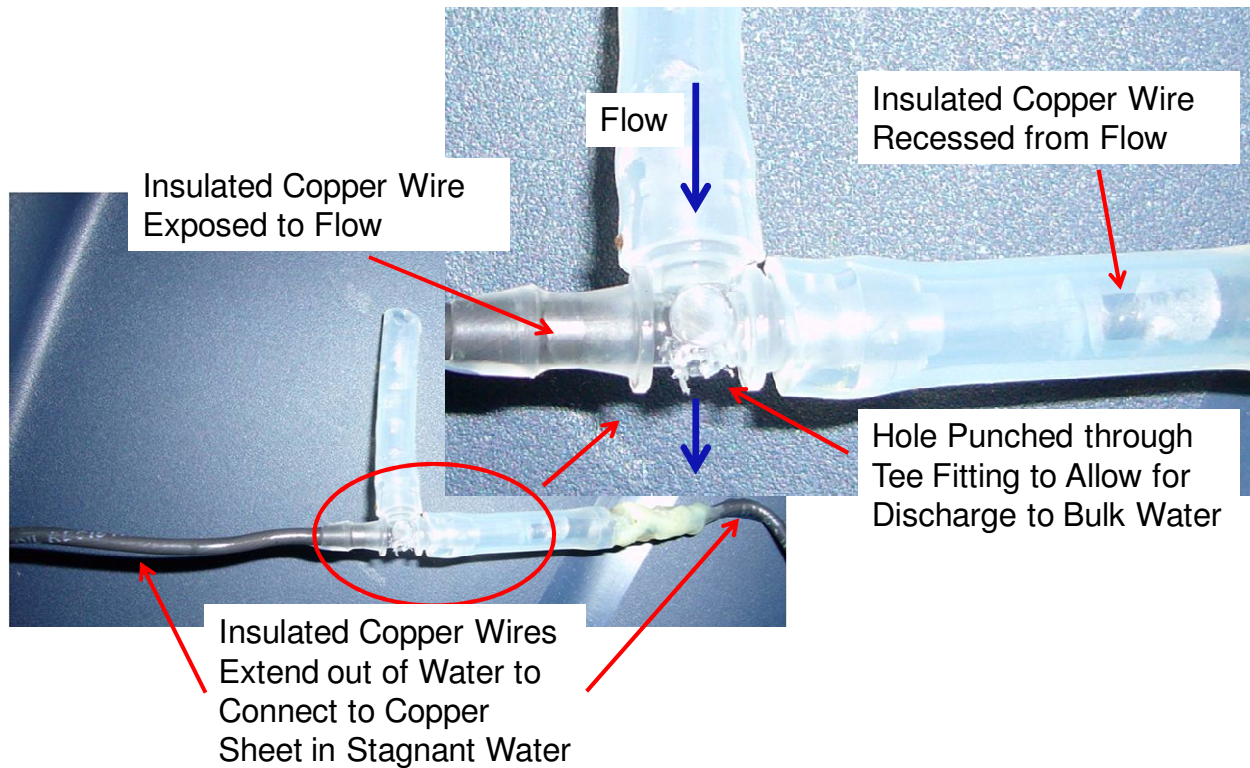


Figure 2-8: Concentration Cell Testing Apparatus with Copper Wires Exposed to Both High Flow and Stagnant Water Conditions in the Tee Sections

A reference water known to cause copper pitting (Marshall, 2004) was used in these experiments at the following recipe: 25.0 mg/L $\text{CaSO}_4 \cdot 2\text{H}_2\text{O}$, 56.85 mg/L NaHCO_3 , 41.296 mg/L $\text{CaCl}_2 \cdot 2\text{H}_2\text{O}$, 2.0 mg/L aluminum solids, 4.0 mg/L chlorine and pH 9.1-9.3. This pitting water was then varied throughout the study by altering the solution pH (pH 5, 6.5, 8, and 9.5) or other factors. Waters at pH 6.5 and pH 8 were then tested with additions of either orthophosphate (2 mg/L as P), ammonia (4 mg/L as N), or chlorinated NOM (2 mg/L TOC). The effect of temperature was also considered by heating the pitting water to 37.5° C (+/- 2.5° C) at pH 6.5 and 8. Heated salt water, synthesized using a powder Instant Ocean Sea Salt mix, was also tested as it was reported to cause serious flow induced damage by Bengough and May (1924). In this apparatus, water velocities in the range of 15 - 20 ft/sec were possible.

The primary data collected during this study was electrochemical measurements of voltage and corrosion currents via a handheld multimeter (Fluke 189 True RMS Multimeter). The multimeter was capable of measuring current above +0.07 μA . During data collection, the multimeter was placed temporarily in line electrically between the insulated copper wire and the

large copper plate submersed in bulk water. All corrosion currents, as per convention, were converted to a *current density* using the known surface area of the insulated wire. These values were referenced to a standard corrosion current density of $1 \mu\text{A}/\text{cm}^2$, which would translate into a hole or leak in new type M copper tubing in 35 years (Figure A-1). All positive currents presented in this work indicate that the copper wires exposed to the high flow are anodic relative to the large copper sheets (the copper sheet is the cathode); whereas negative currents indicate the copper wires are cathodic relative to the copper sheets.

Complications can arise in this type of apparatus from flow electrification (Edwards et al., 2007). To eliminate this issue a small hole or leak was placed in the tubing directly preceding each of the tees (holding pit wires) which effectively shorted-out the flow electrification problem (Figure A-2 and A-3) and was proven to significantly eliminate its influence (Figure A-4).

Long-term Concentration Cell Tests

Due to the informative results obtained with the short-term concentration cell experiments, additional experiments were designed to isolate possible longer-term effects of concentration cells arising due to differential flow patterns. A second apparatus consisted of a 1/15 HP centrifugal pump, PVC pipe, and tygon tubing, recirculating water through a closed loop connected to a 40 L reservoir (Figure 2-9). Similar to the short-term experiments, two copper wires (insulated by silicon tubing) were placed into tee fittings, one placed directly in the flow (subject to high velocity) and one recessed from flow (subject to zero velocity). Evaluations indicated that flow electrification affect was insignificant with this new setup due to the short tubing path between the in-flow copper and copper sheet (Figure A-5).

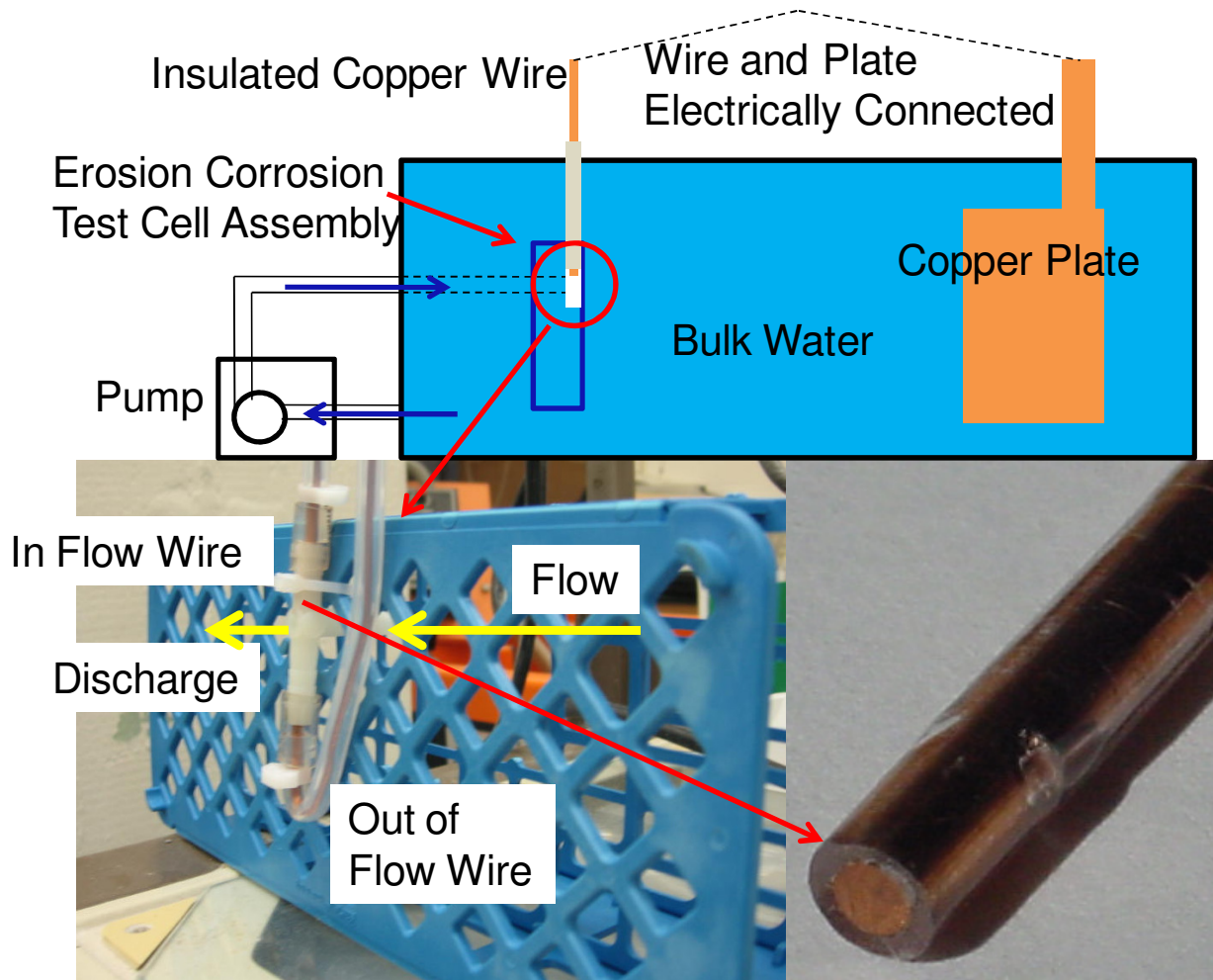


Figure 2-9: Experimental Setup of Long-term Concentration Cell Testing Apparatus

Pit wires of a known diameter (about 0.20 cm or 0.08") were used in this experiment to mimic the surface area (about 0.03 cm²) of a real pit, and this assembly also allowed for weekly weight loss measurements of the copper. The bulk exterior of the copper wires were sealed in a water-tight silicon tubing (Figure 2-10), such that only the tip of the wire was exposed and contacted water. Similar to the previous concentration cell experiment, a tee assembly allowed for one copper pit wire to be flush to longitudinal flow (if the wire was exposed to flow) and a second wire recessed in essentially stagnant water. Both pit wires were externally electrically connected to the large copper plate submerged in the bulk water reservoir. The exterior silicon tubing was removed periodically for weight loss measurements of the copper pit wires.

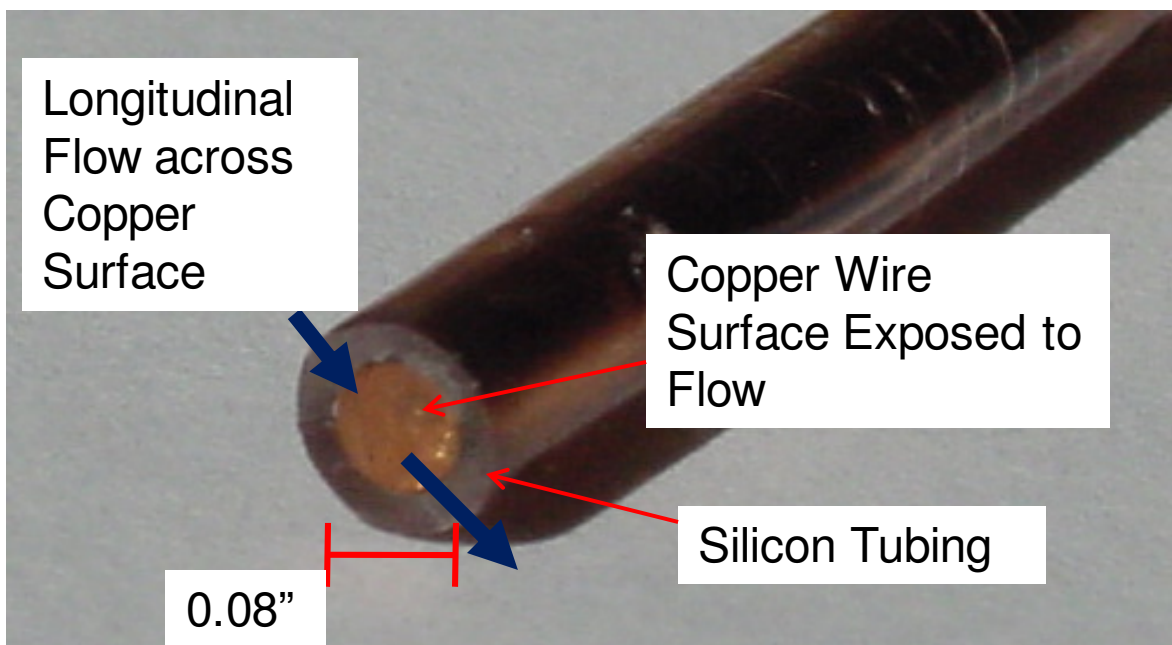


Figure 2-10: Copper Wire Sealed in Silicon Tubing

In order to better monitor electrochemical activity of this copper system, electrochemical data were continuously collected using a Gamry ECM-8 multiplexer in a zero resistance ammeter mode. This setup allowed for measurement of current between the insulated copper wires and copper plates every minute for the duration of the experiment. A handheld multimeter (Fluke 189 True RMS Multimeter) was used periodically to verify the Gamry data.

Four different variations of the known pitting water (Marshall, 2004) were tested. Three tests were conducted at room temperature (at pH 6 with 4 and 0 mg/L Cl_2 and at pH 8 with 4 mg/L Cl_2) (unless otherwise noted, all temperature conditions were room temperature and unlabeled as such). One test was conducted in water heated to 37.5°C ($\pm 2.5^\circ\text{C}$) at pH 6 without chlorine. Three test cells were simultaneously tested in each water quality. Each test cell included 1 copper wire exposed to flow and 1 copper wire recessed from flow thereby subject to stagnant water conditions (Figure 2-9). The wires in two of these test cells (both exposed to flow and recessed from flow) were electrically connected externally to copper plates submersed in stagnant bulk water and the third test cell was left without electrical connection. This long-term concentration cell test lasted for about 23 days except for the heated water

condition. The average velocity with each test cell ranged between 26 – 29 ft/sec. Copper plates and insulated copper wires were sanded prior to the test to ensure uniform starting conditions.

RESULTS

Short-term Concentration Cell Tests

Copper Exposed to High Flow Conditions

The concentration cell that was produced as a result of differential velocity is typified by a result obtained for water at pH 6.5 heated to 37.5° C. The current density between the insulated copper wire exposed to flow (on the suction side of the pump) and the copper sheet in stagnant bulk water gradually increased to almost 60 $\mu\text{A}/\text{cm}^2$ over the duration of the test. Thus, the copper wire exposed to flow progressively became more anodic (relative to the copper sheet in stagnant bulk water) over time. A higher current density for the wires on the suction side versus the discharge side of the pump (Figure 2-11) was nearly always observed in this apparatus and, unless otherwise stated, only “suction side” data is presented in this chapter. Some tests were performed in duplicate (Figure 2-14), but overall, the corrosion currents appeared to attenuate over the course of a few hours so duplicate testing was deemed unnecessary for most of these preliminary tests.

Water quality profoundly affected the magnitude of the current between copper surfaces exposed to differential velocities. For example, simply lowering the solution pH from 8 to 6.5 in this pitting water caused a dramatic increase in current density (Figure 2-12). In unchlorinated water at pH 8, the measured current densities were always negative, indicating the insulated copper wire subjected to high flow was actually cathodic and seemingly passivated relative to the copper plate submerged in stagnant bulk water. This is consistent with expectations based on Figure 2-3, in which the copper surface exposed to higher velocity is expected to be cathodic if the water makes the overall corrosion reaction cathodically limited. As mentioned earlier, the condition of greatest concern with respect to pipe failure occurs when a high anodic current density is observed on the copper wire exposed to high velocity.

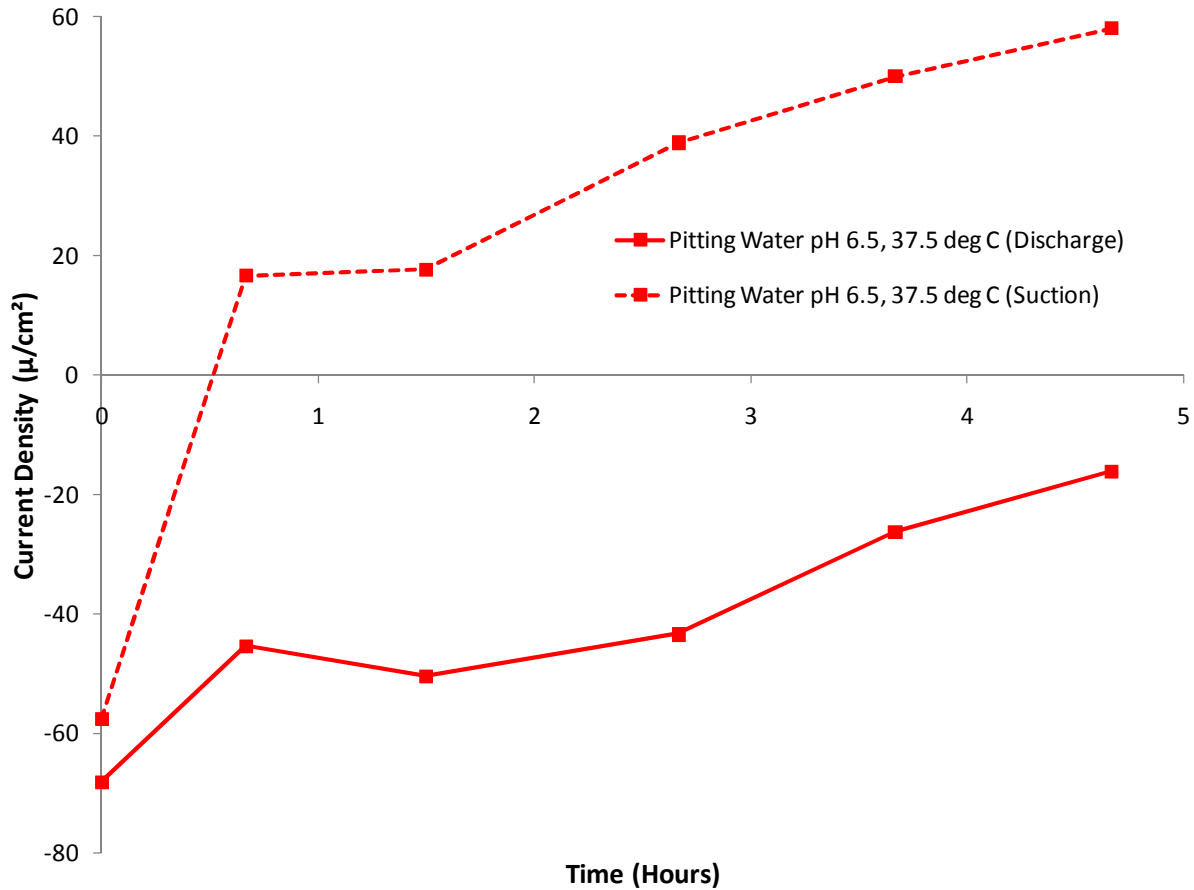


Figure 2-11: Example of Typical Data Collected with Short-term Concentration Cell Testing Apparatus

Solution temperature also affected the magnitude and sign of the currents resulting from differential flow activity of this system. Increasing temperature to 37.5° C increased the current density in the unchlorinated pitting water at both pH 6.5 and 8 (Figure 2-12). The current densities increased further (from 40 μA/cm² to 58 μA/cm² after 4.7 hours) in the pH 6.5 heated water. Even the pH 8 system had some anodic activity at the pit wire (as high as 35 μA/cm² in heated water), but after a few hours, this current density decreased to almost 10 μA/cm² and appeared to be trending towards zero, suggesting that the copper surface in this condition natural passivated to alleviate the attack.

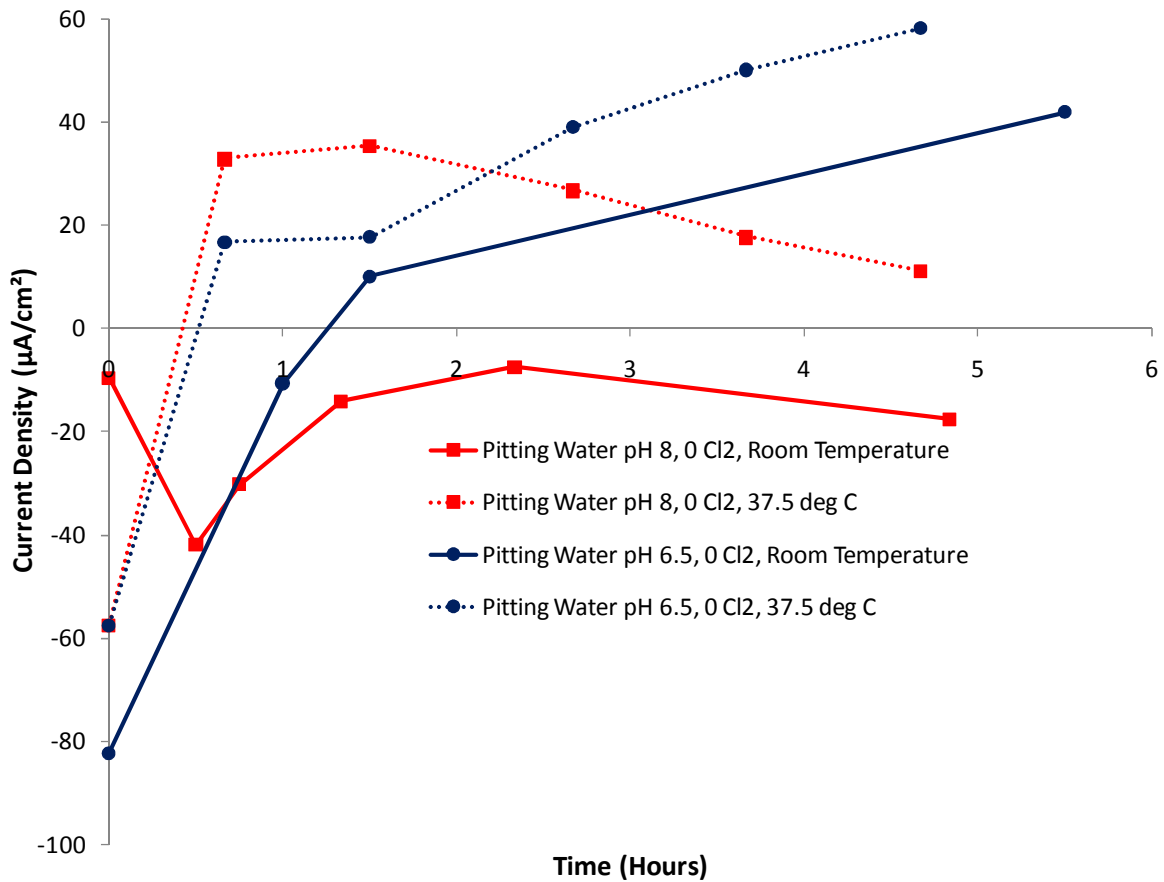


Figure 2-12: Current Density between Insulated Copper Wires Exposed to High Flow and Copper Plates in Stagnant Bulk Water

Various other water qualities were evaluated in this study using this experimental apparatus (Table 2-2 and Figure A6-A9). Water qualities with a sustained high peak current density (i.e. pitting water with 4 mg/L Cl₂ at pH 9.5) seem to confirm that the system is anodically rate limited and would be more susceptible to damage from concentration cells formed by differential flow. In this example (chlorinated pitting water at pH 9.5), based on the average current density measured over the 6 hour experiment, failure in new 3/4" Type M copper tubing would be expected in about 6 months if a scale did not form on the copper surface to reduce the rate of attack.

Table 2-2: Anodic Corrosion Peak Current Density Observed during the Short-term Concentration Cell Testing

Water Quality	Copper Wires Exposed to High Velocity	
	Peak Current Density ($\mu\text{A}/\text{cm}^2$)	% of Peak Current at end of Test ($\mu\text{A}/\text{cm}^2$)
pH 5, 4 mg/L Cl_2	72	100
pH 6.5	42	100
pH 6.5, 4 mg/L Cl_2	285	11
pH 6.5, 37.5° C	58	100
pH 6.5, 4 mg/L NH_3	33	100
pH 6.5, 2 mg/L PO_4	12	54
pH 6.5, 2 mg/L NOM	35	100
pH 8	Cathodic	-
pH 8, 4 mg/L Cl_2	9	100
pH 8, 37.5° C	35	31
pH 8, 4 mg/L NH_3	25	74
pH 8, 2 mg/L PO_4	Cathodic	-
pH 8, 2 mg/L NOM	20	87
pH 9.5, 4 mg/L Cl_2	97	90

Other water qualities, in contrast, produced only low or cathodic (negative) corrosion current densities, and there was no significant acceleration to corrosion that resulted from the differential flow (Table 2-2). Furthermore, the corrosion activity was unsustainable in some system conditions like the pitting water with 2 mg/L PO_4 at pH 6.5. In many of the tests (Table 2-2), the current had already begun to decline by the end of the test (i.e. chlorinated water at pH 6.5), indicating the system was clearly trending towards passivation and the problem would not persist.

Additions of constituents like orthophosphate, ammonia, chlorine and NOM to pitting waters had mixed results. For example, adding 2 mg/L PO_4^{3-} to water at pH 6.5 significantly decreased current density (Figure A-8), while the same adjustment to water at pH 8 had relatively little affect (Figure A-9). In the same respect, adding 2 mg/L NOM to water at pH 6.5 only slightly decreased the anodic current density (Figure A-8), while adding 2 mg/L NOM to water at pH 8 increased current densities above 0 where they remained slightly anodic (ppendix A-9).

Copper Exposed to Stagnant Water Conditions

All of the preceding data was for pit wires subjected to high velocity flow conditions. Data were also collected for insulated copper wires at the same location in the flow path but recessed from flow and therefore subjected to stagnant conditions. As expected, corrosion activity in these wires was very low (relative to the copper plates submersed in stagnant bulk water) compared to most of the wires in the high flow pattern exhibiting strongly anodic activity (Table 2-3). For example, the average current density of the wire recessed from flow for chlorinated water at pH 6.5 was only 12% of the average current density of the wire exposed to flow in the same water, proving that the exposure of the copper wire surface to the high flow drove the attack in water conducive to concentration cell attack. Of the 15 water qualities tested, only 4 conditions produced average current densities of $10 \mu\text{A}/\text{cm}^2$ or above in the recessed/stagnant-water pit wires.

Long-term Concentration Cell Tests

Since the short-term experiments confirmed that very significant concentration cells could be produced from differential flow in certain water chemistries on new copper surfaces, longer-term testing was undertaken to determine if the accelerated rate of attack could be sustained. The copper wires exposed to the high flow in the experimental apparatus were found to be either anodic or cathodic relative to the copper plate in stagnant water depending on the water quality tested (Figure 2-13, Table 2-4). For example, the copper wires exposed to high flow in the pitting water at pH 6 at room temperature and also pH 6 heated to 37.5°C exhibited positive current densities, indicating copper wires were rendered anodic relative to copper plates in the stagnant bulk water. In contrast, the copper wires exposed to flow in the pitting water with 4 mg/L Cl_2 at pH 6 and pH 8 exhibited negative current densities, indicating the copper wires were cathodic relative to plates in stagnant bulk water.

Table 2-3: Corrosion Current Density Observed during the Short-term Concentration Cell Testing (*Wire Exposed to Flow was Cathodic or less Anodic than Wire Recessed from Flow)

Water Quality	Copper Wires Recessed from Flow	
	Average Current Density ($\mu\text{A}/\text{cm}^2$)	% of Average Current Density for Inflow Wire (if Lower)
pH 5, 4 mg/L Cl_2	7	15
pH 6.5	8	*
pH 6.5, 4 mg/L Cl_2	15	11
pH 6.5, 37.5° C	9	45
pH 6.5, 4 mg/L NH_3	6	*
pH 6.5, 2 mg/L PO_4	7	*
pH 6.5, 2 mg/L NOM	0.5	*
pH 8	9	*
pH 8, 4 mg/L Cl_2	13	*
pH 8, 37.5° C	7	63
pH 8, 4 mg/L NH_3	7	*
pH 8, 2 mg/L PO_4	10	*
pH 8, 2 mg/L NOM	7	*
pH 9.5, 4 mg/L Cl_2	22	29

Chlorine, therefore, acted to reduce concentration cell corrosion in this apparatus. This was not unexpected, as free chlorine was found to dramatically reduce concentration cell corrosion in short-term tests with heated salt water (Figure 2-14). The average current density of the wire subject to flow relative to the plate in stagnant bulk water was $443 \mu\text{A}/\text{cm}^2$ in testing without chlorine, and $-722 \mu\text{A}/\text{cm}^2$ in testing with chlorine. These are very significant result since a new $\frac{3}{4}$ Type M copper pipe would be expected to fail in about a month based on the average corrosion rate without chlorine, while the pipe would be expected to passivate and form a protective layer in tests with chlorine. This result counters previous research on copper pitting, which has found that chlorine propagates a pitting effect for one particular water quality (also used a reference water in this work) and type of pitting (Marshall, 2004).

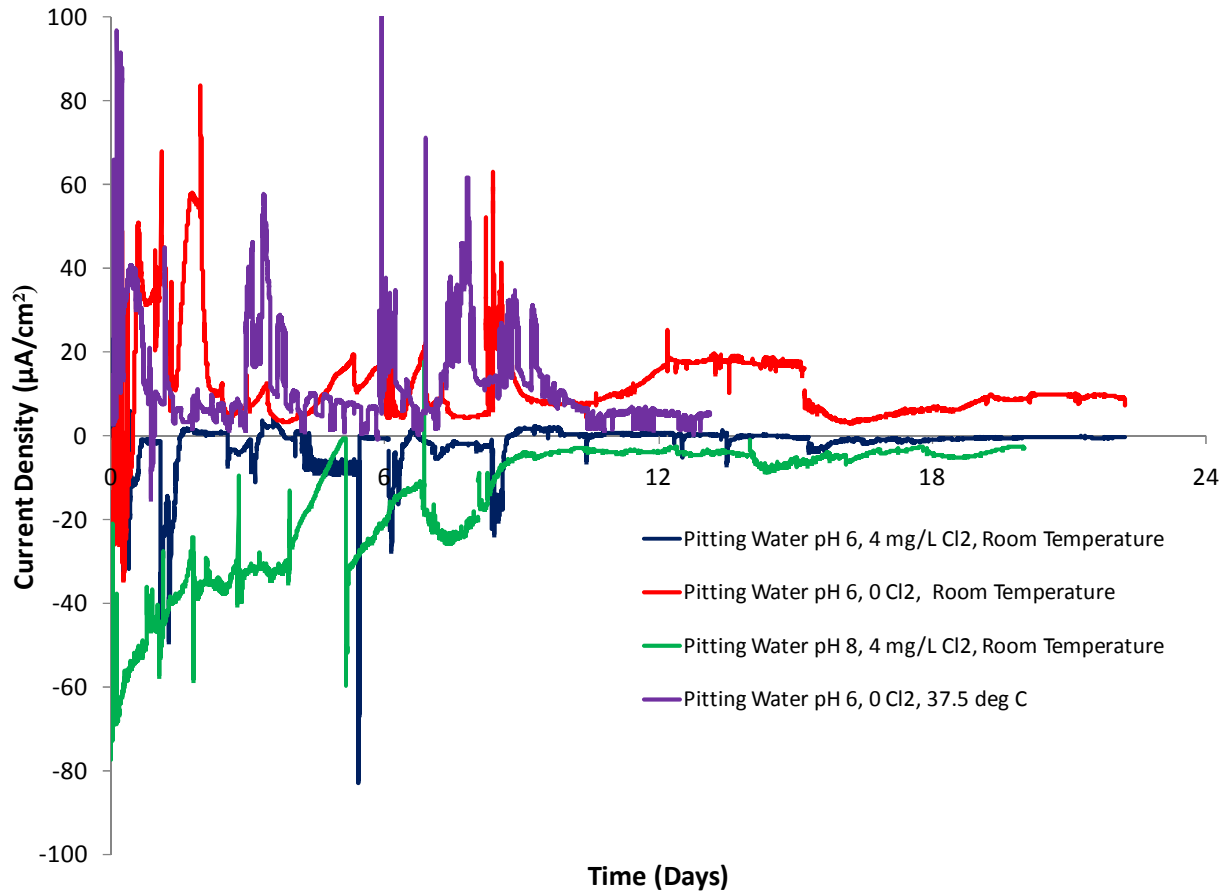


Figure 2-13: Average Current Density between Electrically Connected Insulated Copper Wires Exposed to Flow and Copper Plate in Stagnant Bulk Water in the Long-term Experimental Apparatus

Table 2-4: Average Current Density of Wires for Various Orientations as Observed in the Long-term Concentration Cell Experiment

Condition	Average Current Density ($\mu\text{A}/\text{cm}^2$)			
	Electrically Connected Wires Exposed to Flow	Electrically Connected Wires Recessed from Flow	Unelectrically Connected Wires Exposed to Flow	Unelectrically Connected Wires Recessed from Flow
pH 6 4 mg/L Cl_2	-1.75	2.18	1.73	2.84
pH 6 0 mg/L Cl_2	11.50	5.19	25.06	3.31
pH 8 4 mg/L Cl_2	-14.64	4.06	1.10	1.86
pH 6 37.5°C	11.70	4.79	9.41	2.87

Weight loss of the wires was measured through the duration of the test. After the test ended, a Dremel tool with a soft brush was used to remove any accumulated scale on wire tips. The initial expectation was for much higher weight losses to occur in wires exposed to flow in the systems with more positive (anodic) corrosion current densities; however, results tended to be inconsistent with this expectation (Figure 2-15). For instance, both of the chlorinated waters, which exhibited characteristically cathodic tendencies (negative corrosion current densities), had a greater average weight loss for electrically connected wires exposed to flow when compared to the corresponding wires in the unchlorinated pH 6 waters, which were also the most anodically active (Figures 2-13 and 2-15). Furthermore, the lower average current densities in the wires recessed from flow (Table 2-4) should have translated to less weight loss (than wires exposed to flow) or even a weight gain due to formation of a scale layer, yet the average weight loss was greater in all but one of the wires recessed from flow (Figure 2-15).

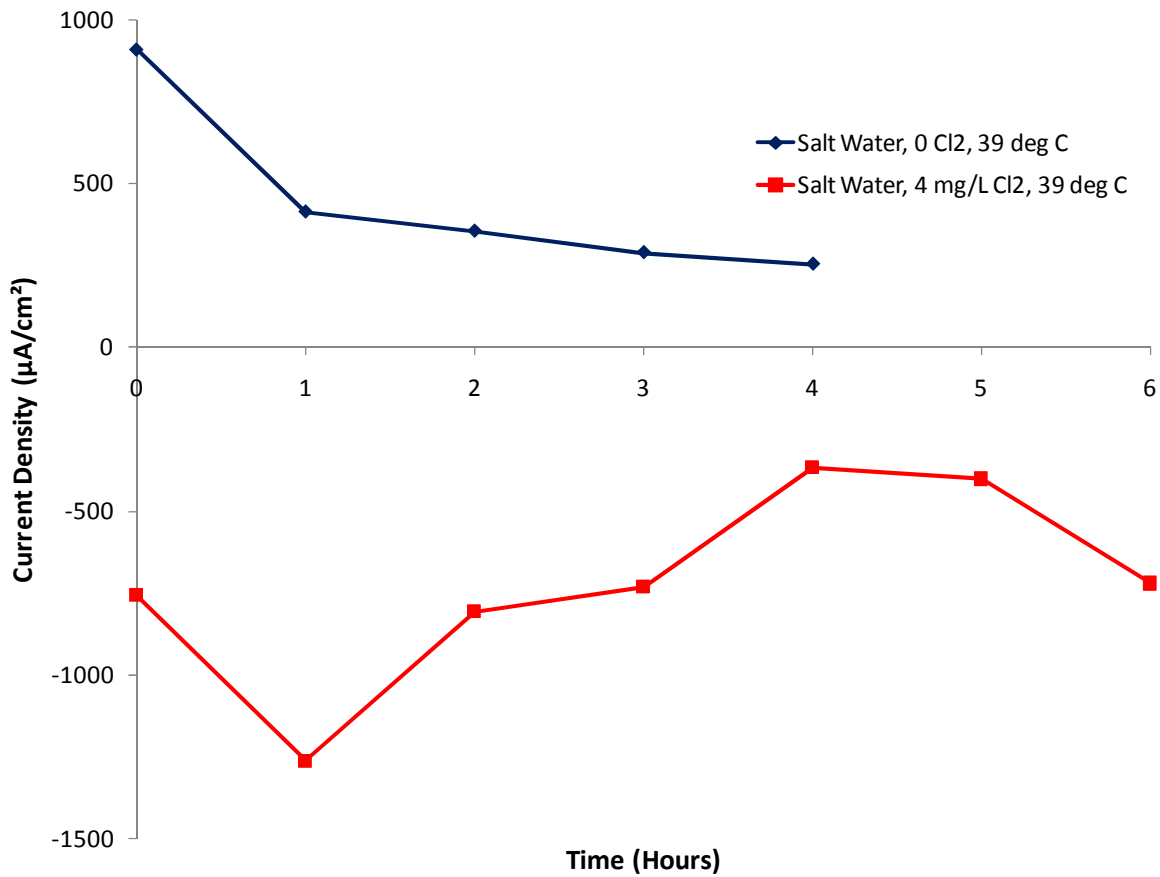


Figure 2-14: Current Density between Electrically Connected Insulated Copper Wires Exposed to Flow and Copper Plate in Stagnant Bulk Water in Heated Salt Water with and without Chlorine in Short-term Tests (Note: Corrosion Rates are from Wires are on Discharge Side of Pump)

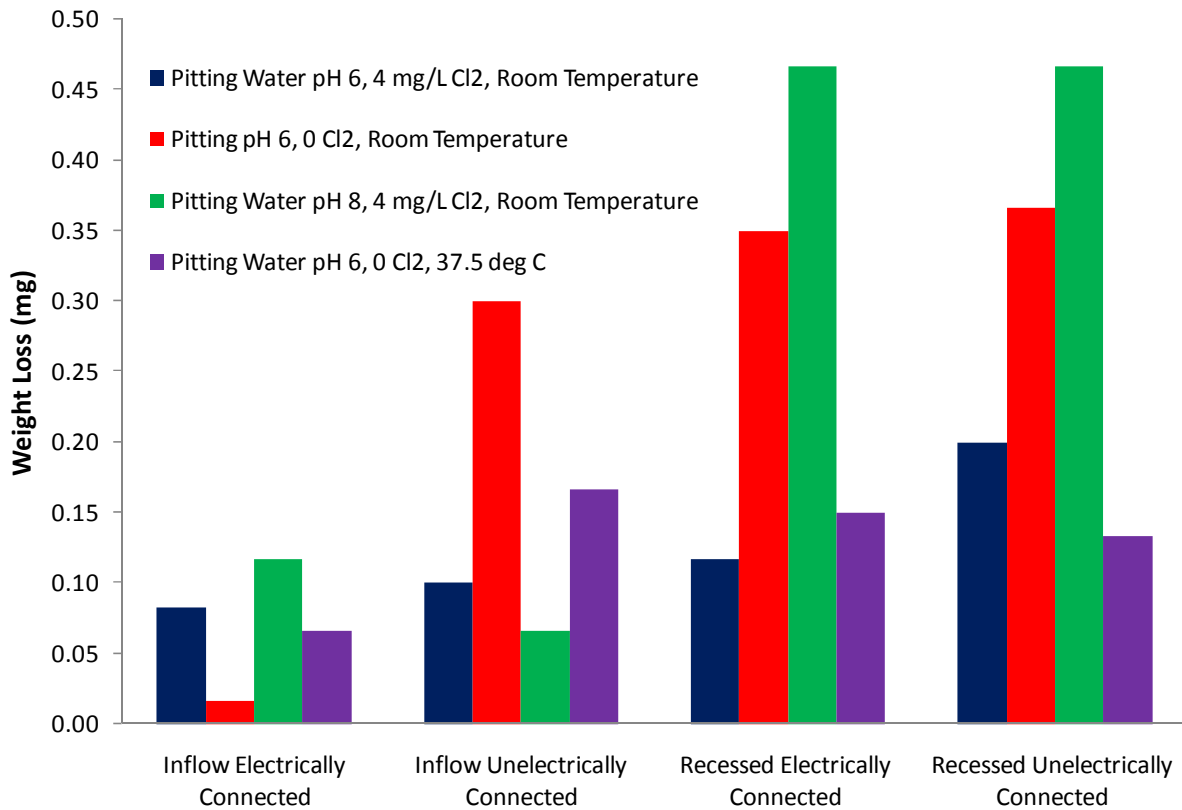


Figure 2-15: Weight Loss of Wires in Long-term Concentration Cell Experiment

It was also theorized that electrically connected wires (wires in external electrical contact to plates in stagnant bulk water) exposed to flow in water qualities exhibiting electrochemical concentration cell characteristics would have greater weight loss than the wires that were isolated, exposed to flow, but not in electrical contact with the copper plates. Currents were periodically measured on the un-electrically wires with a handheld multimeter (Table 2-4). Due to the lack of electrical contact (preventing migration of electrons from anode to cathode), the damage was by acceleration to the baseline corrosion (anodic dissolution from normal corrosion) by water flow, and not from the concentration cell corrosion between in-flow and out of flow copper produced by galvanic electrical connection. Interestingly, the average weight loss of un-electrically connected wires exposed to flow in water at pH 6 at room temperature was 18 times greater than similar wires electrically connected to the plate in stagnant bulk water (Figure 2-15). Similarly, the average weight loss of un-electrically connected wires exposed to flow in water at

pH 6 heated to 37.5° C was more than double the average weight loss for comparable electrically connected wires (Figure 2-15).

The average weight loss of electrically connected wires recessed from flow in 3 of 4 waters tested were quite similar to weight loss of un-electrically connected wires recessed from flow (Figure 2-15). These results are consistent with the fact that less concentration cell corrosion should be occurring in both the electrically connected and un-electrically connected recessed wires. Despite the consistency of the electrically and un-electrically connected wires recessed from flow, overall trends for weight loss and current density did not correlate.

There were striking visual differences for wires exposed to the different chemistries (Figure 2-16). In the chlorinated waters, more and thicker scale accumulated on wires recessed from flow than wires exposed to flow, which is consistent with the theory that rapidly moving water enhances transport of copper cations from the copper surface, preventing a protective scale from forming. All of the wires in the unchlorinated waters visually looked similar (Figure 2-16), indicating that water temperature did not influence scale formation.

Visual differences also existed among the copper plates in stagnant bulk water. For example, there were thick scale layers on the plates exposed to stagnant pitting water with 4 mg/L Cl₂ at pH 6 and 8, while there was only a thin scale layer on the copper plates exposed to stagnant unchlorinated pitting water at pH 6 room temperature and 37.5°C (Figure 2-17). These observations are consistent with the measured current density trends (Figure 2-13). Plates in the chlorinated waters were anodic relative to copper wires exposed to flow, indicating oxidation was occurring at the plate surface (based on the reaction: $\text{Cu}^0 \rightarrow \text{Cu}^{1+} + 1\text{e}^-$). The anions in the water combined with cupric ion produced at the metal surface, forming a more significant scale layer.

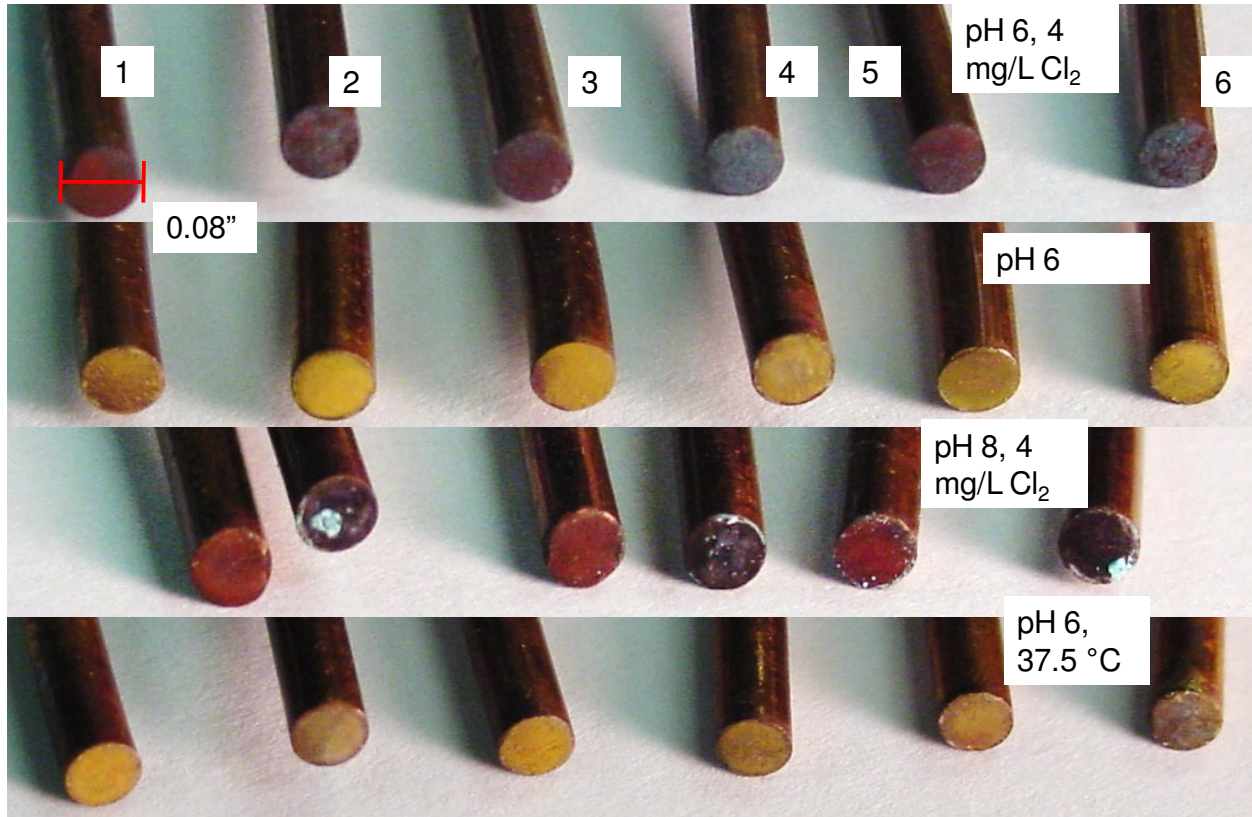


Figure 2-16: Wires used in Long-term Concentration Cell Test – Wires 1, 3 were Electrically Connected/Exposed to Flow; Wires 2,4 were Electrically Connected/ Recessed from Flow; Wire 5 was Un-electrically Connected/Exposed to Flow; Wire 6 was Un-electrically Connected/Recessed from Flow

DISCUSSION

The short-term experiments confirmed that the concentration cell flow induced corrosion mechanism is dependent on water chemistry (Figure 2-12). It was therefore expected that the extent of damage, in the form of weight loss, to the wires in the long-term would be dictated by water chemistry. Weight loss results of the long-term tests, however, were ambiguous. Specifically, weight loss data did not correlate at all to measured corrosion currents (Figure 2-13, Figure 2-15, and Figure 2-18). Furthermore, the greatest weight losses were recorded in the copper wires that were recessed in stagnant water and also for wires electrically isolated (Figure 2-15). Plus, based on experimental results, no water quality tested sustained concentration cell corrosion currents over the long-term.

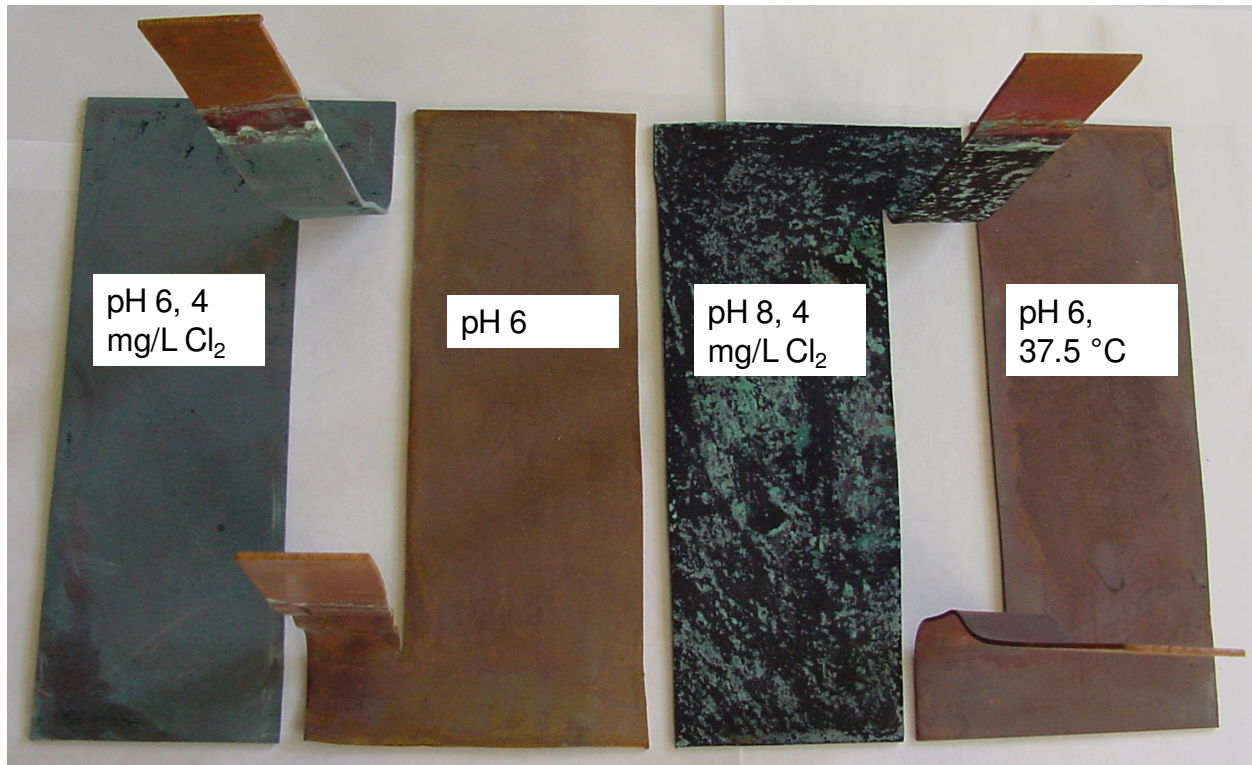


Figure 2-17: Copper Plates in Stagnant Bulk Water from Long-term Concentration Cell Tests

It was noticed during the short-term concentration cell experiment (during which a peristaltic pump was used and currents were measured on both the suction and discharge side of the pump) that the currents measured on the suction side of the pump were always greater than those measured on the discharge side of the pump (Figure 2-11). It was speculated that cavitation may be forming due to the low pressures created by the suction, and that cavitation may be imploding against the copper wires surface, influencing the current. It was clear that a study on the impact of cavitation was necessary.

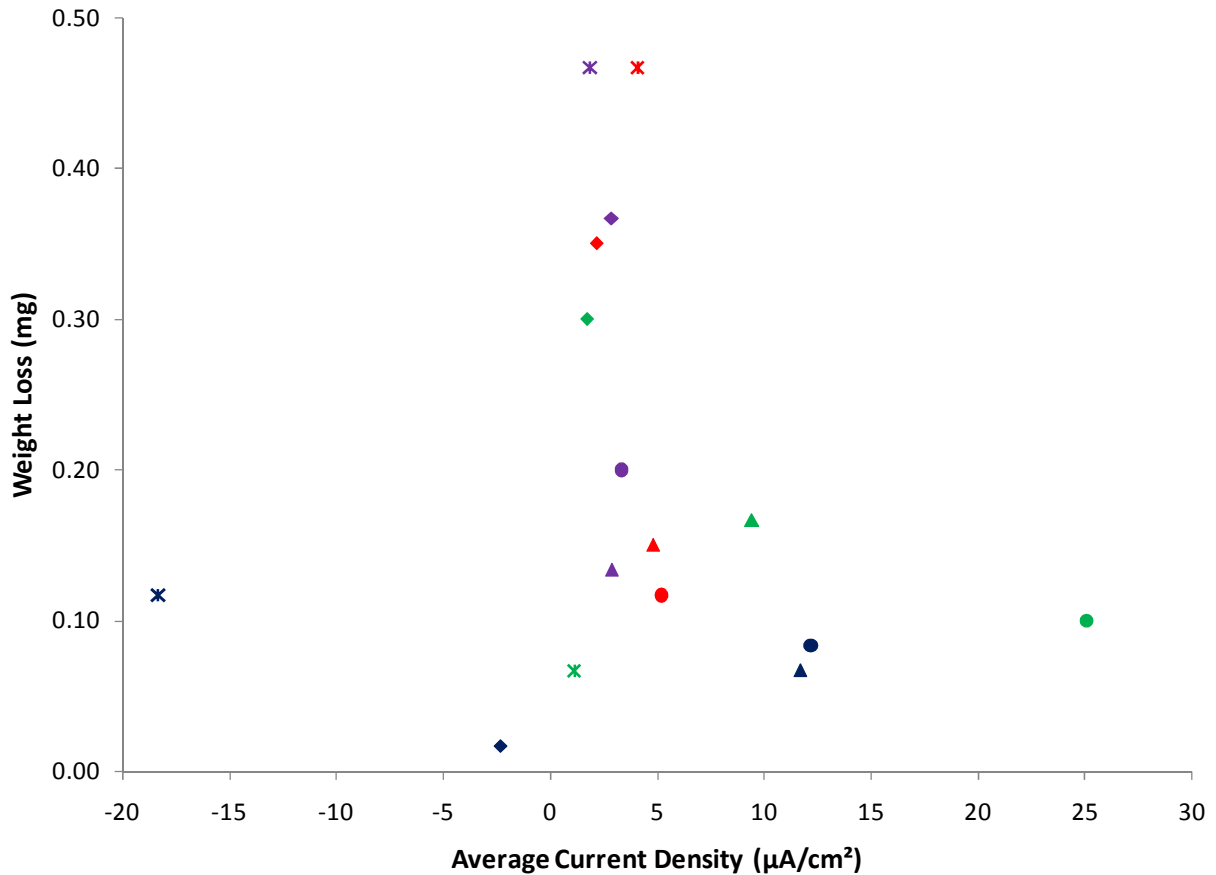


Figure 2-18: Cumulative Wire Weight Loss vs. Average Current Density for all Conditions Tested (i.e. Exposed to and Recessed from Flow, and Electrically Connected and Un-electrically Connected) in Long-term Concentration Cell Test

CONCLUSIONS

- The magnitude and sign of concentration cells induced by differential flow is dependent on water chemistry.
- In long-term concentration cell tests and in short-term testing with heated salt water, dosing at chlorine at 4 mg/L inhibited corrosion currents.
- In short-term concentration cell tests, heated water increased corrosion rate in pitting water at pH 8 and pH 6.
- Under no circumstance were high corrosion rates sustained during long-term testing.

- Weight loss values for wires were largely inconsistent with theory and currents measured.

REFERENCES

- Evans, U. R. Metallic Corrosion Passivity and Protection. London: Edwards Arnold and Co., 1937.
- Marshall, B. J. (2004). “Initiation, Propagation, and Mitigation of Aluminum and Chlorine Induced Pitting Corrosion.” Environmental Engineering. Blacksburg, Virginia. Virginia Polytechnic Institute and State University. **Masters of Science.**
- Nguyen, C., and M. Edwards. “A Novel Method to Predict Copper Pitting.” *Proceedings of the 2006 Annual AWWA Conference*. June 2006.
- Novak, Julia Ann (2005). “Cavitation and Bubble Formation in Water Distribution Systems”. Environmental Engineering. Blacksburg, VA. Virginia Polytechnic Institute and State University. **Master of Science.**
- Obrecht, M.F., and L. L. Quill. “How Temperature, Treatment, and Velocity of Potable Water Affect Corrosion of Copper and its Alloys; What is Corrosion?” *Heating, Piping and Air Conditioning*. (March, 1960f): 109-116.
- “The Copper Tube Handbook”. Copper Development Association Inc. 2006
- Wood, R. J. K., and S. A. Fry. “Corrosion of Pure Copper in Flowing Seawater Under Cavitating and Noncavitating Flow Conditions.” *Transactions of the ASME*. 112 (June, 1990).

CHAPTER 3: BENCH SCALE STUDIES ON CAVITATION IMPLOSION AND PARTICLE IMPINGEMENT AGAINST COPPER SURFACES

Jeff Coyne, Marc Edwards, and Paolo Scardina

INTRODUCTION

Damages that result from impingement of bubbles or particles against metallic pipe surfaces have long been implicated as a contributing factor to flow induced failures in premise plumbing systems. Cavitation gas bubbles in premise plumbing can be either gaseous or vaporous in nature (Novak, 2005). Gaseous cavitation occurs when the local system pressure drops below the dissolved gas saturation pressure, in which case the newly created bubbles are typically comprised primarily of atmospheric gases O₂, N₂, and CO₂. However, if the local system pressure drops below the boiling point of water, it is possible to create bubbles of water vapor (vaporous cavitation) as well as from dissolved gas. Both types of cavitation originate in pressurized premise plumbing systems only due to highly localized flow disturbances that can occur at spinning pump impeller blades, bends, obstructions, or constrictions (i.e. Figure 3-1).

Gaseous cavitation is primarily a mass transfer process involving gases (nitrogen, oxygen, carbon dioxide, water vapor, etc.) between the dissolved aquatic and gas environments (Novak, 2005). Gaseous cavitation bubbles are therefore slower to form and slower to disappear. Conceivably, a gaseous cavitation bubble impacting a surface could remove scale or cause mechanical damage, but in general, gaseous cavitation is still believed to cause relatively little damage to metals and premise plumbing systems. In contrast, vaporous cavitation can create bubbles that appear and disappear almost instantly (on the order of milliseconds) (Novak, 2005). When vaporous bubbles implode at a solid surface, an imbalance of forces causes water to follow the collapsing bubble (Figure 3-1), creating a water jet that impacts the surface with pressures as high as 400 MPa (58,000 psi) (During, 1997), which is sufficient to mechanically damage copper or brass plumbing materials (Novak, 2005).

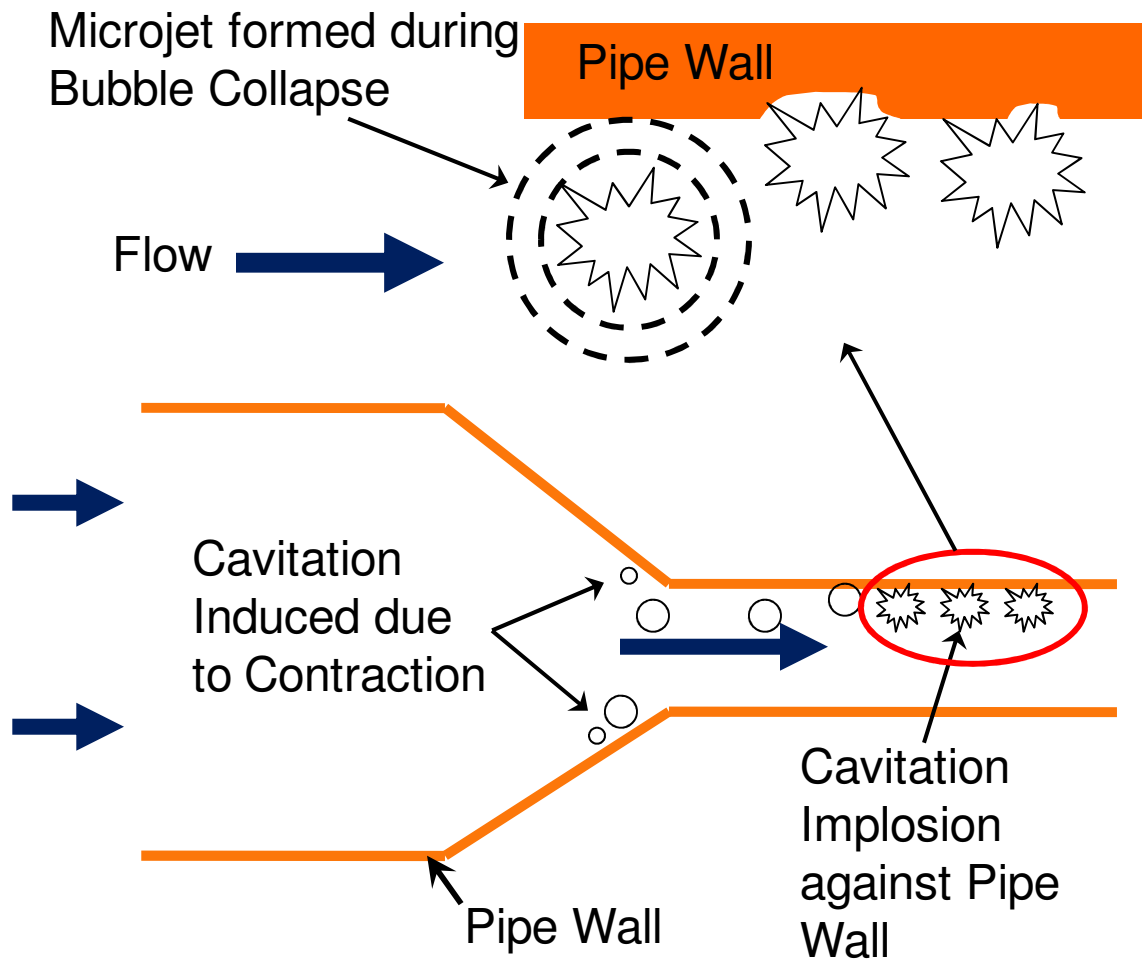


Figure 3-1: Simplified Schematic of Destructive Capability of Cavitation Bubble

Similarly, it has long been believed that particles entrained in flowing water can contribute to copper pitting failures. Based on previous research (Hutchings, 1993) and anecdotal field observations, it has been speculated that solid particles suspended in solution can impinge against and/or gouge the copper metal or induce rapid failures by preventing formation of a passivating scale layer on the pipe surface.

This work investigated flow induced failures resulting from cavitation and particle impingement. Cavitation was induced by use of an ultrasonic processor and also by constricting flow through partially closing a conventional ball valve. A separate test, described herein, investigated the propensity of suspended particles to mechanically damage pipe by jetting sand

particles (which are widely regarded as a very abrasive material) against a copper surface in a recirculating water system.

MATERIALS AND METHODS

Three different phases of experiments were conducted: 1) ultrasonically induced cavitation tests, 2) valve induced cavitation tests, and 3) particle entrained flow tests.

Ultrasonically Induced Cavitation

An ultrasonic processor was used in a previous study to induce cavitation and study resulting damages for a variety of water distribution system metals (Chan et al., 2002). A similar method was adopted in this work by using an ultrasonic processor complete with a stainless steel vibration tip (Figure 3-2). This vibration tip emits a pressure wave by vibrating the tip at 20 kHz. During the low pressure cycles, cavitation bubbles (both gaseous and vaporous) form at the tip and are easily observed in the test solution. The instrument was positioned to direct the bubbles towards copper specimens placed directly below the stainless steel vibration tip (Figure 3-2).

In the tests, flat copper specimens of various thicknesses and dimensions were sanded, cleaned, and photographed. The specimens were subjected to continuous cavitation during the tests, except for brief periods when the specimen was removed for drying, weight loss determination and taking a photo of the surface. The vibrating tip was reproducibly set 1 mm above the copper specimen and steps were taken to make sure the copper was replaced in exactly the same position relative to the tip.

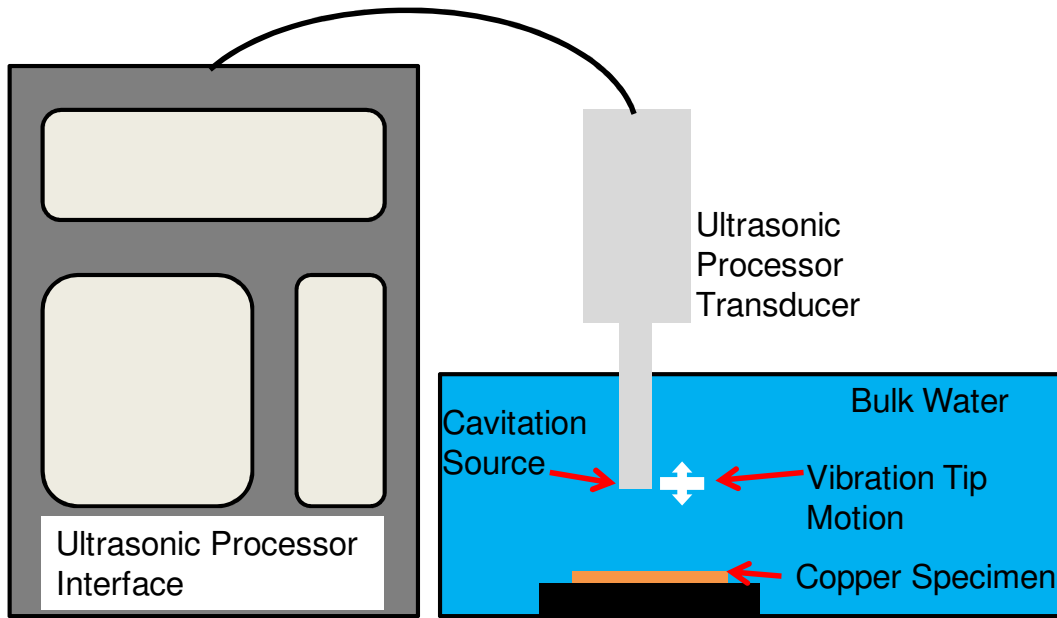


Figure 3-2: Experimental Setup of Ultrasonic Induced Cavitation Apparatus

Valve Induced Cavitation

The experiments with the ultrasonic processor *artificially* induced cavitation, and a second phase of experiments was designed to investigate cavitation damage created under more realistic conditions. Ball valves were plumbed to the local water system (Figure 3-3) and partially closed to create a range of different velocity/headloss and pressure scenarios. An upstream valve was used to create a source of cavitation bubbles that would impinge on a series of copper pipe sections that included a threaded copper adapter (A) (connected to the brass valve), a 1' length of ½" diameter copper pipe (B), and a ½" copper elbow or bend (C) (Figure 3-4).

A second downstream ball valve was used to adjust the hydraulic pressure that was in the test section (Figure 3-4). The pressure upstream from the first valve was fixed at 75 psi (+/- 3 psi) while pressure between the 2 valves was set at 15 psi, 10 psi, or 0 psi (open to the atmosphere) in the three separate tests. The general idea was that the damage resulting from implosion of gaseous or vaporous cavitation bubbles might be controlled by the pressure within the test section.

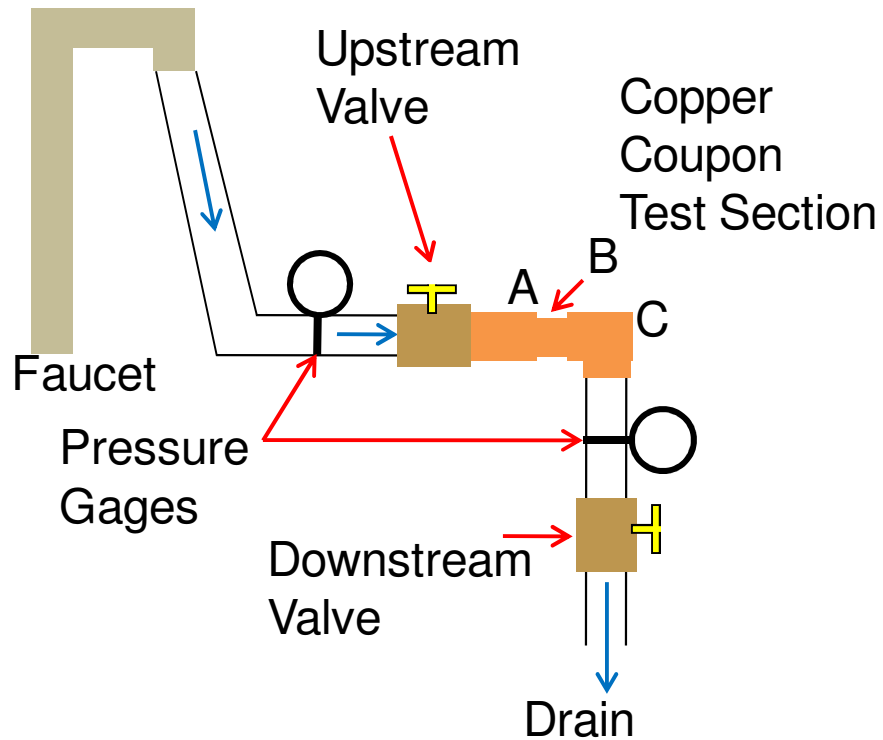


Figure 3-3: Experimental Setup of Valve Cavitation Apparatus

Copper pieces were examined prior to the start of each test. The copper was then subjected to specified flow and cavitation continuously for 3 weeks. The experiment was stopped to allow for visual examination and weighing of the samples. After the third and final week of the test, final weights were measured after gently abrading loose scale from the copper pipe surface.

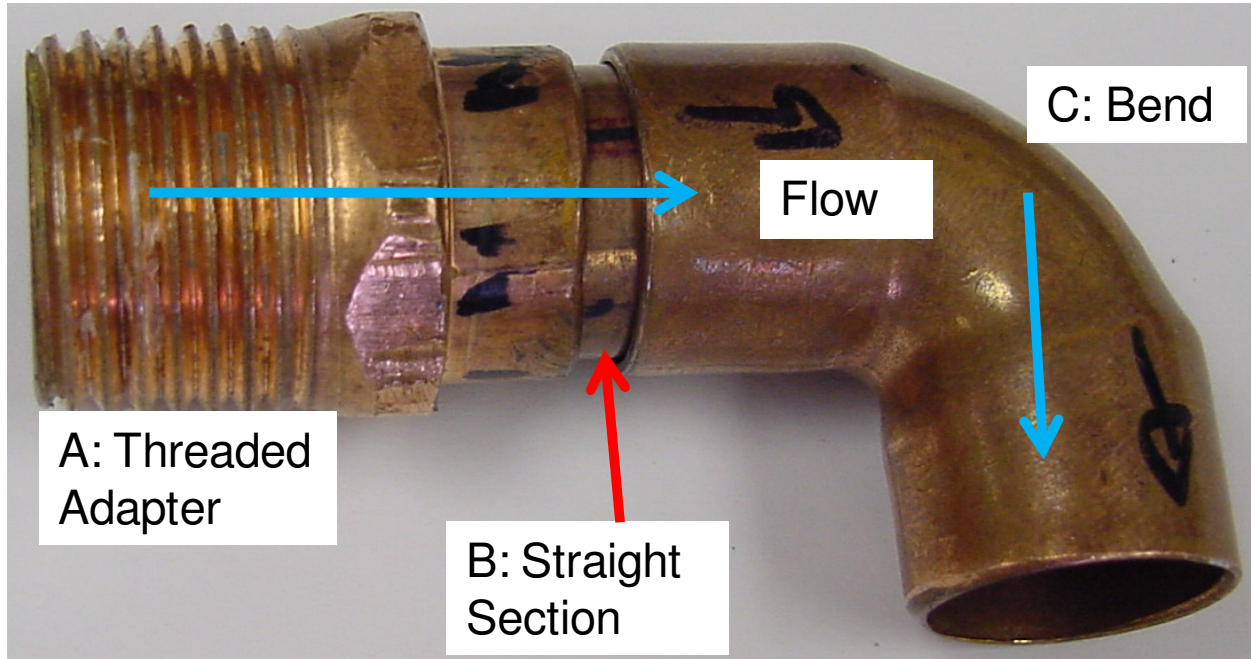


Figure 3-4: Copper Components Subjected to Flow with Cavitation

Particle Impingement

A realistic plumbing system was created to impinge particles entrained in flow against a copper surface. The system used a conventional centrifugal pump sold for use in hot water recirculation systems and ½” diameter copper pipe loop with three bends and one copper constriction (Figure 3-5). The orientation of each component was designed to try and maximize the chance of direct impacts between flowing particles and copper surfaces while replicating essential features of a real plumbing system. Brass threaded adapters were connected the pump to the copper sections. A large funnel located immediately prior to the pump was used to collect the particles at the start and during the experiment to eliminate settling during the course of the test.

A known pitting water, (Marshall, 2004) with 0 mg/L Cl_2 and no aluminum solids at pH 8 (relatively noncorrosive), flowing at an average velocity within the copper pipes of 9.5 ft/sec carried sand of various concentrations and size fractions was used during this study: the first three trials incorporated sand with a size fraction between 0.152 mm (0.006”) and 0.422 mm

(0.017”), and particles between 0.84 mm (0.033”) and 1.0 mm (0.04”) were used in the final trial (Figure 3-6). Copper pipe components were weighed and inspected before and after testing.

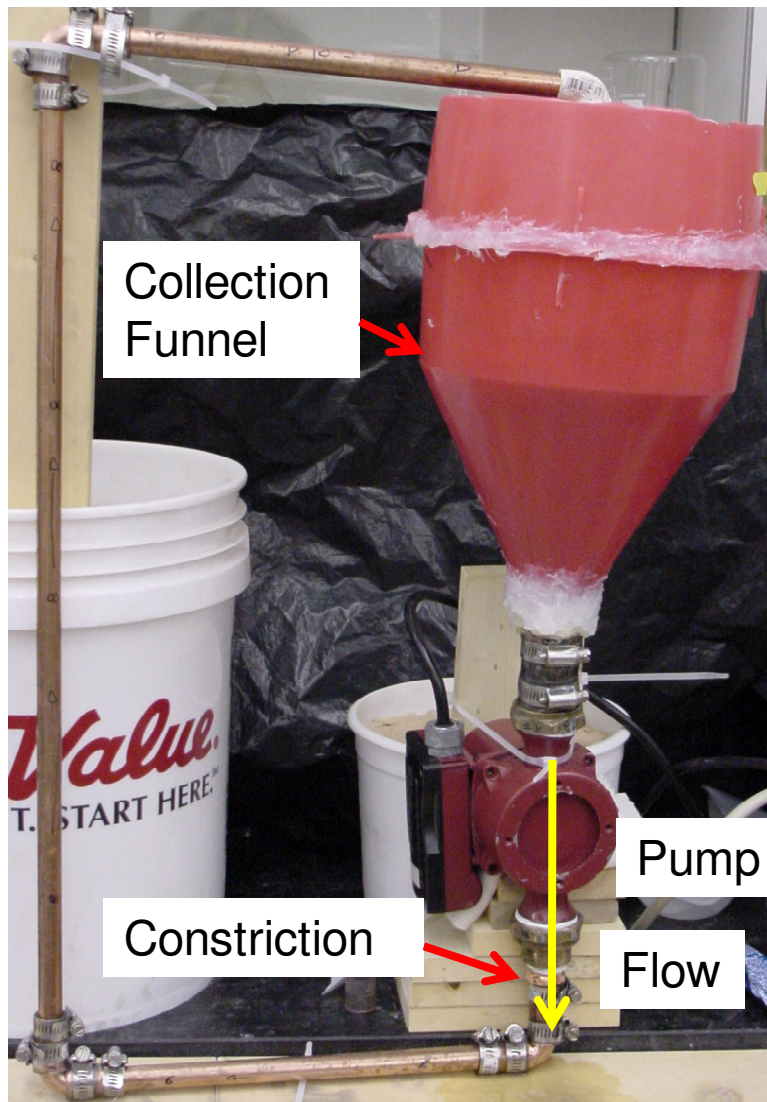


Figure 3-5: Experimental Setup of Particle Entrained Flow Rig (Trial 2)



Figure 3-6: Grain Size Comparison

RESULTS

Ultrasonically Induced Cavitation

The ultrasonic processor clearly induced cavitation bubbles which were easily visible within the solution, and copper damage commenced relatively quickly. For example, damage was visible on copper plate less than 30 minutes after starting the ultrasonic processor and subsequent cavitation (Figure 3-7). During all ultrasonically induced cavitation tests, the implosion force of the cavitation bubbles eroded small particles of copper from the specimen plate, and small chunks of copper were found settled at the bottom of the surrounding holding container.

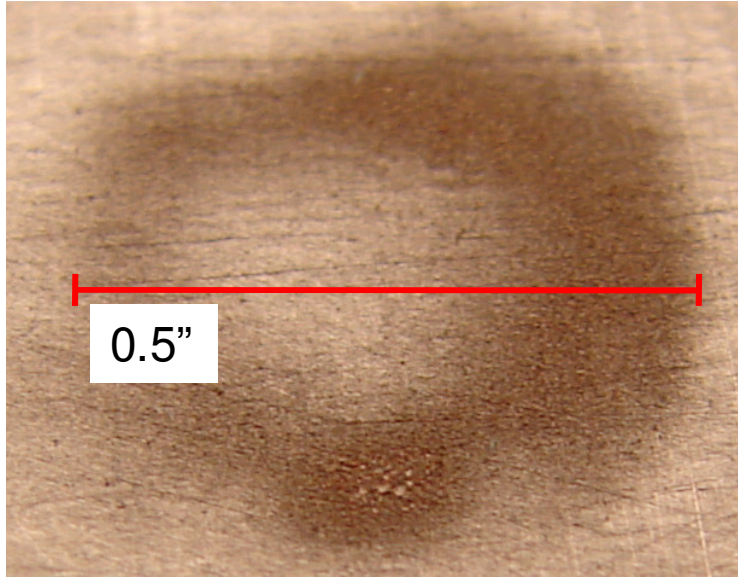


Figure 3-7: Copper Specimen after 30 Minutes of Cavitation

With continued cavitation, the copper surface became more roughened with crevices protruding into the copper (Figure 3-8) and corresponding weight loss (Figure 3-9). After 124.5 hours of continuous cavitation (using a vibration amplitude of 0.0037" or 93 μm) in unchlorinated pitting water (Marshall, 2004) at pH 6 and without aluminum solids, a hole or leak formed in the 0.032" thick copper plate along with extensive pitting within the 1/2" diameter of cavitation attack (Figure 3-8).

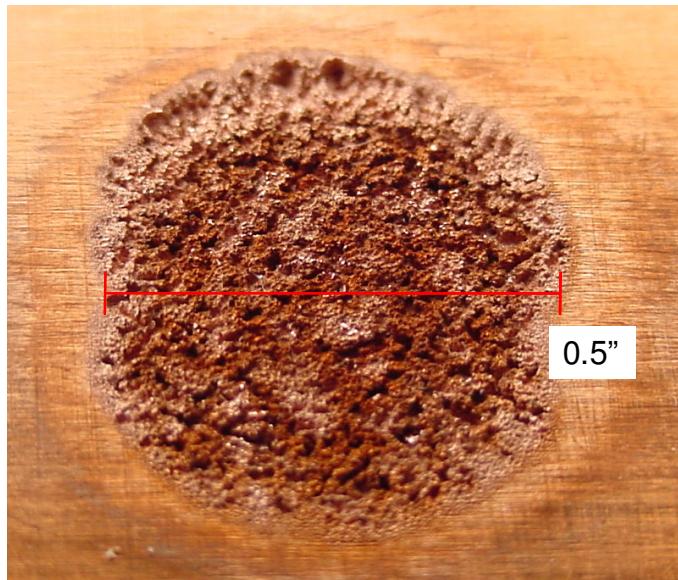


Figure 3-8: Copper Specimen (2"x2"x0.032") after 124.5 Hours of Continuous Cavitation

Surprisingly, the extent of cavitation damage seemed to lessen over time as the pits deepened, as indicated by the plateau reaching in the weight loss data (Figure 3-9). This was unexpected, since the pitted roughness of the ½" diameter damaged area was perceived to be just as susceptible to cavitation damage as freshly sanded specimens. While this might be the case in a real plumbing system with flowing water, in this modified experimental apparatus the susceptible copper surface was apparently progressively receding from the cavitation source (the vibration tip). When the vibration tip was lowered from 1 mm to 0.5 mm away from the damaged copper specimen after 94 hours, weight loss again increased, albeit at a slower rate than initially observed (Figure 3-9). These observations suggest that the rate of cavitation damage could decrease over time, since imploding bubbles might not be able to navigate down to the bottom surface as effectively.

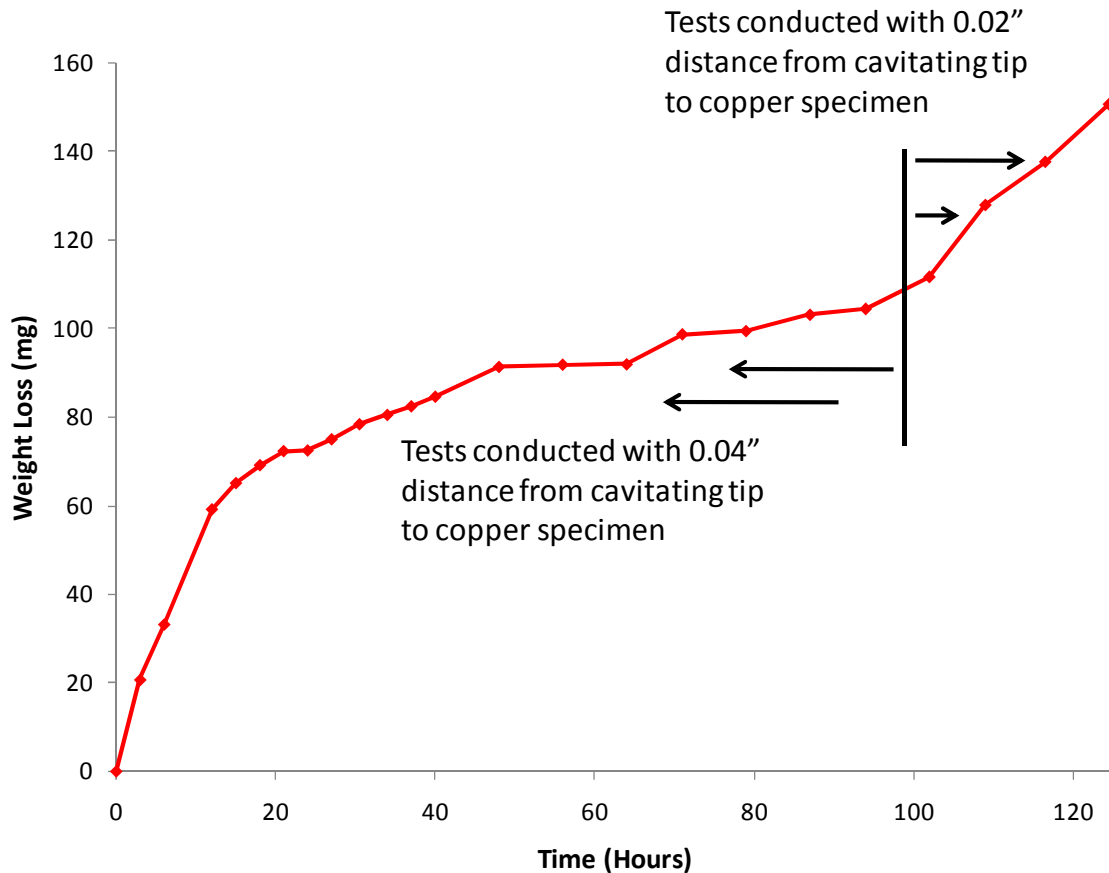


Figure 3-9: Cumulative Weight Loss of Copper Specimen (2"x2"x0.032") Subjected to 124.5 Hours of Continuous Cavitation

Given how the characteristic surface conditions appeared to influence the extent of cavitation, the ability of a corrosion scale layer to withstand or mitigate cavitation damage was also considered. Copper plates (1"x1"x0.062") were pre-exposed to a chlorinated pitting water (4 mg/L Cl₂ at pH 8) developed by Marshall (2004) to allow a representative copper corrosion scale to form (Figure 3-10). The experimental setup was similar to the previous continuous cavitation test (i.e. the vibration tip was placed 0.04" above copper specimen). Since only the effect of pre-existing scale was being investigated (not water chemistry), de-ionized water used as the bulk water. The amplitude of vibration used in this test was 0.00245" (62 μm).

According to visual evidence and specimen weight loss, the pre-existing scale layer offered no protection against cavitation damage. The scale was almost entirely removed from the copper specimen after only 2 hours, leaving bare copper metal exposed to cavitation (Figure

3-10). This was reflected by weight loss measurements as the copper plate with scale actually exhibited more weight loss after the 4 hour test than a freshly sanded copper specimen of the same dimensions subject to the same test conditions (Figure 3-11). Therefore, a scale layer was clearly ineffective protection against cavitation damage.

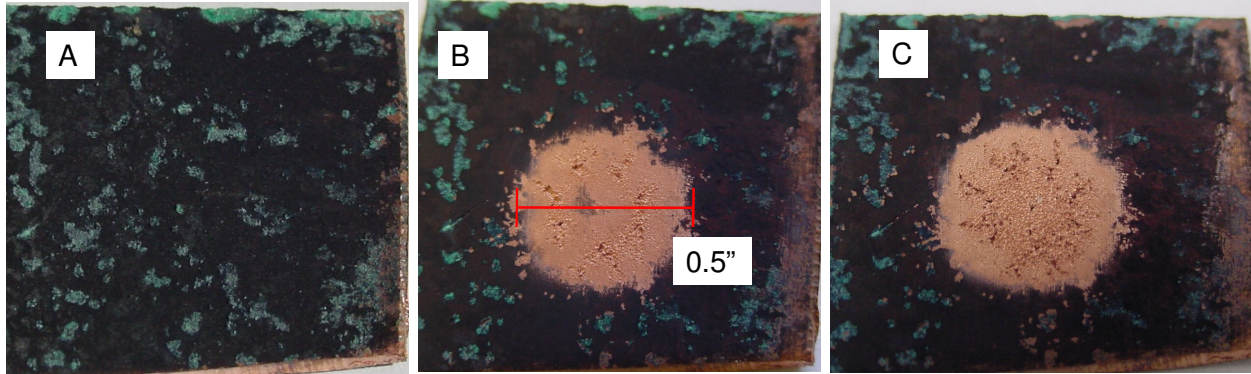


Figure 3-10: A) Initial Copper Specimen with Scale Formed in the Pitting Water with 4 mg/L Cl₂ at pH 8, B) Damage Caused after 2 Hours of Cavitation, and c) Damage Caused after 4 Hours of Cavitation

A previous cavitation study using similar methods (Chan et al., 2002) found a synergistic effect between the electrochemical attack of corrosive water and mechanical cavitation erosion. In a test designed to replicate the experiments performed by Chan et al., a variety of water chemistries were investigated including a synthesized tap water similar to that used by Chan et al. in Hong Kong (2002), a synthesized California tap water believed to be prone to flow induced failure, and the pitting water developed by Marshall (2004) with multiple variations (pHs and with corrosion inhibitors). Flat copper plate specimens, measuring about 1"x1"x0.05" were sanded, cleaned, and photographed prior to the tests. Copper specimens were tested in duplicate and subjected to 4 hours of cavitation with weight loss measurements taken at 30 minute intervals (after specimens were cleaned, dried and photographed). The vibrating tip was set at 1 mm above the copper specimen. The amplitude of vibration used in this test was 0.00245" (62 μm).

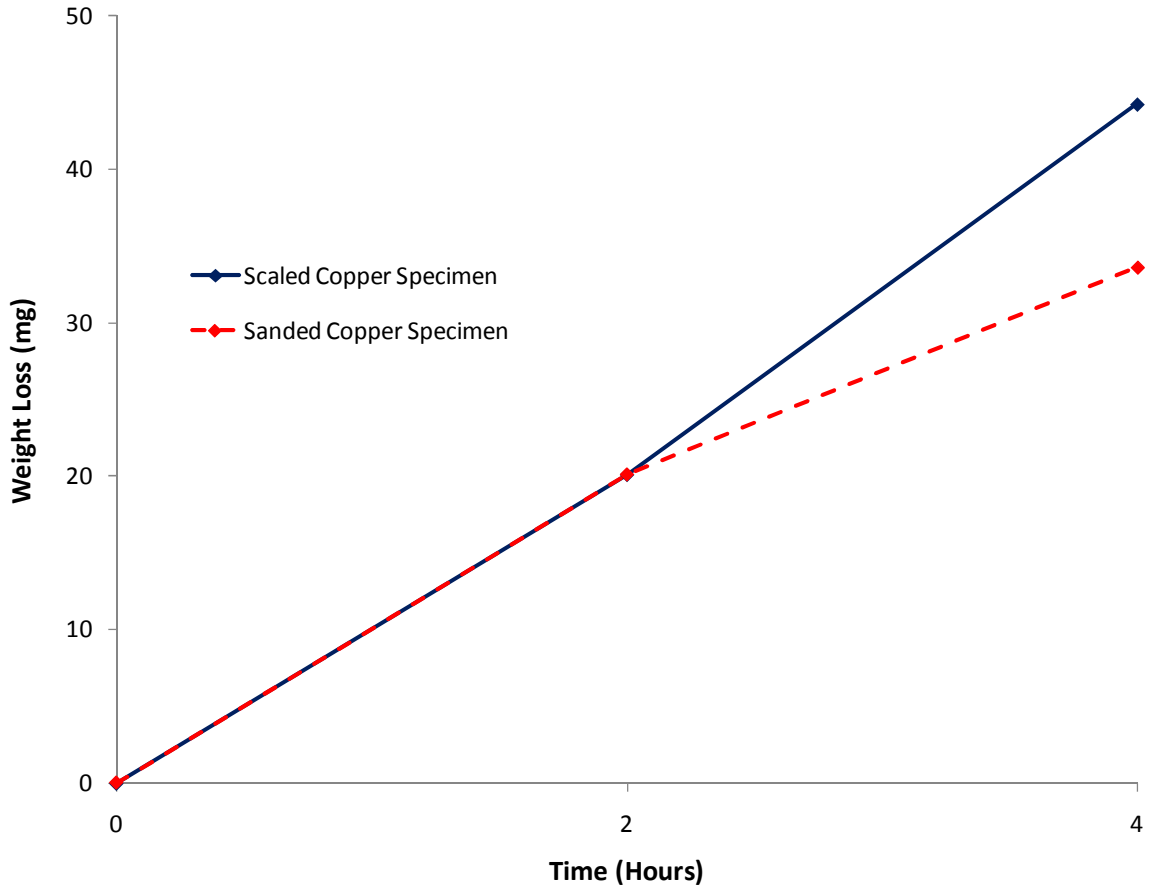


Figure 3-11: Cumulative Weight Loss of Sanded vs. Scale Covered Copper Specimen after 4 hours of Cavitation

Water chemistry seemed to have relatively little effect in altering or mitigating cavitation damage or weight loss within this experimental apparatus (Figure 3-12). Following exposure to cavitation, each copper specimen looked similar regardless of the bulk water quality. In addition to water chemistries presented in Figure 3-12, the dosing of known corrosion inhibitors phosphate (dosed at 2 mg/L PO_4^{3-} as P) and natural organic matter (NOM dosed at 2 mg/L TOC) to the known pitting water without aluminum solids at pH 6 did not dramatically reduce weight loss (Figure 3-13) when tested against the same water without inhibitors. Similarly, average penetration of copper plates does not appear to be inhibited markedly by water quality adjustments (Table 3-1).

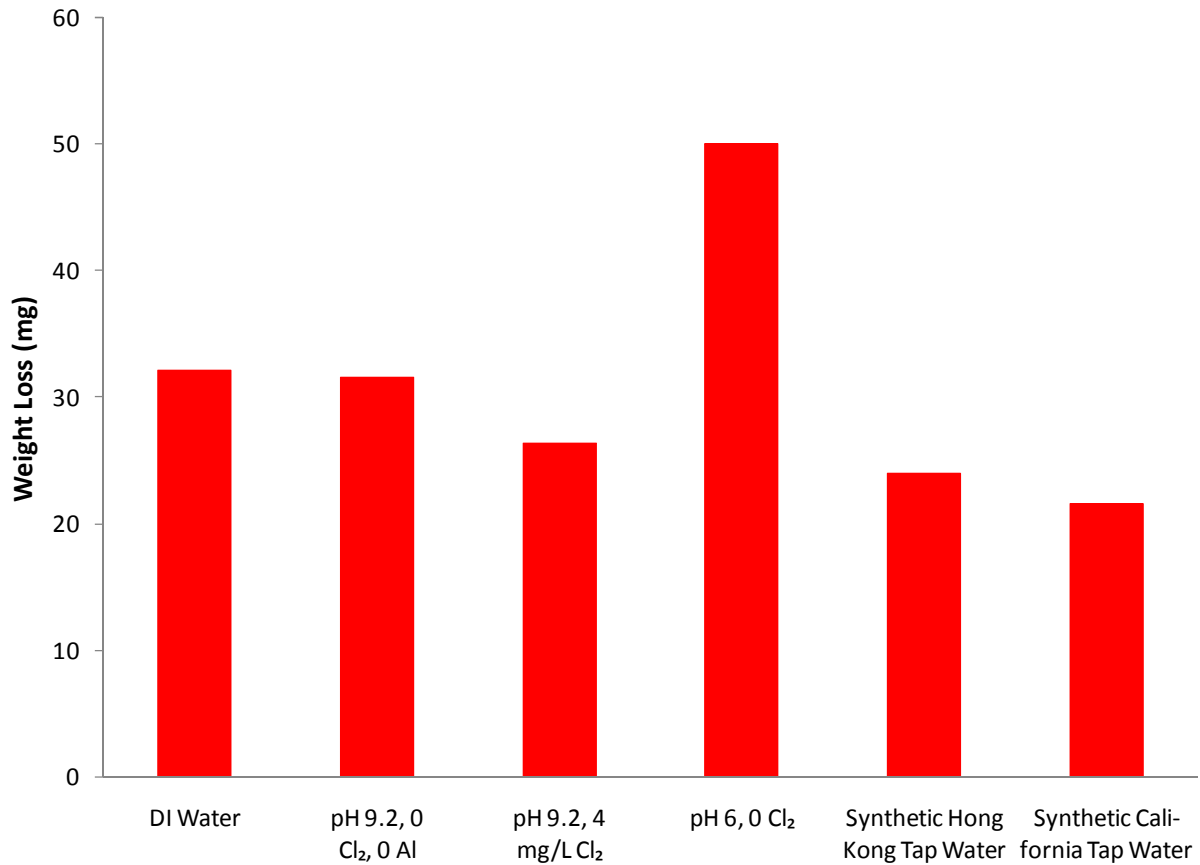


Figure 3-12: Cumulative Weight Loss of Copper Plates after 4 Hours of Cavitation under Various Water Conditions

Of the different parameters considered thus far, only the wall thickness of the copper itself appeared to markedly influence the rate of pinhole formation due to cavitation, since the extent of damage (weight loss) lessened as the pits deepened (Figure 3-9). Consequently, the relationship between different copper thicknesses were considered with respect to that time necessary for cavitation to cause a leak, with goal of determining whether a specific pipe wall thickness would greatly reduce the long-term susceptibility of failure. The set up of this experiment was identical to the continuous cavitation tests (test specimens spaced at 0.04” from the cavitation source for the duration of the test). Tests on copper plates less than 0.032” thick were performed in triplicate. Typically, holes or leaks formed in the copper plates were so small that they were only visible if a light was positioned behind the specimen, illuminating the hole against the darker copper surface (Figure 3-14).

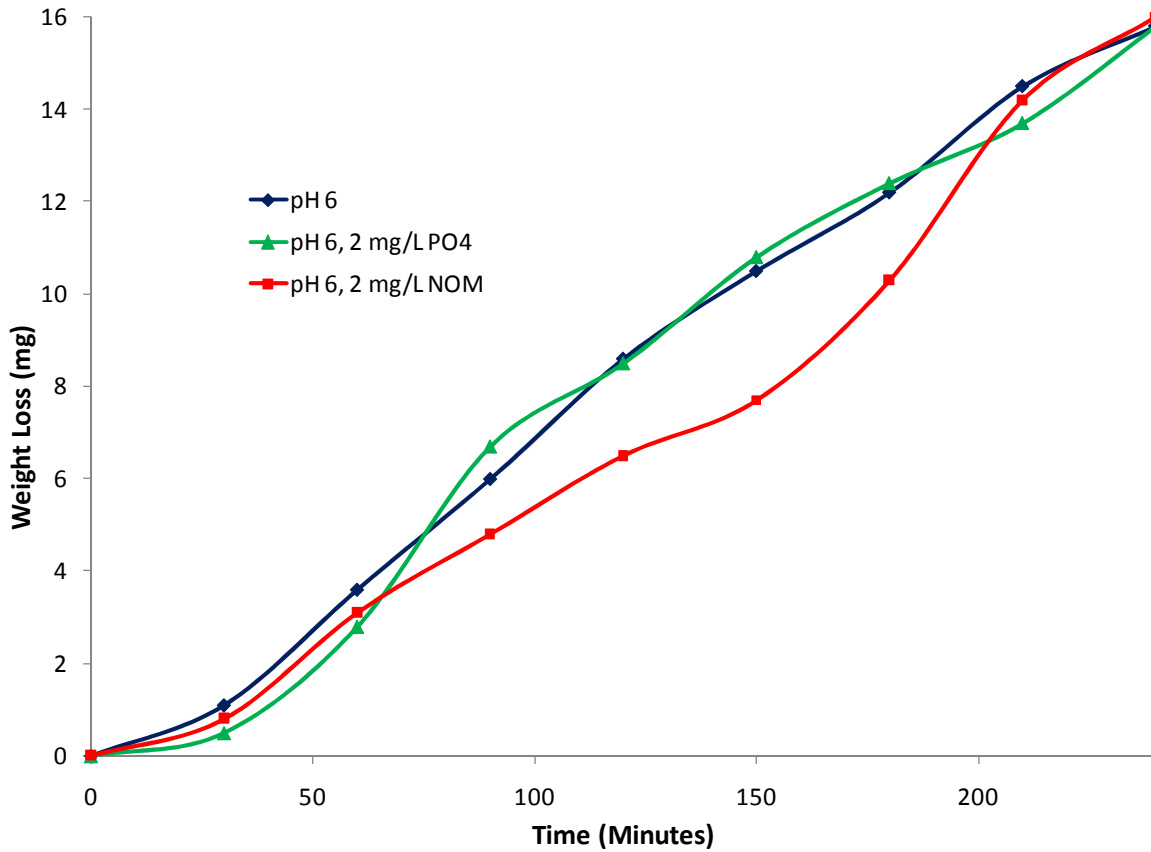
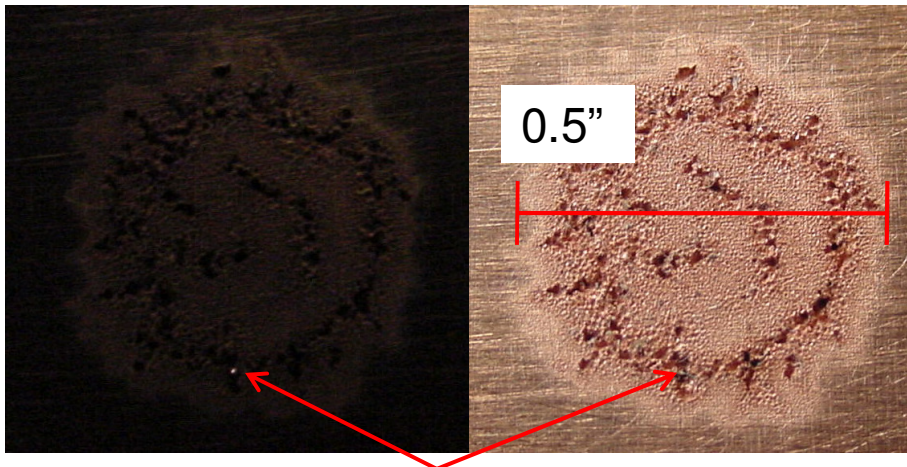


Figure 3-13: Cumulative Weight Loss of Copper Plates after 4 Hours of Cavitation using the Pitting Water at pH 6 and 2 Common Corrosion Inhibitors

An exponential relationship was found between the actual copper wall thickness penetrated and the subsequent time necessary to form a leak (Figure 3-15). As the wall thickness increased from 0.008” to 0.032”, significantly more time was required for leak formation, which is consistent with the initial observations presented in Figure 3-9. It appears that the greater the initial wall thickness of the copper pipe, the more resistant it is to failure from cavitation bubble implosion. Based on the exponential trend line fit to the data for time necessary to cause a leak vs. wall thickness, it is expected that over 4 months would be required to form a leak in new ¾” Type L copper tube (0.045” thick), and 45 years would be required to form a leak in ¾” Type K copper tube (0.065” thick) under the same experimental set up.

Table 3-1: Cumulative Penetration of Copper Plates after 4 Hours of Cavitation for various Water Qualities

Water Quality	Penetration (Inches)	% of Original Thickness
DI Water	0.0055	10.9
pH 9.2, 0 Cl ₂ , 0 Al	0.0054	10.8
pH 9.2, 4 mg/L Cl ₂	0.0066	13.1
pH 6, 0 Cl ₂	0.0054	10.8
Synthetic Hong Kong Tap Water	0.0050	10.1
Synthetic California Tap Water	0.0051	10.2
pH 6, 2 mg/L NOM	0.0042	8.3
pH 6, 2 mg/L PO ₄	0.0064	12.7



Leak Formed in Plate from Cavitation – Illuminated from behind with Flashlight

Figure 3-14: Leak Formed in 0.02” Thick Copper Plate after 6.5 hours of Cavitation

opposed to breaking. An example of this phenomenon has been observed in real plumbing samples (Figure 3-17), where cavitation attack appeared to have caused leaks, pitting, and bending of a subsequently thinned copper pipe. Cavitation clearly can dramatically affect of plumbing materials.

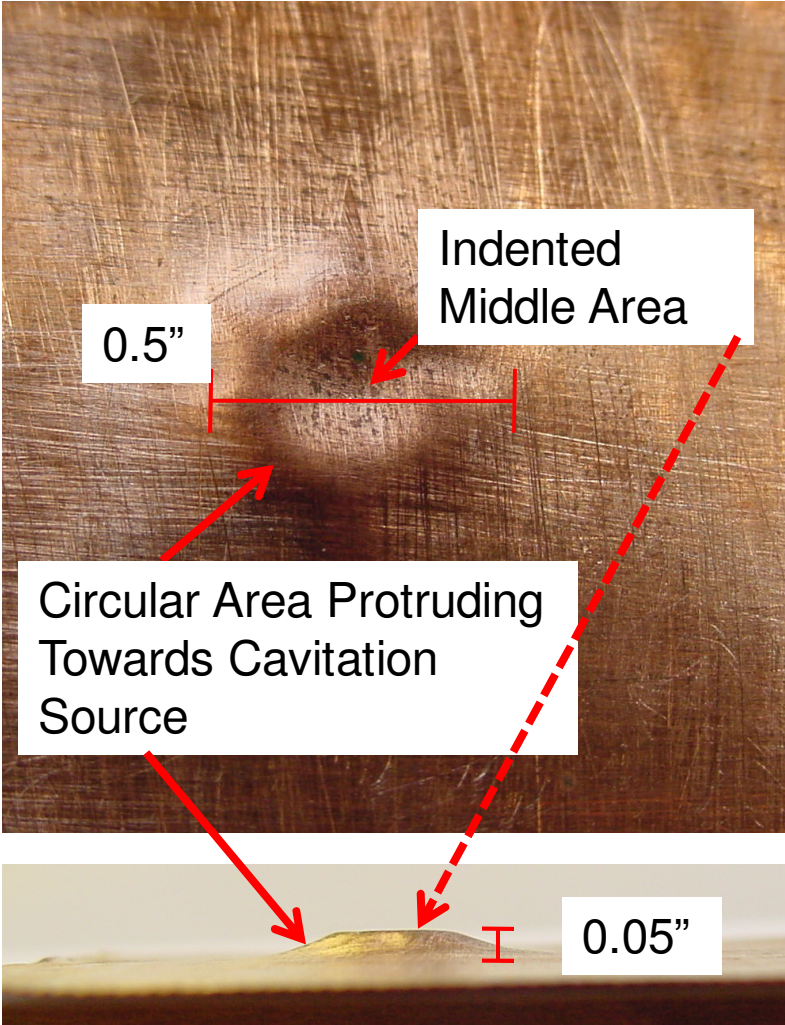


Figure 3-16: 0.004" Thick, Very Thin-walled Copper Plate after Cavitation

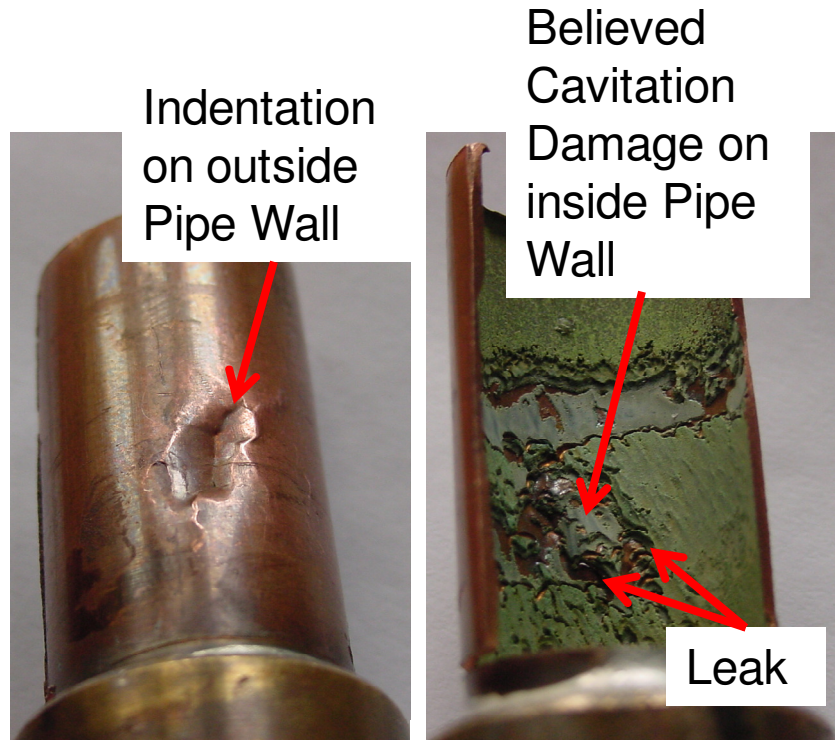


Figure 3-17: Copper Pipe from Real Plumbing System Suspected to have Failed and Flexed via Cavitation

Valve Induced Cavitation

Because such significant pitting and surface roughness resulted from ultrasonically induced cavitation tests, it was believed cavitation created in more realistic plumbing conditions would also result in copper damage. In the valve induced cavitation tests, cavitation was created by partially closing the first or upstream valve in the system, effectively reducing the diameter of the flow and increasing the fluid velocity and headloss thereby inducing cavitation. Bubble formation was clearly audible in all three tests conducted, evidenced by a screeching or constant crackling sound resonating in the upstream brass ball valve. The bubbles were also visibly entrained in the flow (through clear tubing downstream from the series of copper pipes) when the downstream pressure was set to 0 psi. When downstream pressure was set to 15 psi and 10 psi, cavitation was not visible.

Damage to the pipe did not occur as was observed in tests with the ultrasonic processor, as illustrated via visual inspections and weight loss measurements (Table 3-2). For example, at

the end of the 3 week of the test, the maximum weight loss (prior to surface film removal) in any piece was only about 1/10 of 1% of that pieces original weight (Figure 3-18). Inspection of the copper coupons after the test revealed little if any damage; there were no pits or indentations present on the internal copper surface (Figure 3-19) even after removal of a slight surface film which covered most of the inside of every coupon. The film was most likely a combination of corrosion product or scale and a thinly accumulated layer of iron or brass from the bulk solution.

Table 3-2: Cumulative Weight Loss of Copper Coupons in Valve Cavitation Damage Tests (Prior to Film Removal Film)

Experimental Component	Cumulative Weight Loss (mg)		
	75 psi, 15 psi	75 psi, 10 psi	75 psi, 0 psi
Threaded Adapter	3.9	18.4	27.2
Straight Section	3.4	6.8	4.6
Bend	1.5	6.4	7.7

After the final week of the test, coupons were weighed prior to and after film removal. It is interesting to note that the copper pipe components exposed to cavitation in the 75 psi upstream-0 psi downstream configuration had the greatest mass of accumulated scale (Figure 3-20). This is consistent with theory, which states that gaseous cavitation bubbles are more stable than vaporous bubbles and cause less damage (Novak, 2005). It is possible that the existence of vaporous cavitation bubbles in the 75 psi upstream-10 psi or 15 psi downstream tests, while not causing damage to any metal surface, prevented significant scale from forming or film from accumulating. Despite this result, overall it was not possible to reproduce cavitation damage using the practical approach attempted in this research.

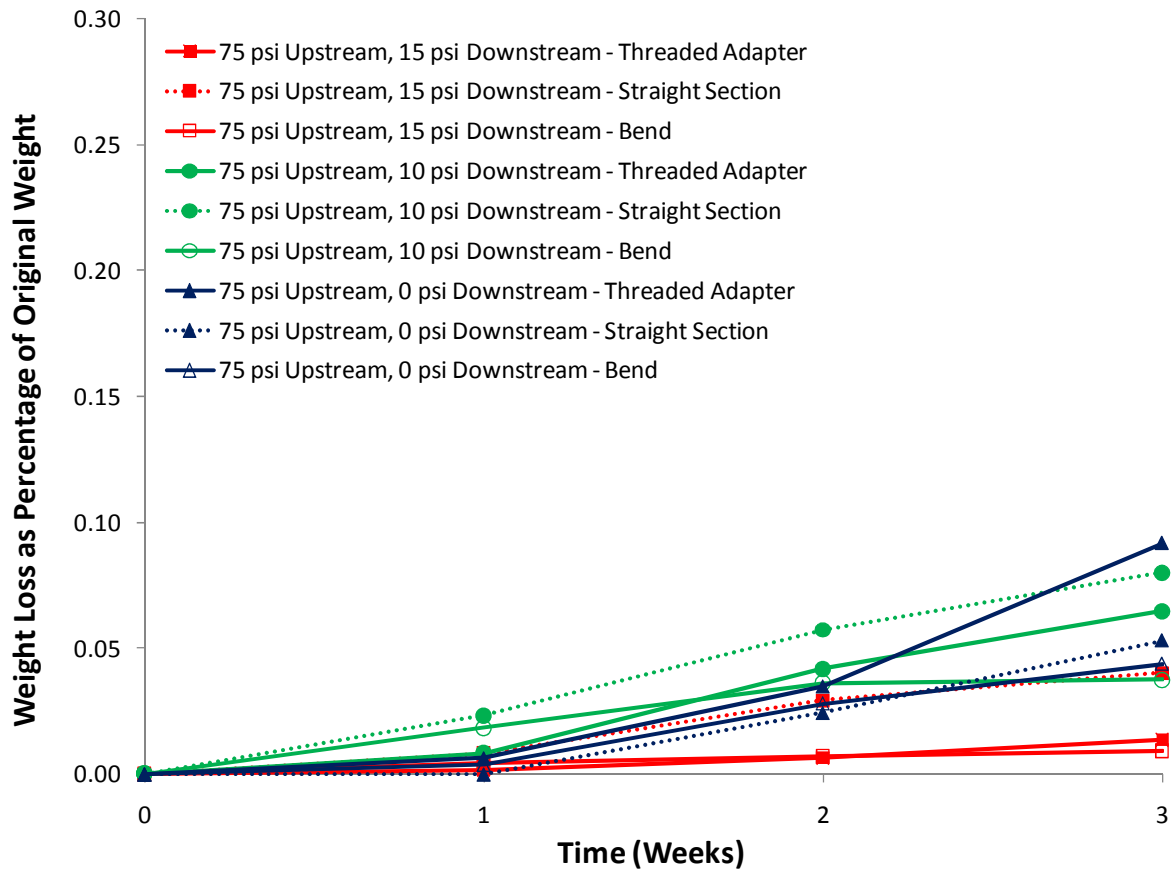


Figure 3-18: Weight Loss of Copper Components Subjected to Flow with Cavitation Prior to Film Removal

	Threaded Adapter	Straight Section	Bend
75 psi Upstream – 0 psi Downstream			
75 psi Upstream – 10 psi Downstream			
75 psi Upstream – 15 psi Downstream			

Figure 3-19: Copper Coupons used in Valve Cavitation Experiment After Film Removal (Flow Directed into the Page)

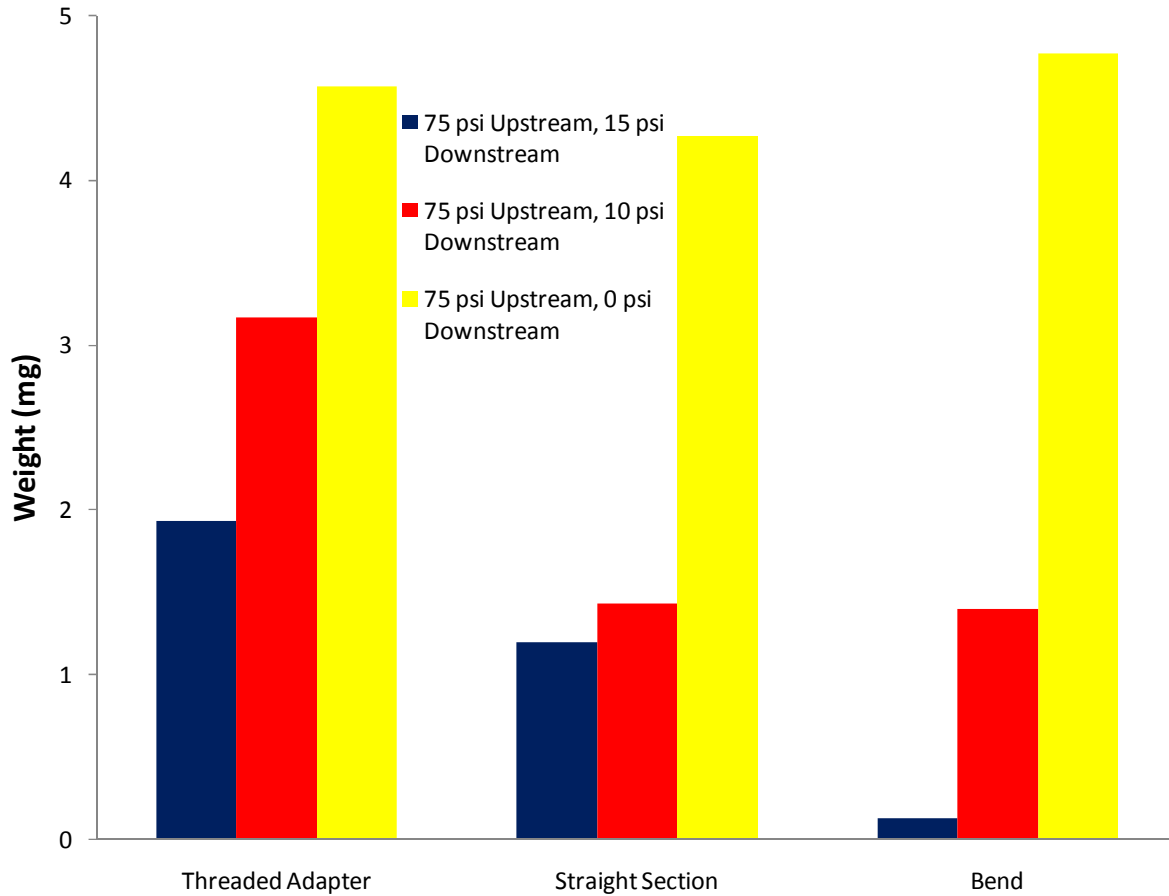


Figure 3-20: Weight of Film Accumulated on Copper Sections during Valve Induced Cavitation Test

Particle Impingement

Even though sand was initially regarded as being highly abrasive, thereby potentially damaging to copper piping by impingement, there was no significant weight loss in any component in any trial following one week on continual circulation of sand entrained in solution (Tables 3-3 and 3-4). Furthermore, an intensive visual inspection did not find any significant gouges or pits as had been expected. The copper and brass components seemed visually unaffected by the presence of the sand.

Table 3-3: Conditions of each Sand Particle Impingement Test

Trial	Duration	Sand Concentration (g sand/L water)	Sand Grain Size Range (mm)	Results
1	5 Hours	25	0.152 - 0.422	Experiment ended early due to sand pulverizing; no weight loss measurement taken
2	6 Days	6.25	0.152 - 0.422	Experiment ended early due to pump malfunction; no significant weight loss measured in copper components
3	7 Days	6.25	0.152 - 0.422	No significant weight loss in copper components
4	7 Days	5	0.84 - 1.0	No significant weight loss in copper components

Notably, the sand was fundamentally altered during these experiments. The sand eventually became pulverized and effectively destroyed, most likely by the centrifugal pump and possibly to a lesser extent by impacting the copper tubing. At the start of the experiment, the water had a yellowish-tan appearance, and individual sand grains could be identified visually flowing in the water. By the end of the week long tests, the water was black and murky in appearance, and the sand became a significantly much smaller size fraction.

The only damage from running the experiment occurred to the centrifugal pumps, which had a tendency of malfunctioning. The initial experimental design had the pump horizontal in the flow pattern, and two pumps subsequently malfunctioned before the end of the week long test. After transitioning to a vertical configuration (Figure 3-5), the pump longevity improved. As would be expected, the particles were highly disruptive to the pump, of which 2 were essentially ruined by pumping the high concentration of sand.

Table 3-4: Results of Sand Particle Impingement Tests

Premise Plumbing Component	Initial Weight (g)	Final Weight (g)	Weight Loss (mg)	% of Original
Trial 2				
Horizontal Copper Tube (9")	88	88	0	0
Vertical Copper Tube (6")	44.5	44.6	-100.00	-
Copper Elbow	16.93	17	-66.67	-
Trial 3				
Brass Union Female (a)	60.011	60.009	1.73	0.00
Brass Union Male (a)	83.277	83.233	43.33	0.05
Copper Contraction	59.179	59.164	15.10	0.03
Copper Elbow (a)	17.185	17.174	10.63	0.06
Vertical Copper Tube (12")	87.45	87.45	0.00	0.00
Vertical Copper Tube (6")	43.755	43.749	5.17	0.01
Copper Elbow (b)	16.889	16.886	2.67	0.02
Horizontal Copper Tube (12")	87.243	87.193	50.00	0.06
Brass Union Male (b)	83.05	83.05	0.00	0.00
Brass Union Female (b)	60.429	60.423	5.50	0.01
Trial 4				
Brass Union Female (a)	60.016	59.992	23.5	0.04
Brass Union Male (a)	83.208	83.126	82.4	0.10
Copper Contraction	60.196	60.148	48.2	0.08
Horizontal Copper Tube (1")	9.395	9.355	39.7	0.42
Copper Elbow (a)	16.966	16.925	40.9	0.24
Horizontal Copper Tube (12") (a)	86.975	86.896	78.4	0.09
Copper Elbow (b)	16.646	16.623	23.4	0.14
Horizontal Copper Tube (25")	181.457	181.339	117.3	0.06
Copper Elbow (c)	16.721	16.703	17.9	0.11
Horizontal Copper Tube (12") (b)	86.920	86.840	79.6	0.09
Brass Union Male (b)	83.018	82.999	18.9	0.02
Brass Union Female (b)	60.431	60.417	14.0	0.02

DISCUSSION

Constituents suspended in water such as solid particles or bubbles have long been suspected to cause damage to plumbing systems. In this work, damage only occurred when vaporous cavitation bubbles were forced to implode on a copper surface, as was observed in experiments using an ultrasonic processor to artificially induce cavitation. In follow-up tests, water was initially deaerated by first boiling it for 30 minutes and then allowing it to cool with the surface closed to the ambient atmosphere. This water, compared to other ultrasonically

induced cavitation tests, had a very low level of dissolved gas, and still exhibited approximately the same degree of cavitation. Since gaseous cavitation bubbles do not form in boiled water, this reinforces that the bubbles formed using the ultrasonic processor were due to vaporous cavitation.

When cavitation was naturally initiated in a separate experiment using a partially closed ball valve, bubbles were not always visible in all test conditions, but rather the presence of cavitation was noted by sound within the valve. In other configurations bubbles were obviously visually entrained within the flow path and swept through the pipe network. Given that the lifetime of vaporous cavitation bubbles is on the order of milliseconds (Novak, 2005), it seems likely that these bubbles were at least partly due to gaseous cavitation considering their persistence for a few seconds as the bubbles moved through the system to the drain. There was never any significant copper pipe damage observed from cavitation bubbles.

Surprisingly, particle impact or impingement also did not induce any real damage to copper surfaces. The sand was actually pulverized quickly, and the pump was ruined during the short time of the experiment due to the high concentration of sand particles - as a result these conditions are considered far worse than would ever be encountered in practice. If suspended particles do in fact cause damage to copper surfaces, it is due to an unanticipated circumstance not recreated in our experiments.

CONCLUSIONS

- Implosion of vaporous cavitation bubbles, as induced with an ultrasonic processor, significantly pitted and even penetrated copper plates with thicknesses comparable to that of copper pipes used in home plumbing systems.
- In experiments using the ultrasonic processor, an exponential trend was found between the actual copper wall thickness penetrated and the subsequent time necessary to form a leak; indicating that the greater the initial wall thickness of the copper pipe, the more resistant it is to cavitation failure.

- As surfaces became progressively damaged by cavitation implosion impinging perpendicular to the surface, the rate of cavitation damage decreased over time possibly due to surface roughness disrupting bubble implosion against the surface.
- Adjustments to water quality including additions of known corrosion inhibitors like NOM and phosphate had no mitigating effect on damage from cavitation attack
- Cavitation induced by partially closed valves did not cause significant cavitation damage to downstream copper components.
- Particle entrained flow was not able to induce significant damage to copper tube surfaces.

REFERENCES

During, E. D. D. Corrosion Atlas. Amsterdam, The Netherlands: Elsevier Science, 1997.

Chan, W.M., F.T. Cheng, and W.K. Chow. “Susceptibility of Materials to Cavitation Erosion in Hong Kong.” *Journal of the American Water Works Association*. 94.8 (2002):76-84.

Hutchings, Ian M. “Monograph on the Erosion of Materials by Solid Particle Impact.” *Materials Technology Institute of the Chemical Process Industries*. 10 (1983).

Novak, Julia Ann (2005). “Cavitation and Bubble Formation in Water Distribution Systems”. Environmental Engineering. Blacksburg, VA. Virginia Polytechnic Institute and State University. **Master of Science**.

Marshall, B. J. (2004). “Initiation, Propagation, and Mitigation of Aluminum and Chlorine Induced Pitting Corrosion.” Environmental Engineering. Blacksburg, Virginia. Virginia Polytechnic Institute and State University. **Masters of Science**.

CHAPTER 4: BENCH SCALE STUDIES ON COMBINED FLOW INDUCED FAILURE MECHANISMS

Jeff Coyne, Marc Edwards, and Paolo Scardina

INTRODUCTION

The conventional wisdom is that flow-induced failures of copper pipe can be caused by a variety of phenomena that include gaseous and vaporous cavitation, particle impingement, concentration cell corrosion, liquid impingement, and electrification. However, when tested in isolation, vaporous cavitation was the only mechanism that caused significant damage (in the form of pitting and weight loss of a copper test coupon) and pipe failure (in the form of fully penetrated copper test coupons). This analysis suggests that the other flow induced failure mechanisms studied must act in conjunction with other factors, if they are to cause significant damage to copper tubing in premise plumbing.

Two studies on combined phenomena were devised to examine the possible effect of combined flow induced failure mechanisms. The first study examined the combined effect of cavitation, high velocity water impingement and concentration cell corrosion by subjecting copper specimens to water jets. The second study examined the combined effect of cavitation and concentration cell corrosion in tests referred to as *cycled cavitation*. This was accomplished by using the ultrasonic processor to induce cavitation bubble implosion against insulated copper wires for a brief period of time, and then examining the corrosion of the cleaned surface after stagnation.

METHODS AND MATERIALS

Two will be described: 1) tests examining high velocity jets, and 2) cycled cavitation tests.

High Velocity Jet Tests

Bengough and May (1924) found that high velocity jets (17.5 ft/sec) moving longitudinally across a submersed copper plate prevented a passivating scale from forming, allowing damage to occur by increasing the corrosion rate. Penetration on the order of 0.002”

over two weeks occurred (Bengough and May, 1924). It was believed at the time that jets mechanically eroded scale and created anodic areas at water impingement sites (relative to copper exposed to stagnant water). According to the interpretation of this work (Part 1), the damaging action of the jets could have been a combination of high velocity impingement (causing detachment of loosely adhered scale at a small part of the surface), cavitation (mechanically eroding copper metal and scale), and a concentration cell (created by the electrochemical imbalance between the small surface area subject to high velocity and a larger cathode area subject to lower velocity).

Cavitation is believed to have been a factor in the damage to the copper plates observed by Bengough and May, because they stated that “the lower layers of scale contained small amounts of disintegrated particles of metallic copper...” (1924, page 134). In cavitation tests described in this paper (with the ultrasonic processor), small chunks of metallic copper were eroded from copper specimens and collected at the bottom of the reservoir container, and no pieces of metallic copper were ever detached by liquid impingement alone. To further investigate the damaging effect of high velocity jets on copper plates, experiments using longitudinal and perpendicular jets were devised.

The general approach and setup of the high velocity jet experiments replicated that of Bengough and May (1924). Experiments were performed with jets which caused high velocity water to impinge against separate copper specimens both perpendicularly and longitudinally while submersed in the same bulk water (Figure 4-1). Centrifugal pumps circulated the 50 L bulk water volume in a closed loop, transporting water through modified pipette tips, which increased the velocity of water forming a “jet” effect, before impinging along or against copper plates.

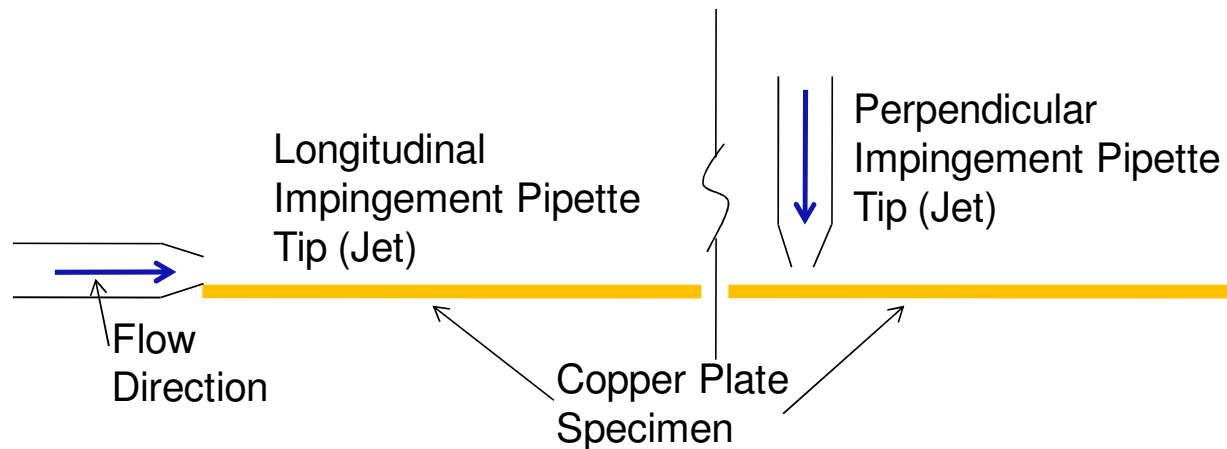


Figure 4-1: Simplified Schematic of Experimental Setup of Jet Tests

One experimental setup allowed for duplicate testing of perpendicular and longitudinal jets. Copper specimens, which measured about 4"x4"x0.062", were sanded prior to each test to eliminate possible influence of any existing corrosion scale. Each copper specimen was photographed, weighed, and measured for thickness (with a point micrometer) throughout the experiment. Pipette tips were modified to have a uniform jet diameter of 0.11" at the tip exit, which created a velocity of 17.5 ft/sec (+/- 1 ft/sec). In the longitudinal test, jet tips were oriented to allow for parallel flow over the flat copper plate surface (Figure 4-1). In the perpendicular test (Figure 4-1), jet tips were placed about 0.012" (3 mm) above the copper plate surface. Pipette tips were connected inline to recirculating pumps through various tubing sizes, adapters, and ½" PVC pipes and elbows (Figure 4-2). A PVC cross or tee was installed downstream from the recirculating pump. Two branches of the PVC tee led to the duplicate pipette jets (either longitudinal or perpendicular), while the other led to a flow/velocity regulation valve which also discharged into the bulk water. Because of the hydraulics of the system, creating significant head loss due to the small diameter of the jet tips, slight and periodic gaseous cavitation arising in the pump was unavoidable.

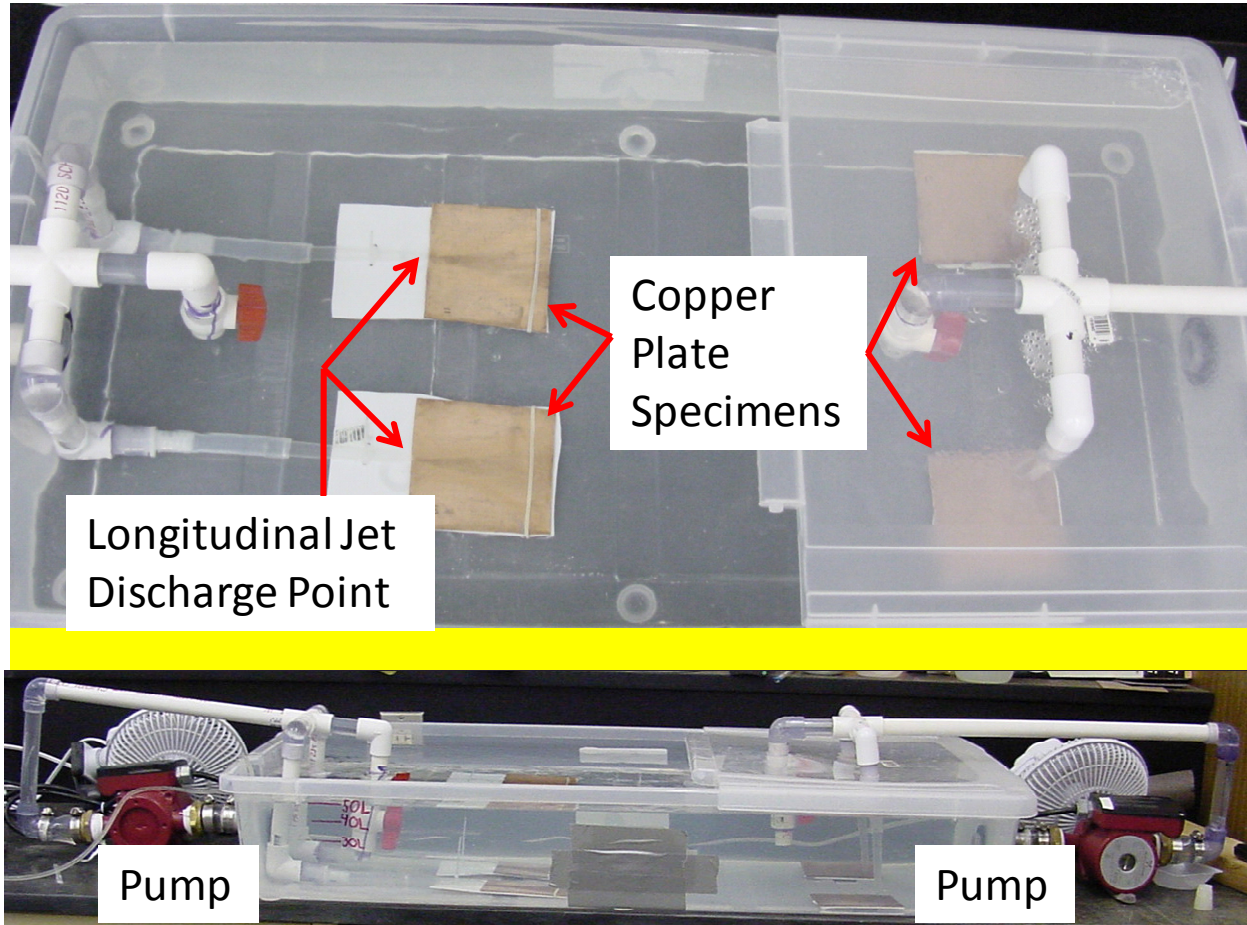


Figure 4-2: Experimental Setup of Jet Testing Apparatus

Multiple water qualities were tested including heated salt water, which was previously identified as causing jet impingement damage to copper plates (Bengough and May, 1924). The salt water was synthesized using a powdered Instant Ocean Sea Salt mix. An electrical submersible heater was used to maintain temperature (39°C ($\pm 2^{\circ}\text{C}$)). Other waters tested include the water known to cause copper pitting (Marshall, 2004) at room temperature, pH 8 and with 4 mg/L Cl_2 , and at pH 6 heated to 39°C ($\pm 2^{\circ}\text{C}$). Aluminum solids were not added to experimental waters because of findings from ultrasonic cavitation tests deeming them insignificant to flow induced failure. De-ionized water was periodically added to the bulk waters to make up for evaporation losses. At weekly intervals, tests were stopped briefly to empty and refill testing containers with fresh experimental water.

In addition to testing flat copper plates (free of flow obstruction), plates with a copper joint edge (simulating an edge formed by a copper elbow connection) (Figure B-1) and a plastic surface blockage (simulating a deposit or a tubercle on the inner copper pipe wall) (Figure B-2) were tested with longitudinal jets in heated salt water. It was theorized that a flow obstruction like a joint edge or a surface blockage would create localized turbulence therefore increasing damage (Landrum, 1990).

Cycled Cavitation

Similar to the ultrasonically induced cavitation tests described previously, a sleeved copper wire (Figure 4-3) was exposed to cavitation emitted from the ultrasonic processor vibration tip. This wire was electrically connected to a large copper sheet, which allowed for a free flow of electrons between wires and plates or vice versa. The Gamry multiplexer was positioned in series between the wire and copper sheet to collect continuous real time electrochemical corrosion currents.

In contrast to the cavitation experiments with the copper plates, the cavitation was cycled similar to what might occur in a real system with on/off flow patterns. Two wires (sanded prior to tests) were positioned directly under the vibration tip and subjected to cavitation episodes that lasted various lengths of time, while two other sanded and sleeved wires were located elsewhere in the holding container at stagnant water conditions (never subjected to cavitation). All wires were electrically routed through the Gamry ECM-8 multiplexer in a zero resistance ammeter mode and connected to their own individual copper sheet submerged in the bulk water at stagnant conditions.

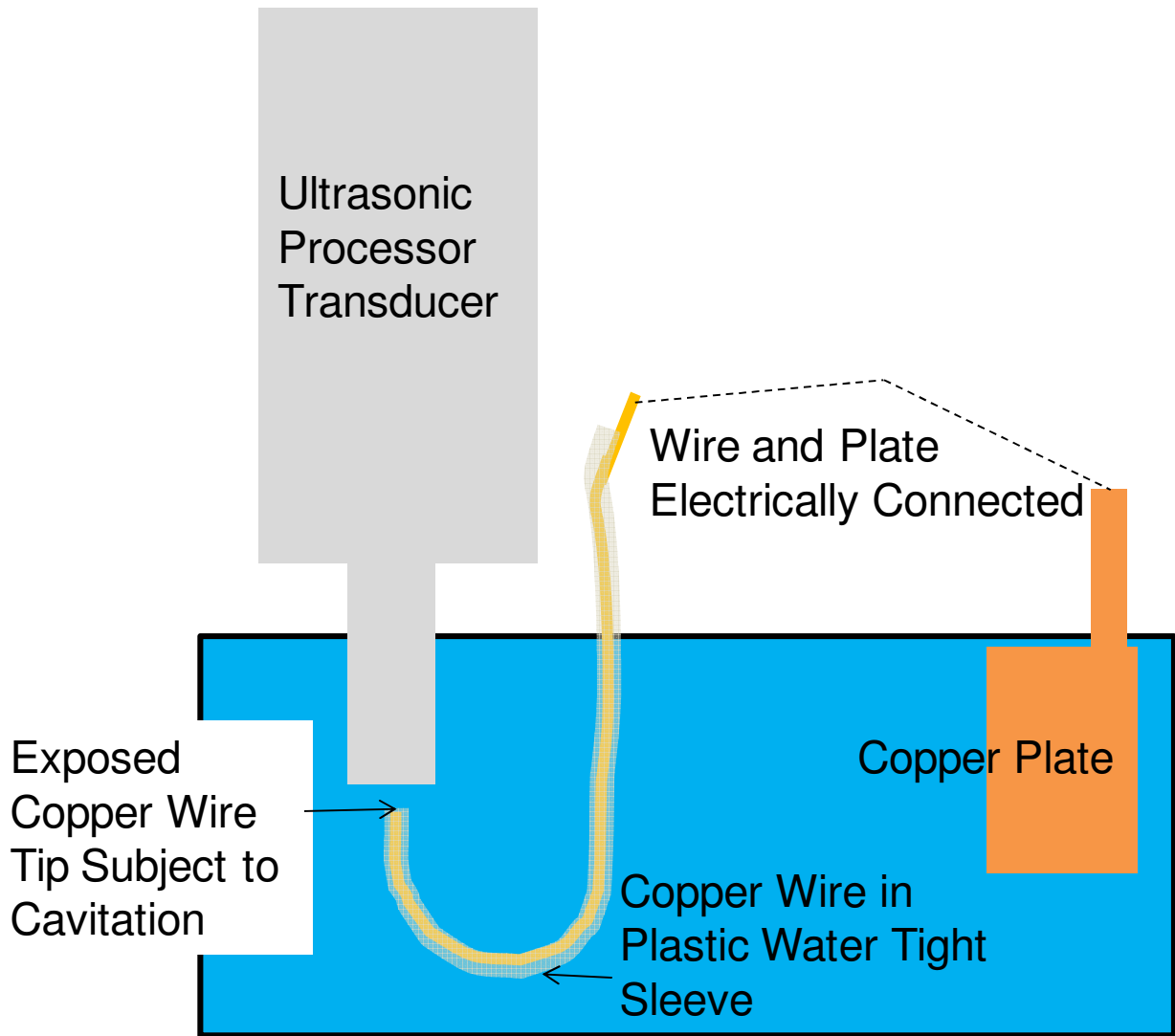


Figure 4-3: Experimental Setup of Cycled Cavitation Tests

Current and voltage measurements were recorded between the wires and the copper plates every 2 minutes. Using the known surface area exposed to cavitation (about 0.033 cm^2), a current density was calculated by dividing current measured by area. For this experimental configuration, a positive corrosion current indicates wires are anodic relative to copper plates, and a negative current signifies wires are cathodic relative to plates. The pitting water developed by Marshall (2004) was used in this test at pH 6 without chlorine or aluminum solids. Currents were allowed to first stabilize before cavitation was initiated for a duration of four hours, followed by another period of stabilization.

RESULTS

High Velocity Jet Tests

No plates exposed to fresh water had significant damage over the 4 or 5 week duration of the tests (Figure 4-4 and Figure 4-5). The plates in heated salt water were subject to extremely aggressive attack. Certain areas of plates subjected to both longitudinal jets (Figure 4-6) and perpendicular jets (Figure 4-7) in heated salt water experienced significant gouging, pitting, and buffing. When removed from water for inspection, damaged areas were comparable in appearance to new, un-corroded copper metal.

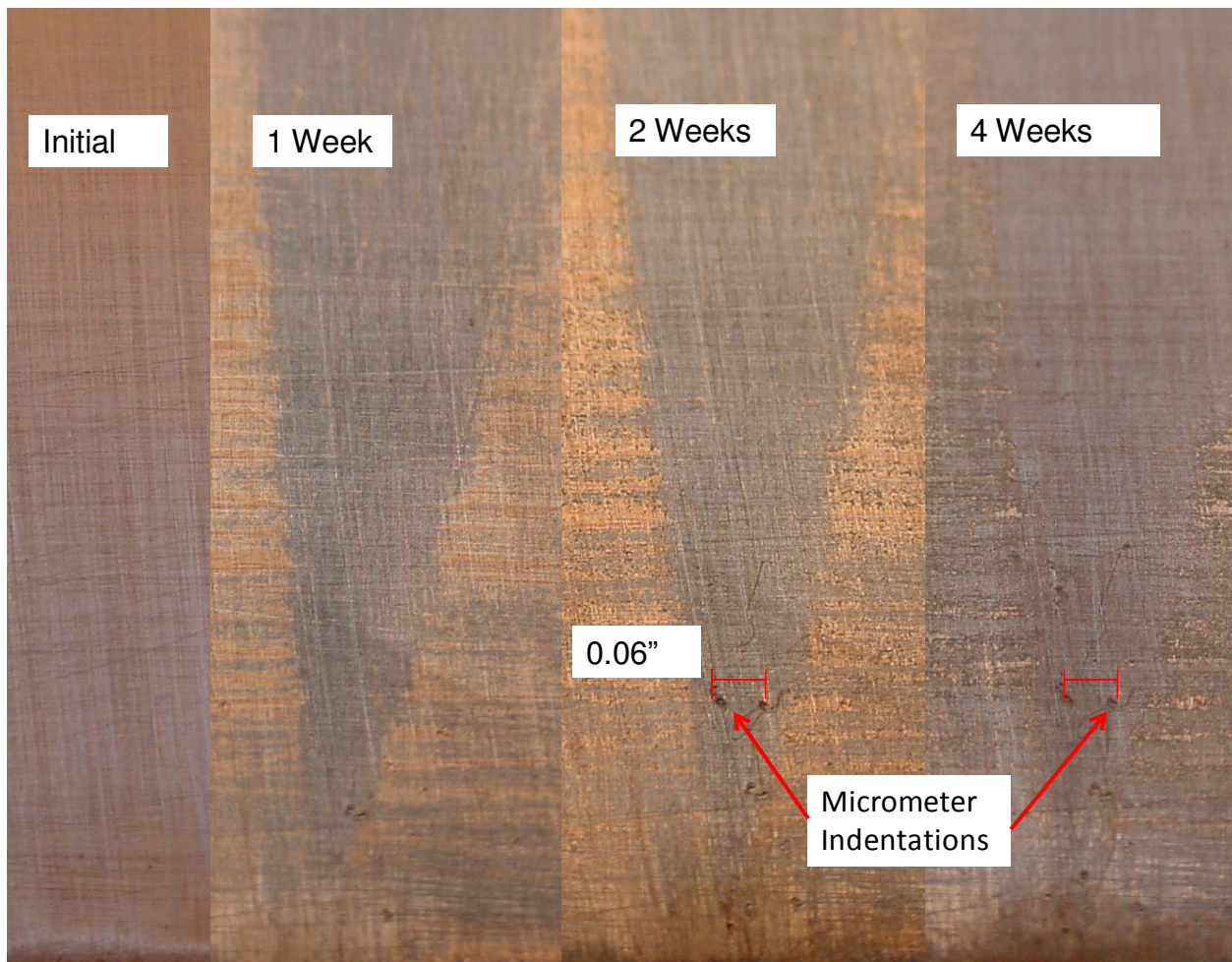


Figure 4-4: Surface Subjected to Longitudinal Jet in Room Temperature Fresh Water at pH 8 and 4 mg/L Cl₂ (Flow from Bottom to Top) (Note: Small Divots in Undamaged Areas are Point Micrometer Indentations)

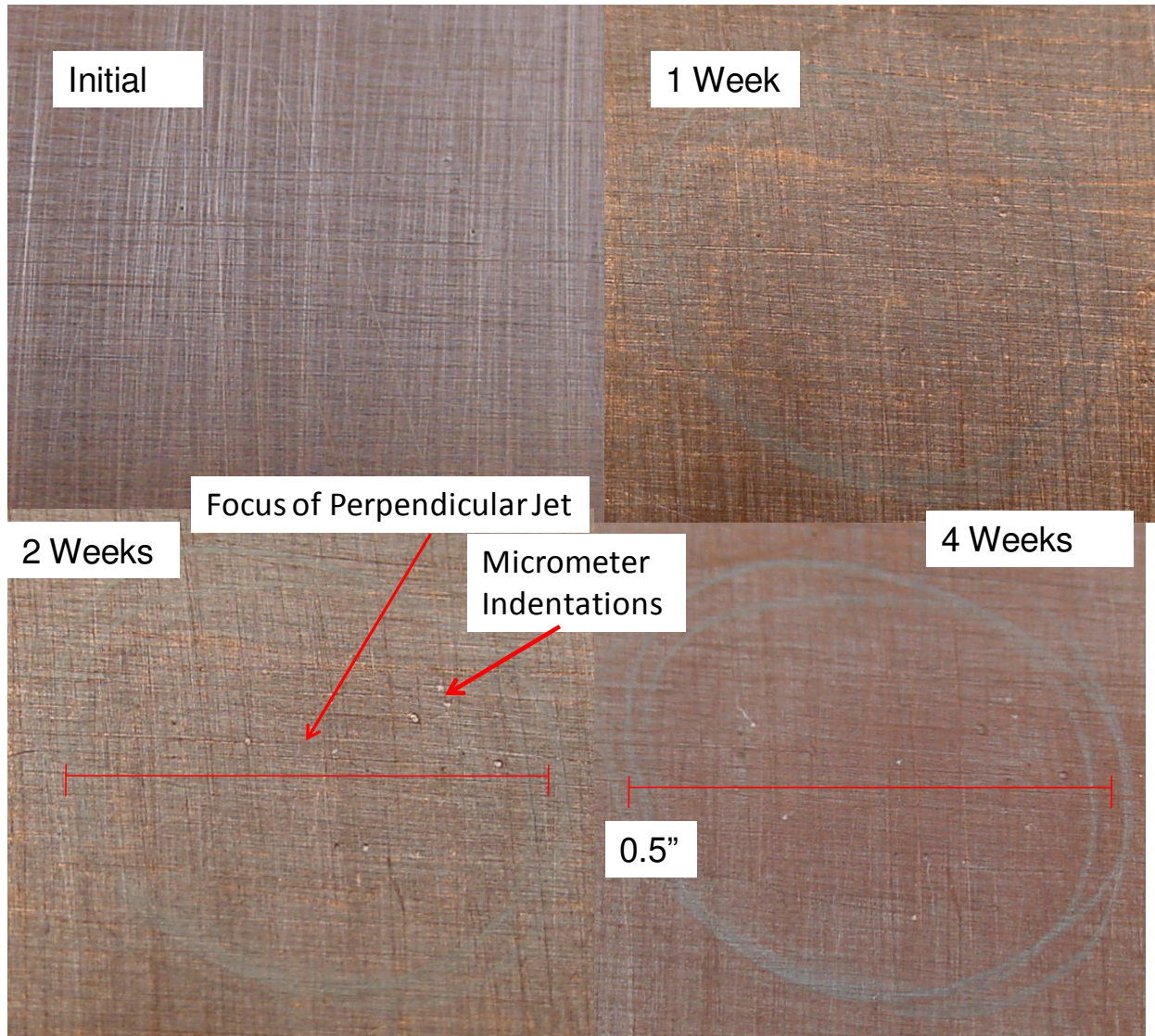


Figure 4-5: Surface Subjected to Perpendicular Jet in Room Temperature Fresh Water at pH 8 and 4 mg/L Cl₂ (Flow from Bottom to Top) (Note: Small Divots in Undamaged Areas are Point Micrometer Indentations)

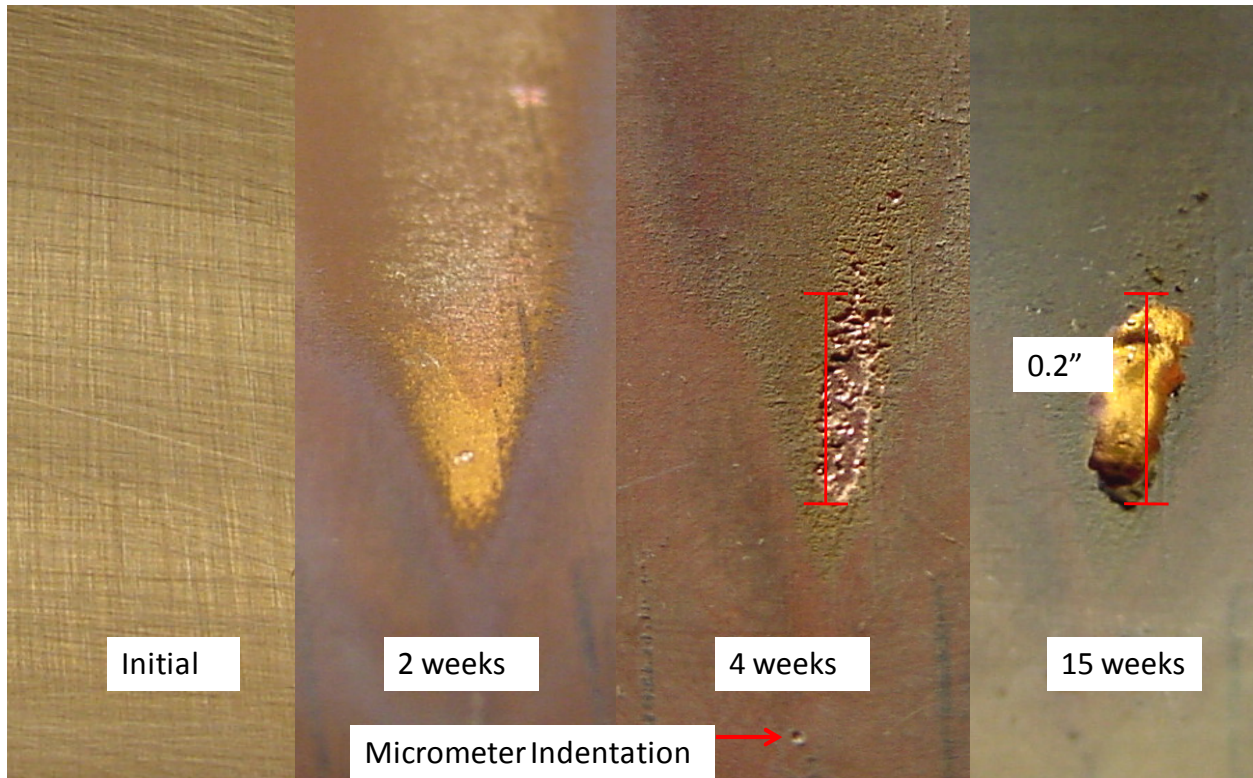


Figure 4-6: Surface Subjected due to Longitudinal Jet in Heated Salt Water (Flow from Bottom to Top) (Note: Small Divots in Undamaged Areas are Point Micrometer Indentations)

It was evident during testing that water impinging against the plates created distinct zones of damage, indicated by a shiny copper surface (Figure 4-6 and Figure 4-7), and “dead zones” (Figure 4-7) and undamaged zones (Figure 4-8), indicated by a dark brown copper surface. It is believed these distinct damaged and undamaged areas are due to the hydraulics of the flow. For instance, as water discharged from the jet tips moving towards the plates, the streamlines of the highest velocity water naturally fanned out, thereby impinging against the copper most aggressively in the circular region surrounding the area that remained relatively undamaged in the case of the perpendicular jet (Figure 4-9), and at a distance downstream from the longitudinal jet tip (Figure 4-10)

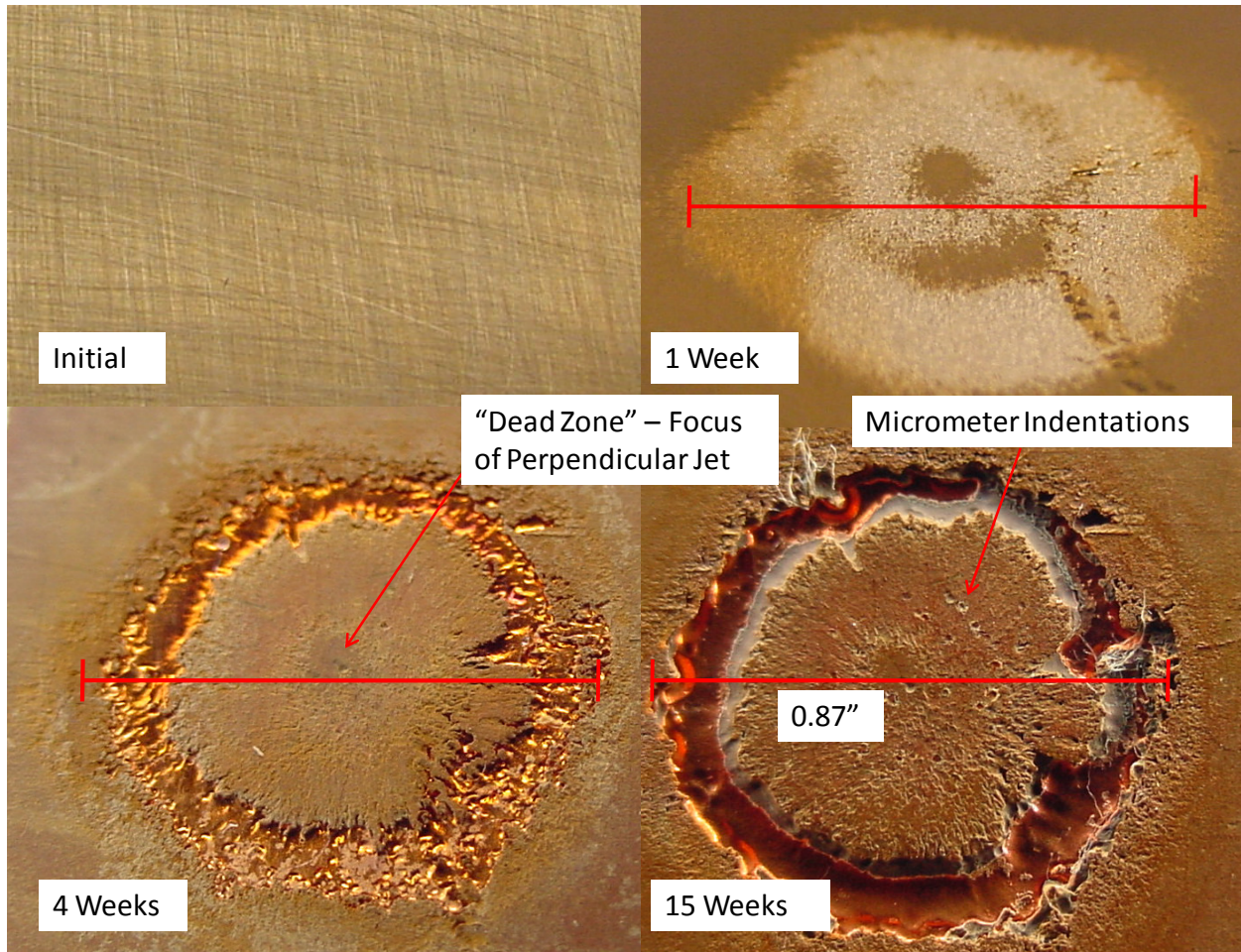


Figure 4-7: Surface Subjected to Perpendicular Jet in Heated Salt Water (Note: Small Divots in Undamaged Areas are Point Micrometer Indentations)

Given the extent of damage observed with the heated salt water, other physical configurations were tested. In contrast to the plates free of flow obstructions tested in heated salt water described above, none of these conditions resulted in significant damage (Table 4-1) including the plate with the copper joint edge (Figure B-3), the plate with a plastic flow obstruction (Figure B-4), and the plates subjected to jets in a range of fresh waters (Figure 4-4, Figure 4-5, Figure B-5, Figure B-6).

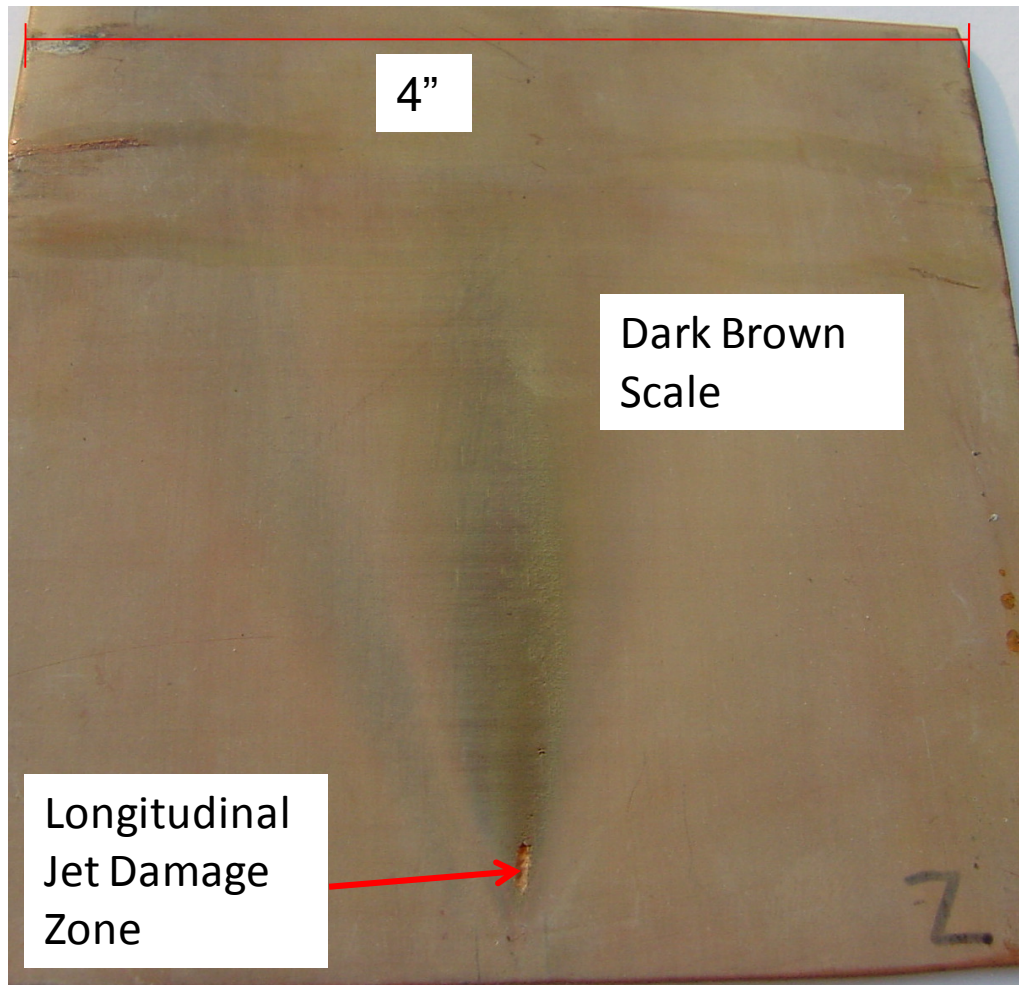


Figure 4-8: Surface Subjected to Longitudinal Jet in Heated Salt Water

After 16 weeks, the average measured depth of the three deepest areas in the damaged zone on one of the plates subjected to a longitudinal jet in heated salt water was over 0.034" (Figure 4-11), which is deep enough to form a leak in typical 3/4" Type M copper tube (0.032" thick). A similar measurement of the damaged zone resulting from the perpendicular jet in the heated salt water was over 0.022" after 16 weeks (Figure 4-11) but the penetration appears to be leveling off over time. In comparison, all of the other areas of the copper plate were seemingly unaffected with less than 0.0002" of thickness loss or even gained thickness during the course of the testing (Figure 4-11). Unlike tests with heated salt water, there was virtually no penetration in plates tested in room temperature water with 4 mg/L Cl₂ at pH 8 (Figure 4-12) and water heated to 39° C at pH 6 without chlorine (Figure B-7). Similar to the penetration results,

cumulative weight loss was greatest in plates subject to jets in heated salt water (Figure B-8, Figure B-9, and Figure B-10).

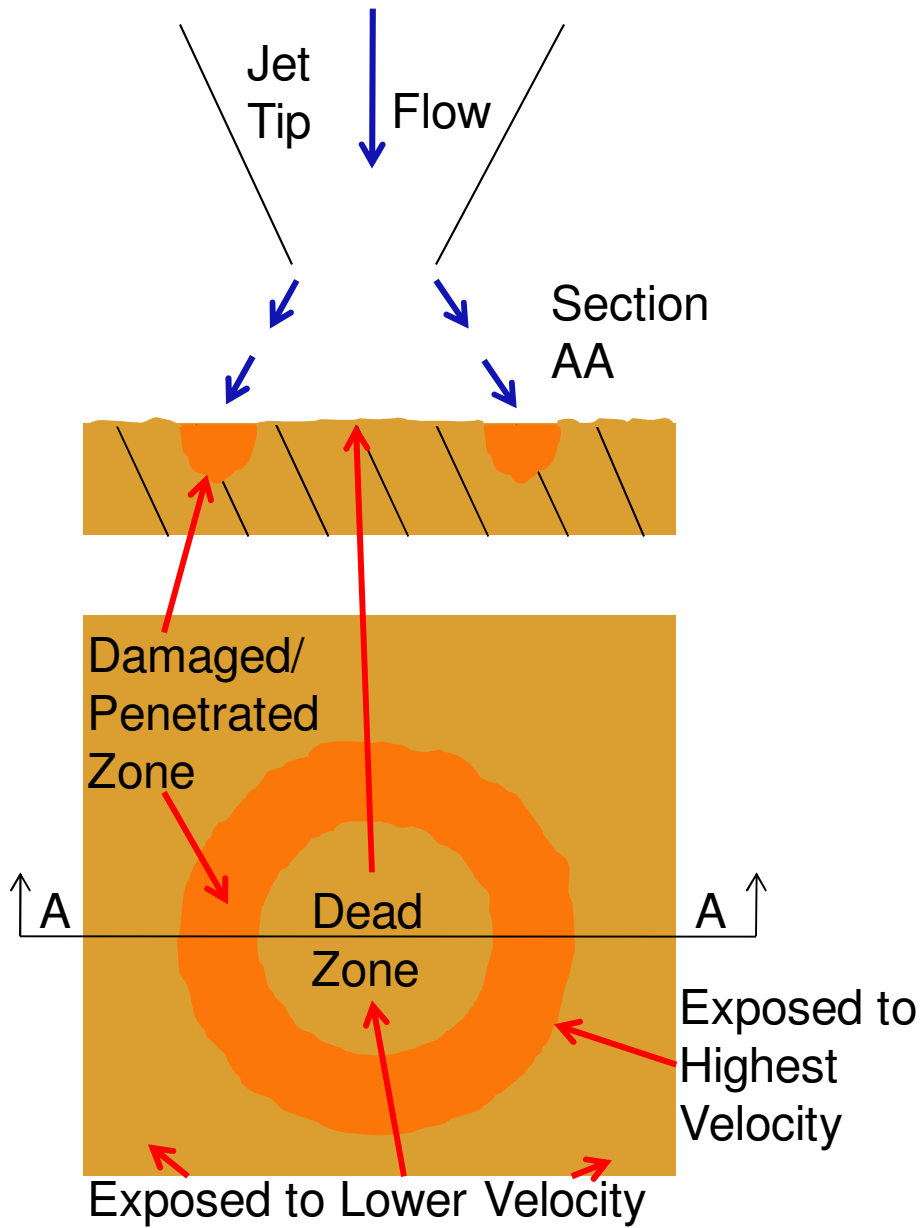


Figure 4-9: Schematic of High Velocity Streamline Impingement in Perpendicular Jet Test in Heated Salt Water

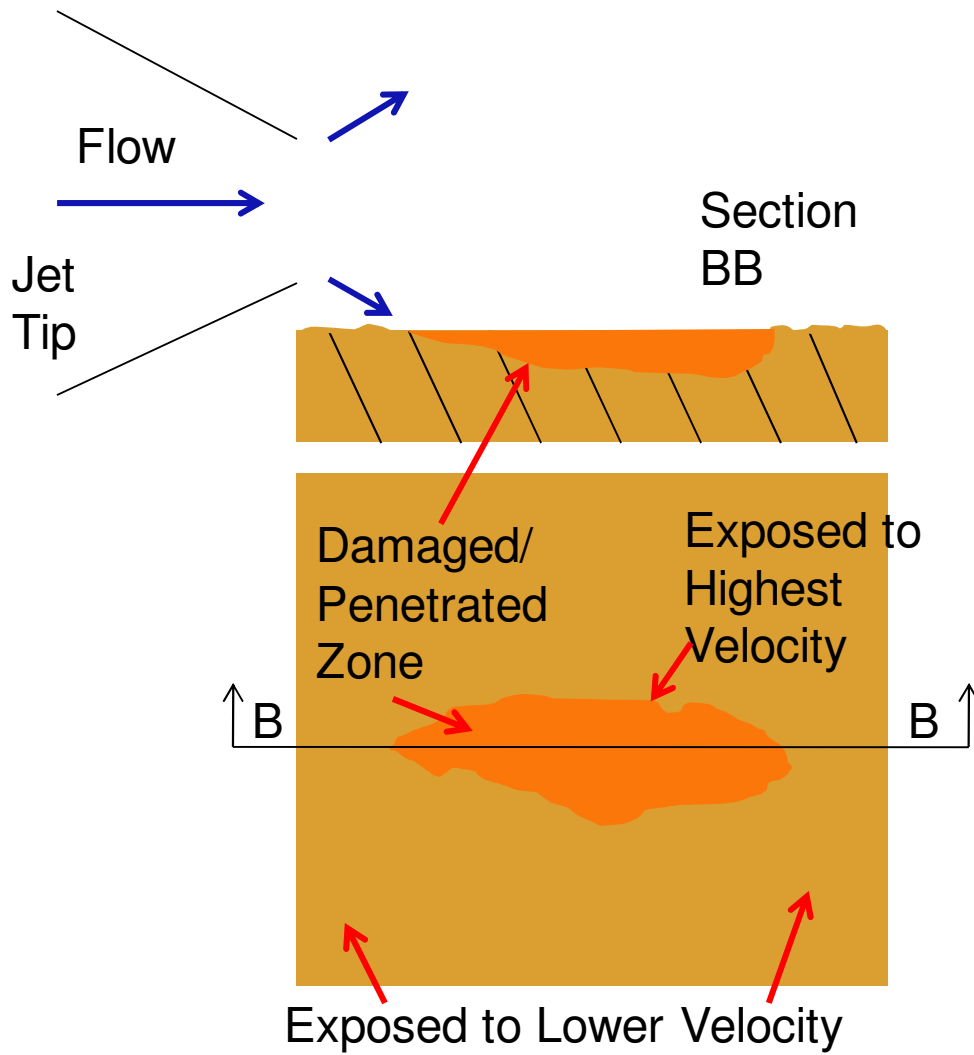


Figure 4-10: Schematic of High Velocity Streamline Impingement in Longitudinal Jet Test in Heated Salt Water

**Table 4-1: Summary of Visual Results from Longitudinal and Perpendicular Jet Tests
(Note: Tests without Damage after 3-5 Weeks were Ended)**

Trial	Conditions	Duration (Weeks)	Visual Results
1	Salt Water, 39°C	15	Significant damage from longitudinal and perpendicular jets
2	Salt Water, 39°C (with Joint Edge)	9	No significant pitting
3	Salt Water, 39°C (with Surface Blockage)	3	No significant pitting
4	4 mg/L Cl ₂ , pH 8, Room Temperature	4	No significant pitting
5	pH 6, 39°C	5	No significant pitting

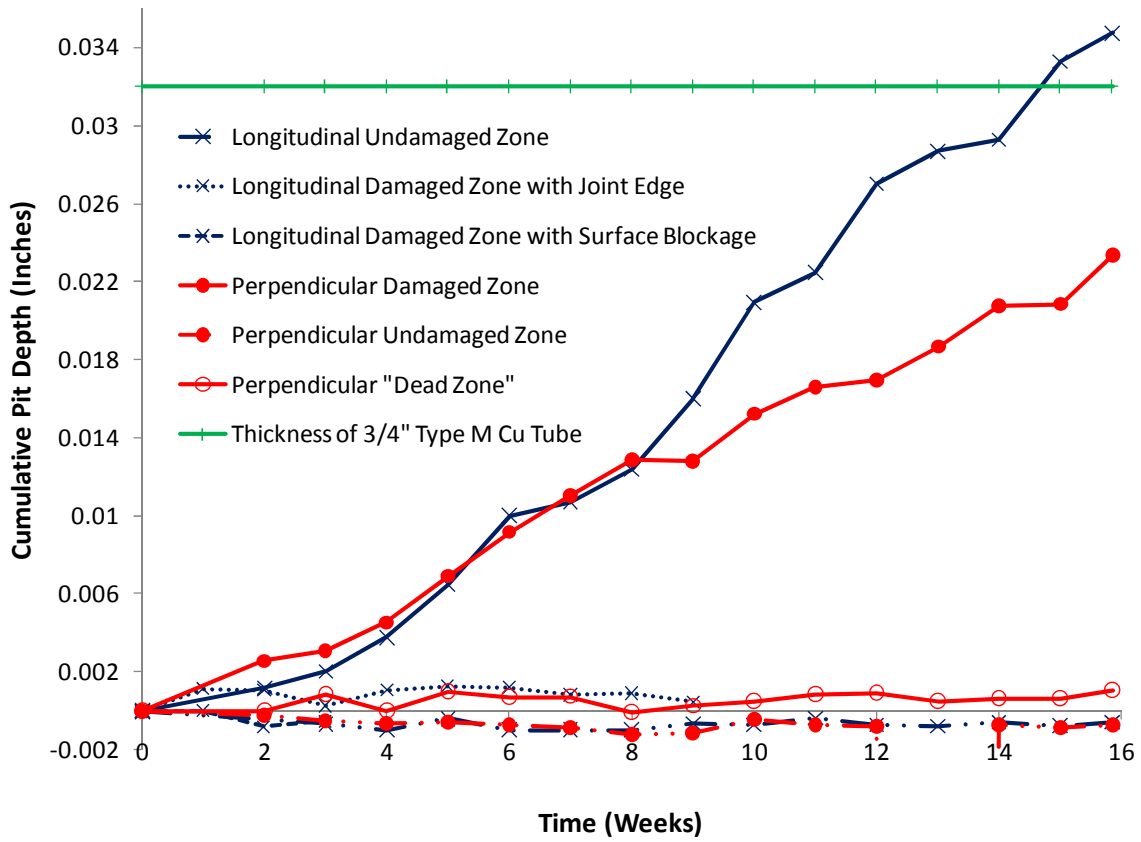


Figure 4-11: Cumulative Penetration for Various Longitudinal and Perpendicular Jet Test Plates in Heated Salt Water

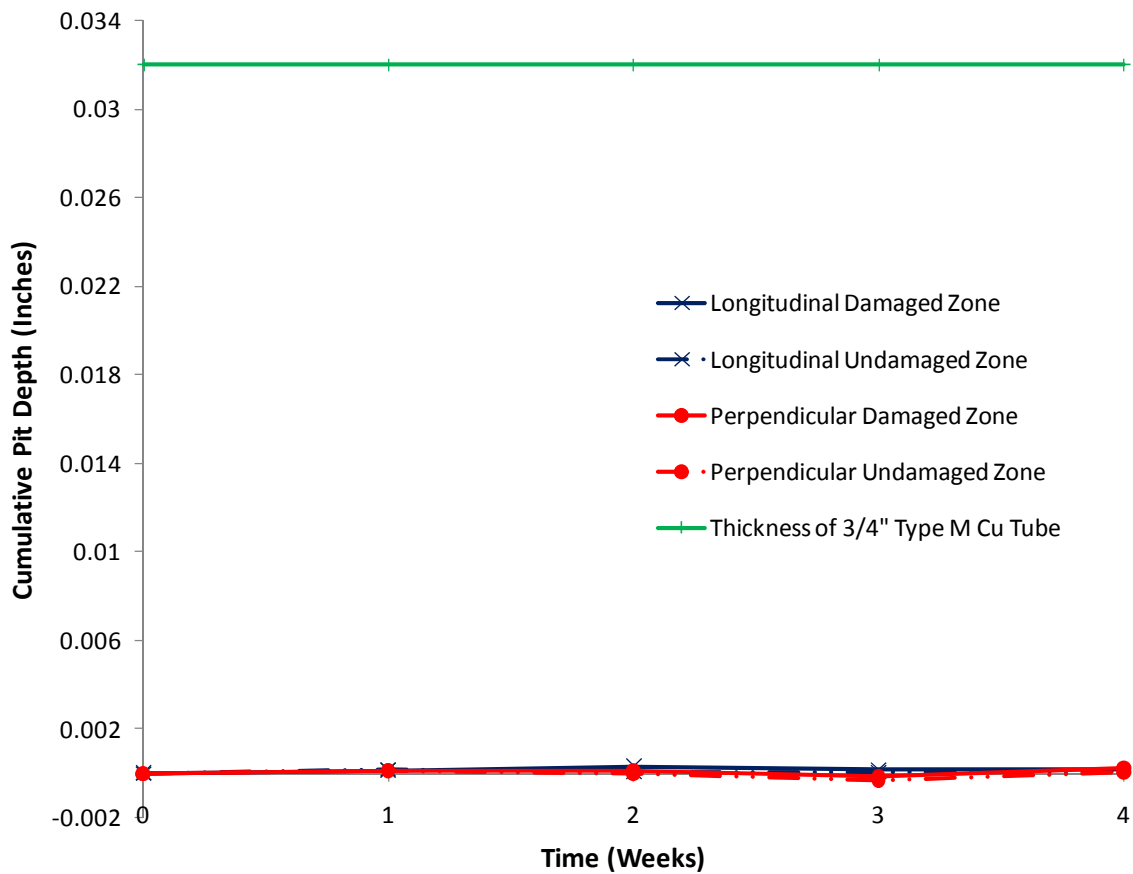


Figure 4-12: Cumulative Penetration for Various Longitudinal and Perpendicular Jet Test Plates in Room Temperature Fresh Water at pH 8 and 4 mg/L Cl₂

In the test using heated salt water, the penetration depth due to perpendicular jet impingement eventually leveled off markedly while penetration due to longitudinal jet impingement remained relatively constant (Figure 4-11). The decreased penetration in the plate subject to a perpendicular jet may have been due to cavitation bubbles imploding prior to reaching the penetrated surface as the surface receded, which is believed to have been the case in previous cavitation experiments (Figure 3-9). The sustained penetration rate in the plate subject to a longitudinal jet may have been due to the acceleration in the rate of attack due to turbulence in the growing gouge or pit (Figure 4-6).

It is not understood why tests in heated salt water had such a dramatic pitting compared to tests in fresh water. One possible reason is the influence of a concentration cell in heated salt

water. A short-term concentration cell test in un-chlorinated heated salt water (Figure 2-14) resulted in dramatically higher anodic currents than tests conducted using various fresh waters (Figure 2-11). For instance, the current density of the wire subject to flow on the discharge side of the pump in un-chlorinated heated salt water initially spiked to over $900 \mu\text{A}/\text{cm}^2$, and over the duration of the 4 hour test decreased to only about $250 \mu\text{A}/\text{cm}^2$ (Figure 2-14), which is still over 4 times higher than the current density measured at the end of the short-term test for the same wire on the discharge side of the pump in heated pitting water at pH 6 (Figure 2-11). The average current density of the wire subjected to flow discharge side of the pump throughout the duration of the test was $443 \mu\text{A}/\text{cm}^2$, 20 times higher than the average current density measured for the same wire in heated pitting water at pH 6. Based on this average current density ($443 \mu\text{A}/\text{cm}^2$), a leak would be expected to form in a new $\frac{3}{4}$ " Type M copper pipe in about 1 month. While it is understood that heated salt water is not typically transported through premise plumbing systems, this result provides a possible reason as to why plates subject to jets in heated salt water incurred dramatically more damage than plates in fresh water.

Cycled Cavitation

Initially, currents measured between the sleeved wires and copper plates stabilized at about $0 \mu\text{A}/\text{cm}^2$ (Figure 4-13). During cavitation, the corrosion rate decreased to less than $-30 \mu\text{A}/\text{cm}^2$, indicating the copper surface in contact with cavitation actually became cathodic with respect to the copper sheet not exposed to cavitation. In other words, the wires were electrochemically protected from corrosion during cavitation. Immediately following cavitation, the wires subjected to cavitation experienced a current spike and became highly anodic, while there was no change in the control wires in stagnant water that did not experience any cavitation. For example, the current of one of the wires subject to cavitation spiked to about $50 \mu\text{A}/\text{cm}^2$, indicating the wire was anodic with respect to the submerged copper plate. If this current density could be sustained, it would be predicted to cause a leak in the wall of a typical copper tube in less than 1 year. The anodic current spike proceeded to decrease over the next 72 hours back to the stable, starting value. During this time, however, the current density did remain significantly high, above $20 \mu\text{A}/\text{cm}^2$, for over 12 hours.

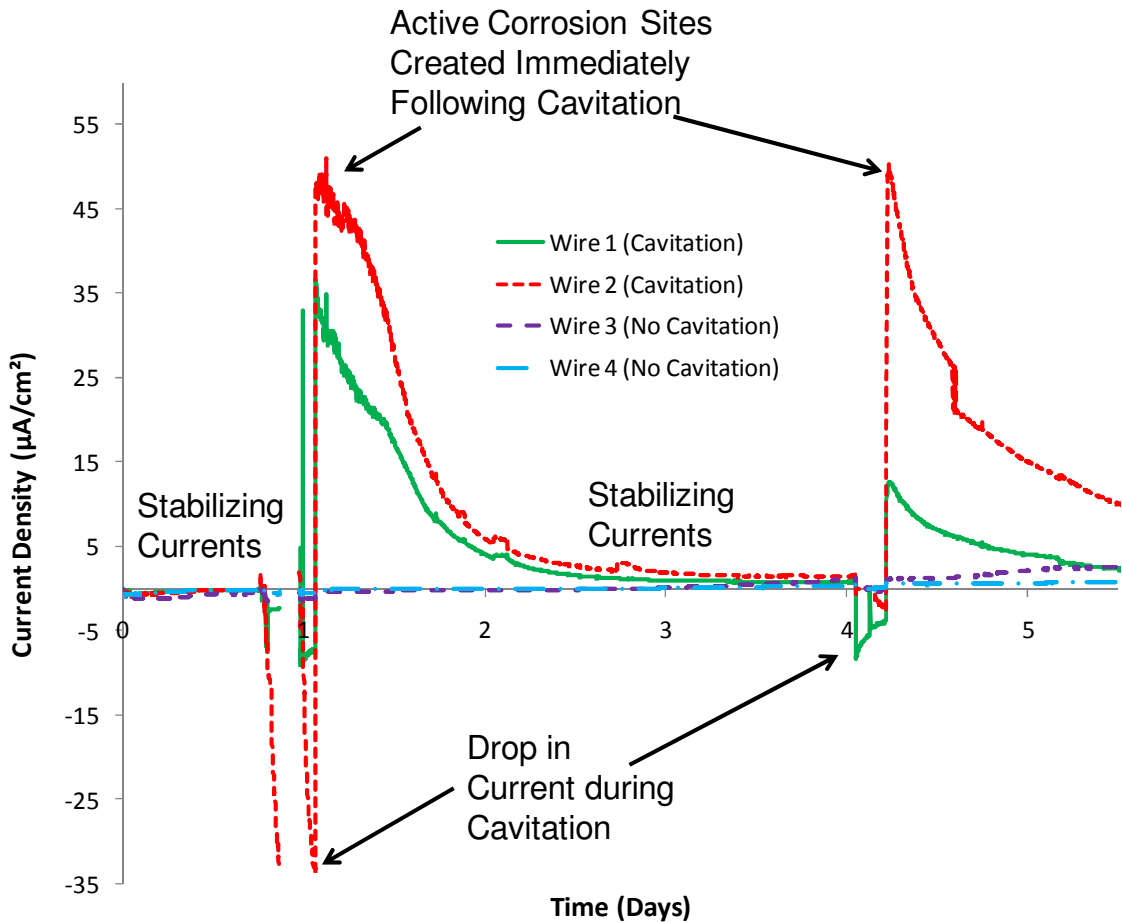


Figure 4-13: Current Density between Insulated Copper Wire Subjected to Periodic Cavitation and Copper Plate in Stagnant Bulk Water at pH 6

After wires were allowed to stabilize, cavitation was initiated for a second time, and another anodic current spike was recorded once again, up to almost the same value of $50 \mu\text{A}/\text{cm}^2$ in one of the wires subject to cavitation. These results imply that the cavitation removed the protective scales that normally form on the copper pipe surfaces subject to very high flow. To verify this, a similar apparatus was set up, but instead of being subjected to cavitation, one wire surface was sanded after corrosion currents stabilized, effectively removing any protective or passivating surface scale that had formed. Similar to the cycled cavitation test, the corrosion current density spiked after the copper wire surface was “cleaned” by sanding (Figure 4-14). Even though the high current density for the sanded wire did not sustain as long as the wire subjected to cavitation, a significantly high current density ($60 \mu\text{A}/\text{cm}^2$), sufficient to eat a hole through a new $\frac{3}{4}$ ” Type M copper pipe in less than 3 years, was sustained for 3 hours. These

results indicate that if small surfaces received periodic cavitation with some regularity, then it could disrupt the “healing” of the surfaces that normally prevents excessive corrosion from conventional corrosion mechanisms.

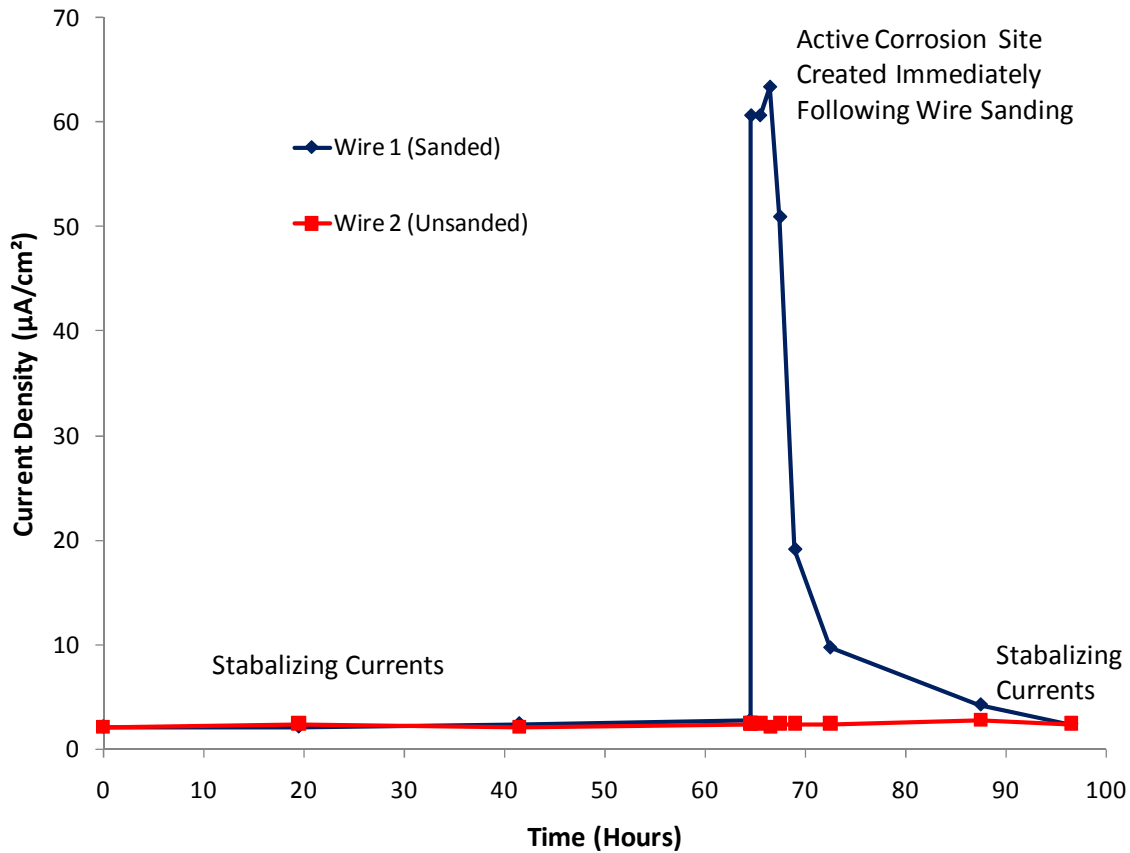


Figure 4-14: Current Density between Insulated Copper Wire Subjected to Periodic Cavitation and Copper Plate in Stagnant Bulk Water at pH 6

To ensure that the current density spikes was not merely a “false positive” caused by cavitation-generated pits increasing copper surface area exposed to water, a test was conducted with identical setup except a sanded copper wire protruded ¼” out of the water tight sleeve, exposing a greater surface area to the stagnant bulk water. Currents measured were divided by the surface area of the original copper wire set up (about 0.033 cm²) to produce a comparable current density. Highly anodic current spikes did not occur when these wires were exposed to the same pitting water but without any cavitation (Figure 4-15); therefore, it was deemed likely

that the cavitation was the cause of the increased corrosion currents (and not an increase in surface area).

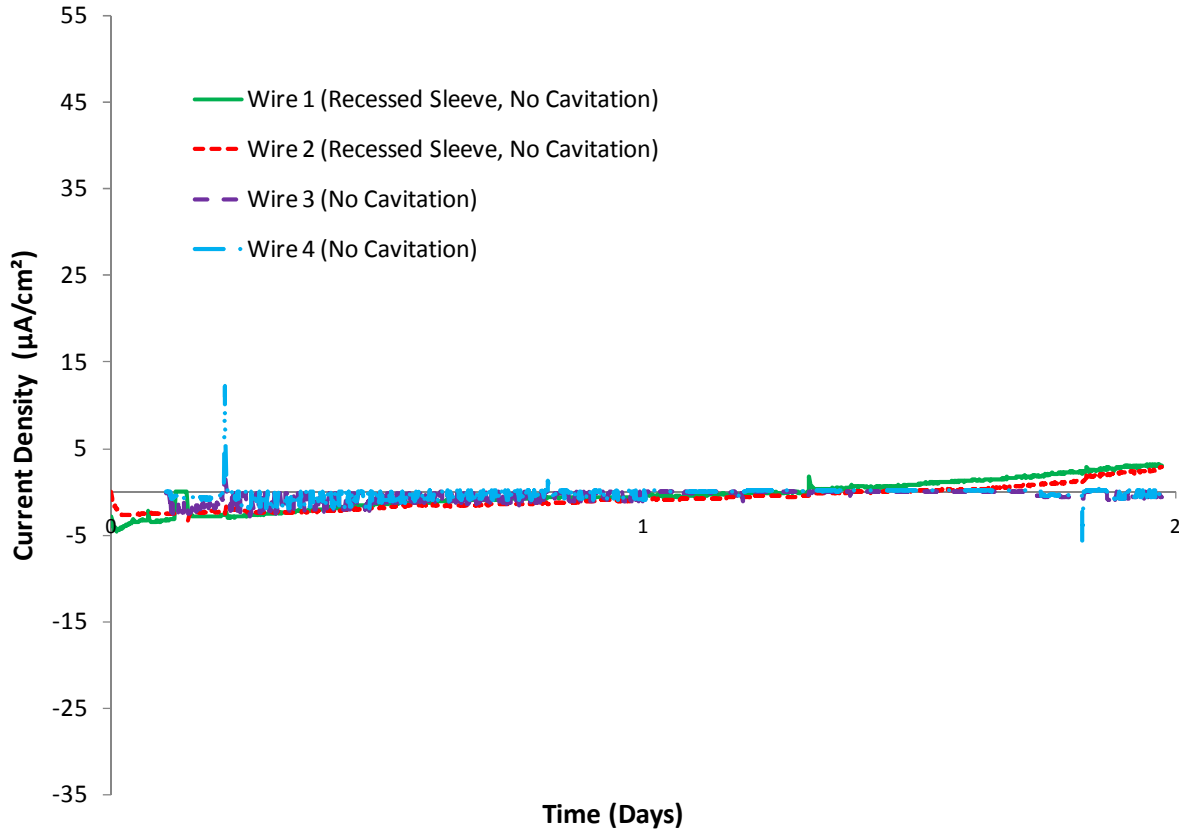


Figure 4-15: Current Density between Insulated Copper Wire with Greater Surface Area Exposed and Copper Plate in Stagnant Bulk Water

DISCUSSION

High Velocity Jet Impingement

It is unknown how or why the damage to copper surfaces occurred in the jet tests for heated salt water described above. If cavitation erosion was the only mechanism responsible for initial damage, then plates in all waters tested would have pitted or gouged surfaces since it was found in Chapter 3 that water chemistry has no mitigating affect cavitation damage to copper specimens (although there is evidence that cavitation forms differently in salt water (Ceccio et al., 1997)). Once copper plate damage was initiated in the jet tests, however, it is believed that a

combination of high velocity impingement, cavitation, and concentration cell corrosion contributed to the extent of the pitting. The net result is that under certain conditions flow induced corrosion can be dramatically damaging. Unlike Bengough and May (1924), metallic copper particles were never observed in our apparatus.

One proposed mechanistic explanation is that high velocity impingement may prevent scale from sufficiently adhering to copper plates in the damaged zones or even detaching loosely adhered scale, exposing bare copper metal to the jet. According to Bengough and May, carbonate scales form slowly on copper in salt water and can be expected to become “detached and redistributed” due to rapidly moving water (1924). While the extent of corrosion scale prevention due to high velocity impingement is unknown in the tests conducted and described in this paper, there is evidence that scale formation can at least be manipulated by rapidly moving water. Even in waters where copper plates were not pitted (in waters with 4 mg/L Cl_2 at pH 8 and heated at pH 6), there is some visible differences between the scale formed on the area of the plate subject to flow and the scale formed on the areas subject to stagnant/low flowing water; indicating that high velocity flow did indeed influence the scale formation (Figure 4-16). While this high velocity impingement may have affected scale distribution, it is not believed to have been the main cause of damage in these experiments.

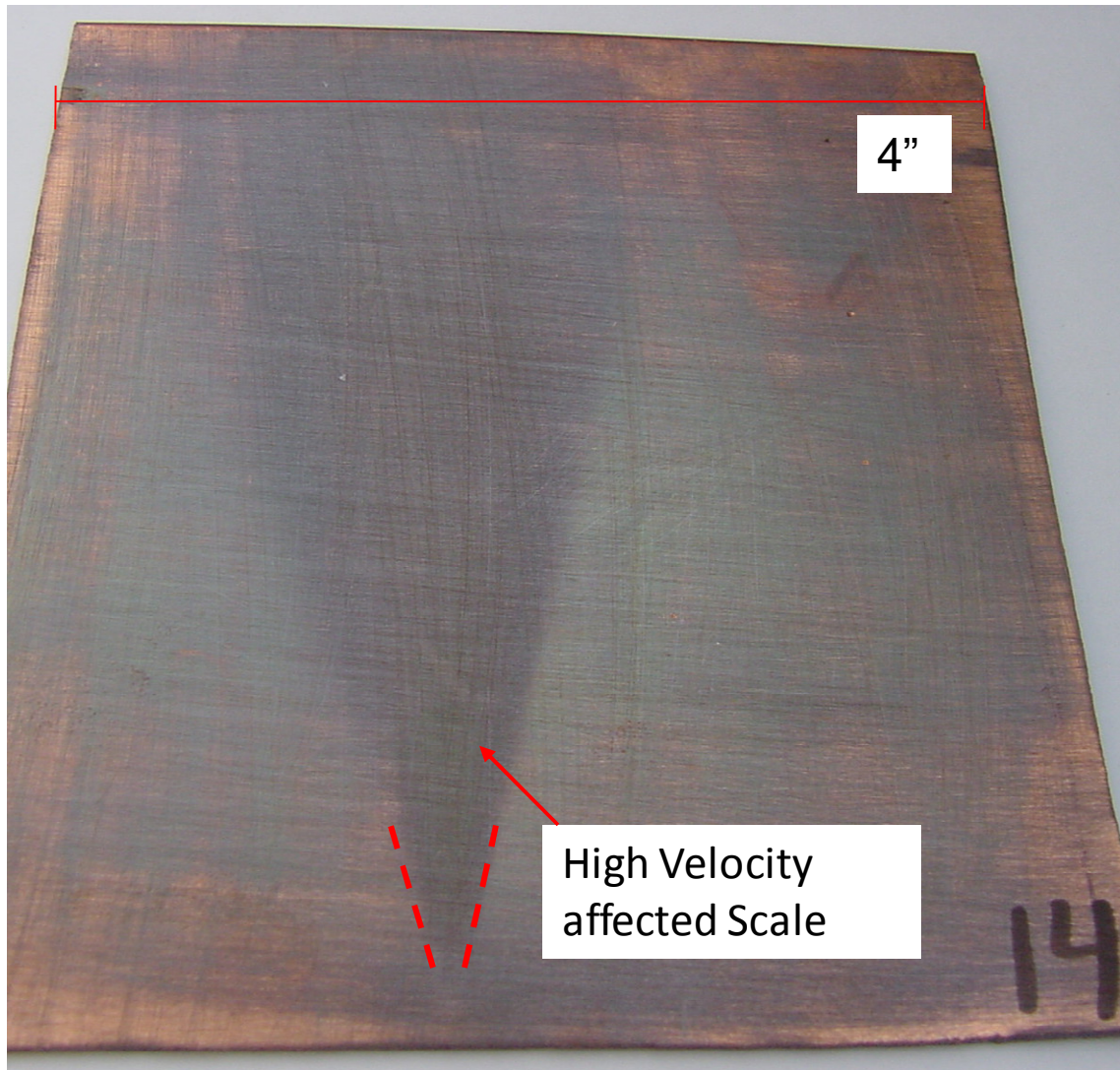


Figure 4-16: Copper Plate Subject to Longitudinal Jet in Heated Pitting Water at pH 6

Cycled Cavitation

Preliminary tests described above suggest that brief periods of cavitation may effectively remove passivating scales from copper surfaces and create hyperactive corrosion sites (Figure 4-13). Hypothetically, this action could be highly detrimental in a system subjected to on/off flow patterns, because repeated removal of the passivating scale and creation of hyperactive corrosion sites by cavitation could allow accelerated corrosion attack (observed for short periods of time) to continue indefinitely. That is, a section of pipe may be subjected to damage from a brief cavitation event (when a faucet is turned on), but then subject to even more damage from a

subsequent high corrosion rate from exposure to stagnant water (when the faucet is turned off) for a period of hours. This result is significant because it suggests cavitation does not have to be continuous in order to cause damage. Brief periods of cavitation followed by exposure to stagnant water may be sufficient to cause pipe damage and penetration due to a combination of bubble implosion and dramatically increased corrosion rate.

To further illustrate the potential for damage caused by a combination of cavitation and concentration cell corrosion, the following describes a hypothetical scenario where a specific portion of a copper premise plumbing system is subjected to an on/off cavitation flow pattern similar to the cycled cavitation experiments described above (Figure 4-13) (i.e. a spot on the pipe with the area of a typical pinhole leak is subjected to cavitation damage while water is flowing, following by periods of stagnation). Following cavitation and during stagnation the small portion of the surface becomes the anode and the current decays almost exponentially with time (Figure 4-13 and Figure 4-17) as the scale reforms and the copper surface returns to stabilized corrosion activity. For this hypothetical example, the independent variable is the number of 100-second cavitation events per day, which controls the scale removal and resulting corrosion rates.

Three data sets are presented: 1) predicted penetration per month attributable only to cavitation damage against the copper surface, 2) penetration per month attributable to the concentration cell corrosion current between the small area subjected to cavitation and the rest of the copper pipe following periods of cavitation (Figure 4-13), and 3) penetration per month attributable to the combined (overall) effect of cavitation bubble implosion and concentration cell currents arising after cavitation.

For simplification in making calculations, the concentration cell current decay over time for a typical stagnation event following cavitation over one of the wires was approximated with an exponential function and used for all calculations (Figure 4-13 and Figure 4-17). Penetration from corrosion over an interval was calculated based on the integration of an exponential trend line fit to this curve (Figure 4-17):

$$y=56.2e^{-2 \cdot 10^{-5}t}, t=\text{seconds}$$

After each cavitation event, it is assumed that a hyperactive corrosion site is created and scale is removed, resulting in currents similar to those recorded in previous cycled cavitation experiments (Figure 4-17). To provide some extreme examples, if the interval between each cavitation event is 10,000 seconds (about 9 cavitation events per day), the average corrosion rate during stagnation would be about $43 \mu\text{A}/\text{cm}^2$. In contrast, if the interval between each cavitation event is 85,000 seconds (about 1 cavitation event per day), the average corrosion rate during stagnation would be about $10 \mu\text{A}/\text{cm}^2$.

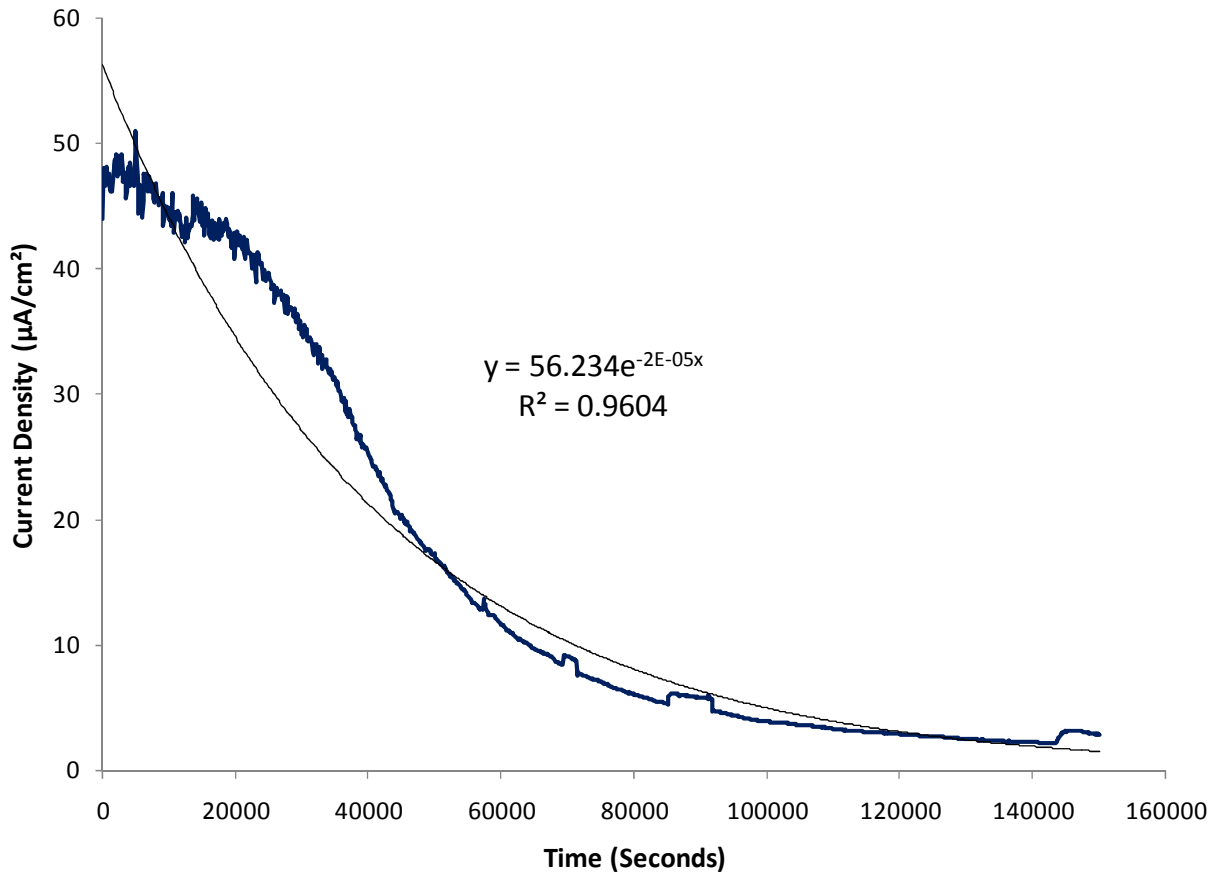


Figure 4-17: Current Density for Wires Subjected to Cavitation relative to Plate in Stagnant Bulk Water following Cavitation

To calculate the rate of penetration attributable only to cavitation bubble implosion, a constant rate of penetration was calculated based on the slope of a portion of a curve showing weight loss vs. time for the cavitation test using the 0.032” thick copper plate (Figure 3-9). It is assumed that the rate of weight loss and penetration of copper behave similarly when subjected

to cavitation (i.e. initially high but leveling off over time). The selected slope value (7.1×10^{-9} inches per second) accounts for a leveling-off effect that was observed to occur after prolonged cavitation. The penetration from the combined effect of cavitation and concentration cell corrosion was obtained by adding the penetration rate of each effect individually.

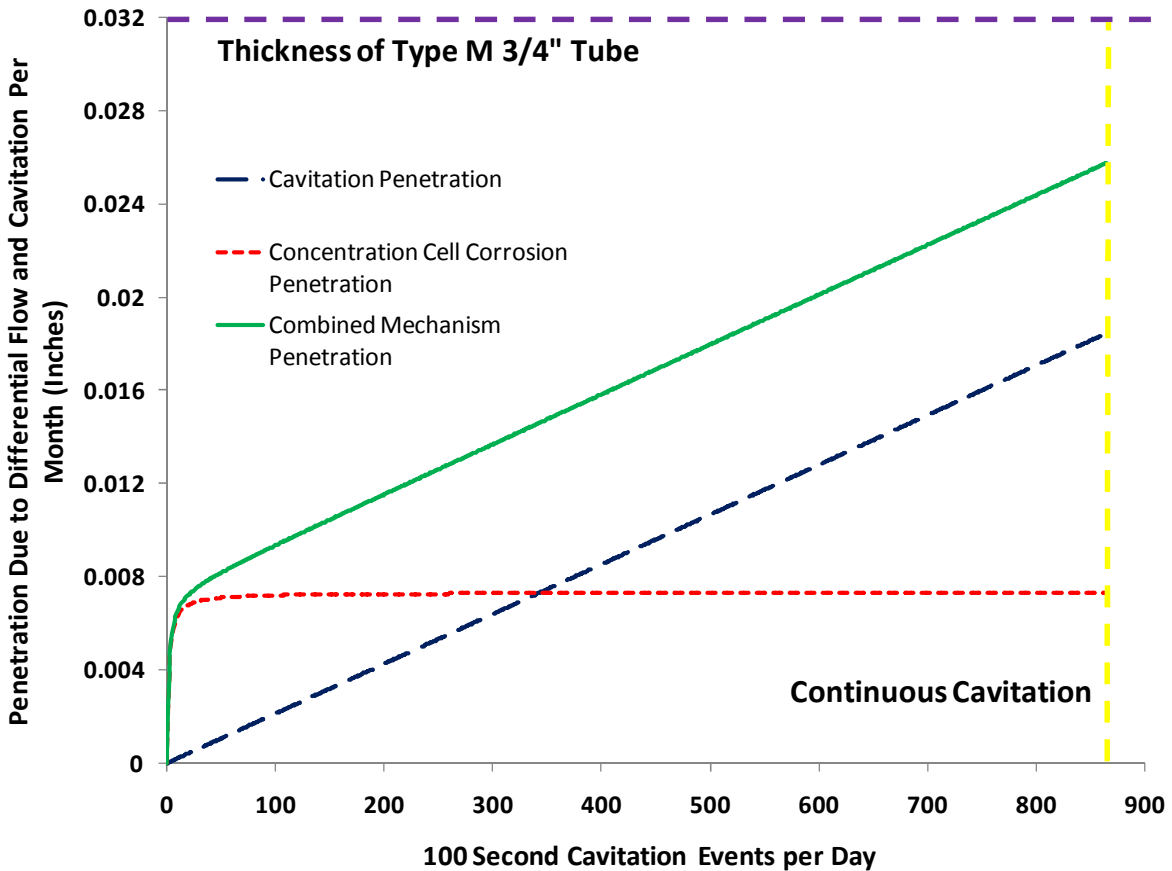


Figure 4-18: Penetration due to Combined Effect of Cavitation and Concentration Cell Corrosion Cycled Cavitation in a Hypothetical Premise Plumbing System

This hypothetical example suggests that the indirect effect of cavitation, producing concentration cell corrosion from cleaning or removal of the passive film, can dramatically exacerbate the cavitation damage. Specifically, the direct effect of cavitation is smaller than the direct effect of concentration cell currents arising during stagnation if the frequency of cavitation is less than 340 events per day (Figure 4-18). Furthermore, penetration resulting from the extra corrosion that occurs after the cavitation can be 100 times higher than that due to cavitation alone at 1 event per day (Figure 4-19). At 340 cavitation events per day the direct damage from

cavitation is about equal to that from subsequent corrosion Figure (4-17). At 50 cavitation events per day a new 3/4" Type M copper pipe could fail in as little as 4 months.

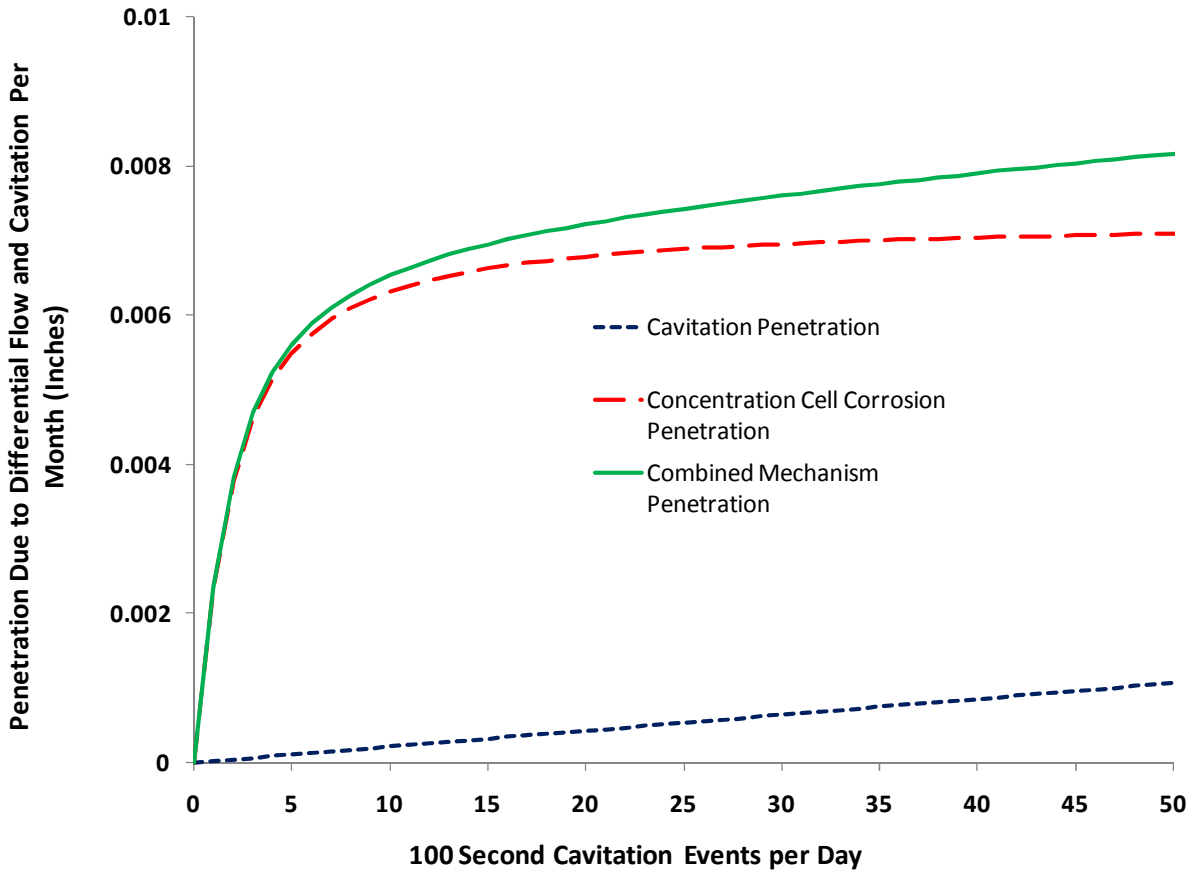


Figure 4-19: Penetration due to Combined Effect of Cavitation and Concentration Cell Corrosion Cycled Cavitation in a Hypothetical Premise Plumbing System

Thus, it remains very possible that water chemistry and concentration cell corrosion contribute to damages resulting from intermittent cavitation. Specifically, in other waters (i.e., Figure 4-20), there was less accelerated corrosion rate resulting from periodic cavitation. Additional research is necessary to examine this issue in more detail.

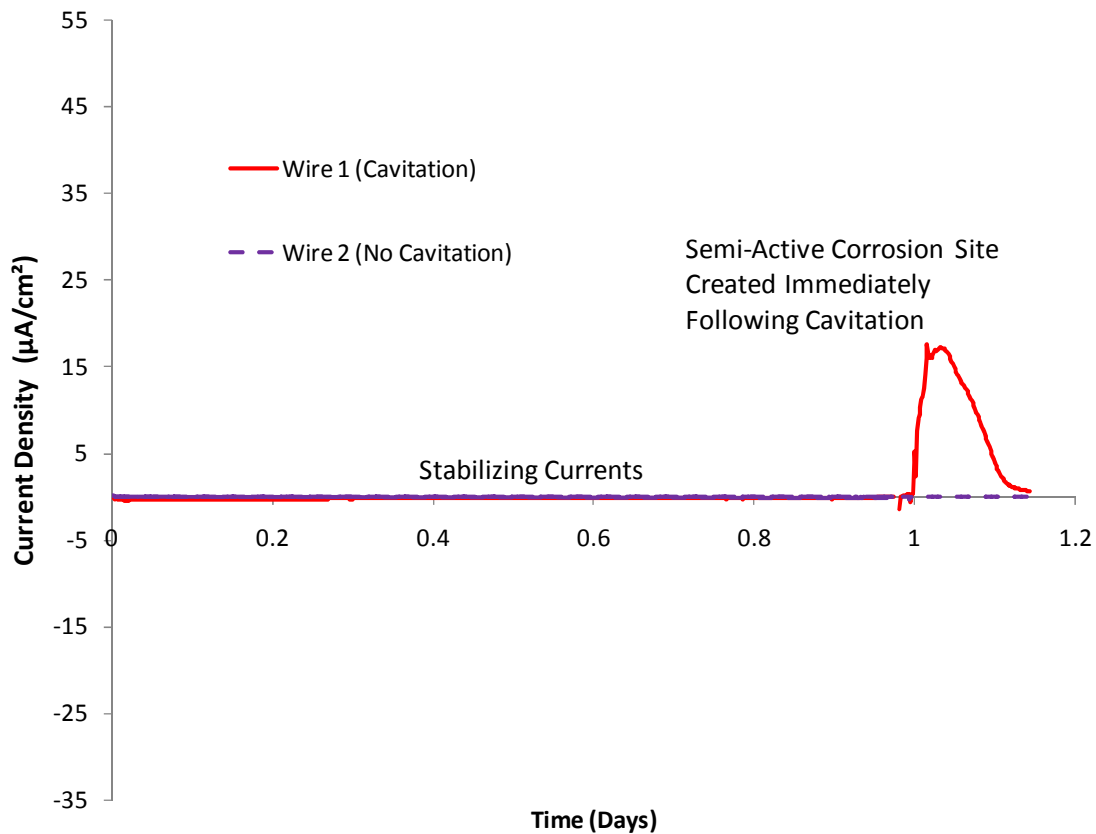


Figure 4-20: Current Density between Insulated Copper Wire Subjected to Periodic Cavitation and Copper Plate in Stagnant Bulk Water at pH 8 with 4 mg/L Cl_2

CONCLUSIONS

- Although not reproduced in synthetic tap water, rapidly moving water caused significant pitting to copper in longitudinal and perpendicular jet tests with heated salt water (possibly due to a combination of cavitation, high velocity impingement, and concentration cell corrosion)
- In the high velocity jet apparatus, the extent of flow induced damage was dependent on water chemistry, in that only heated sea water caused significant damage
- Cavitation may remove protective scales that are normally formed on copper surfaces creating more active corrosion sites, which, when in conjunction with concentration cell corrosion, can promote significant electron flow and lead to failure

REFERENCES

Bengough, Guy D. and R. May. "Seventh Report to the Corrosion Research Committee of the

Institute of Metals". *The Journal of the Institute of Metals*. 32 (1924): 90-269.

Ceccio, S., S Gowing, and Y. T. Shen. "The Effects of Salt Water on Bubble Cavitation". *The*

Journal of Fluids Engineering. 119 (March, 1997): 155-163.

CHAPTER 5: SUMMARY OF KEY CONCLUSIONS

Jeff Coyne and Paolo Scardina

- In conclusion, copper plumbing is susceptible to flow induced damage and premature failure. This was the first work to propose and systematically isolate individual mechanistic factors.
- Flow induced damage can conceivably occur from concentration cell corrosion, cavitation implosion, particle impingement, high velocity impingement, and another fluid flow phenomenon known as flow electrification.
- Cavitation damage from imploding vaporous cavitation bubbles caused the greatest extent of damage in experiments. Concentration cell corrosion and even high velocity impingement further influenced and enhanced copper damage at certain system conditions.
- Short-term and long-term concentration cell experiments demonstrated how changes in water chemistry can dramatically alter currents measured between wires subjected to flow and larger copper plates in stagnant bulk water. For example, chlorination effectively eliminated the concentration cell corrosion currents, and lowering pH increased concentration cell currents. High corrosion rates were unsustainable in long-term tests.
- Vaporous cavitation, induced by an ultrasonic processor, was found to be highly destructive when these bubbles implode against copper surfaces. Pinhole leaks were formed in copper plates with common pipe wall thickness. Based on results, 3/4" Type K and 3/4" Type L copper pipe would be expected to endure 23 and 3000 times more cavitation than 3/4" Type M copper pipe, respectively, before pinhole leak formation.
- Changes to water chemistry and the presence of a pre-existing scale layer did little to mitigate copper cavitation damage from the ultrasonic processor.

- As surfaces became progressively pitted by cavitation implosion, the rate of cavitation damage decreased over time, possibly due to the roughened surface disrupting the ability of an imploding bubble to impact fresh surface.
- Experiments analyzing mostly gaseous cavitation and sand grains entrained in flow revealed very little damage caused by the either of these mechanisms.
- A combination of high velocity impingement, cavitation, and concentration cell corrosion caused significant pitting in plates subjected to perpendicular and longitudinal jets in heated salt water. High velocity jet tests carried out in a range of fresh waters revealed little damage.
- In a test analyzing the combined effect of cavitation and concentration cell corrosion, significant and sustained corrosion rates were produced for wires subjected to a period of cavitation followed by a period of stagnation.
- Various factors affected the extent of damage in some of the tests on flow induced damage causing mechanisms including temperature, water chemistry (including salt water, chlorination, pH adjustments, etc.)

APPENDIX A

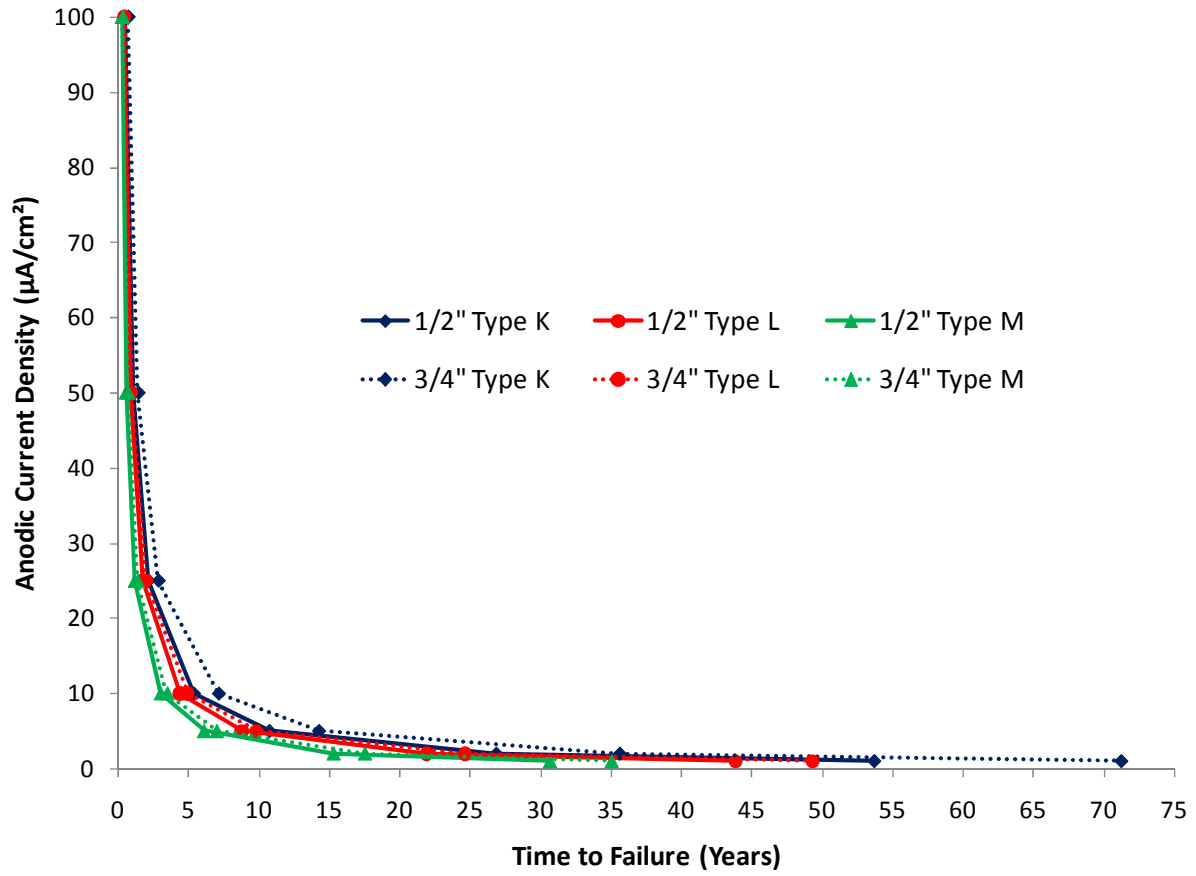


Figure A-1: Anodic Current Density vs. Time to Failure for Different Types and Sizes of Copper Pipe

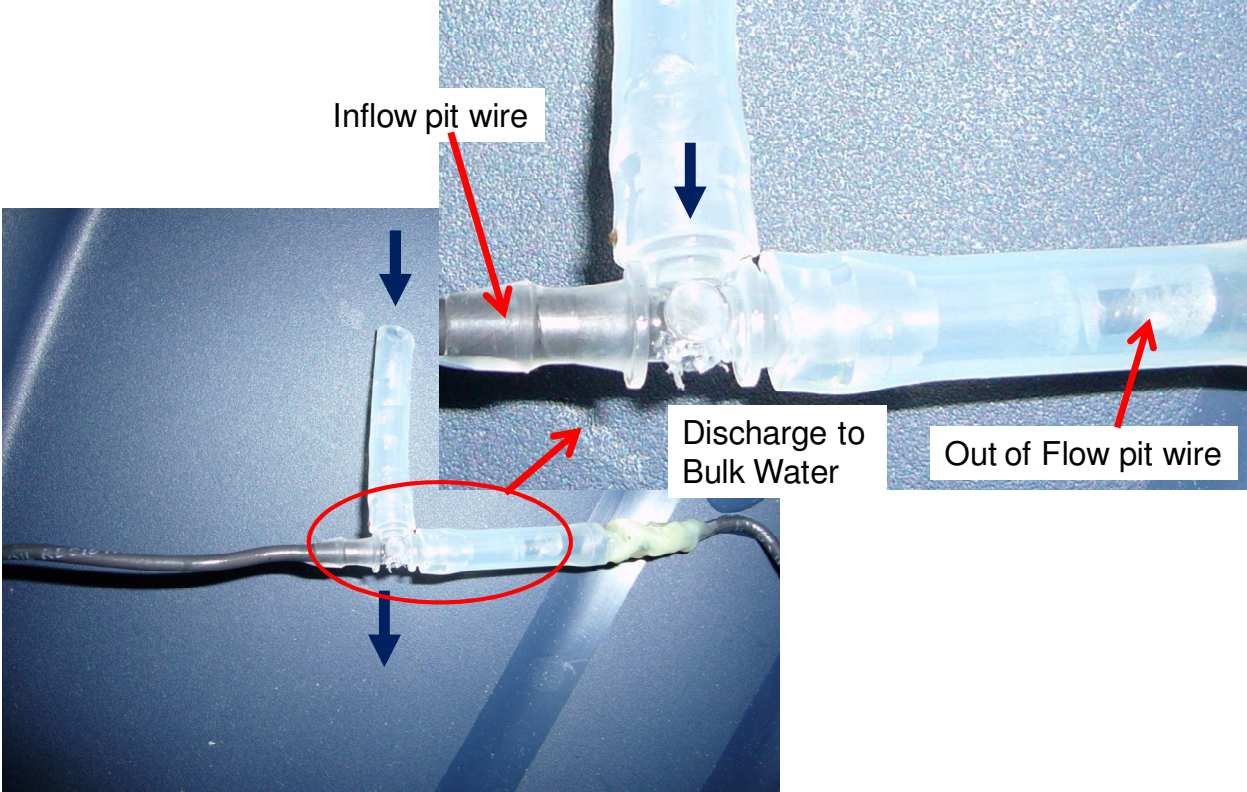


Figure A-2: Short-term Concentration Cell Testing Apparatus before Installation of Leak

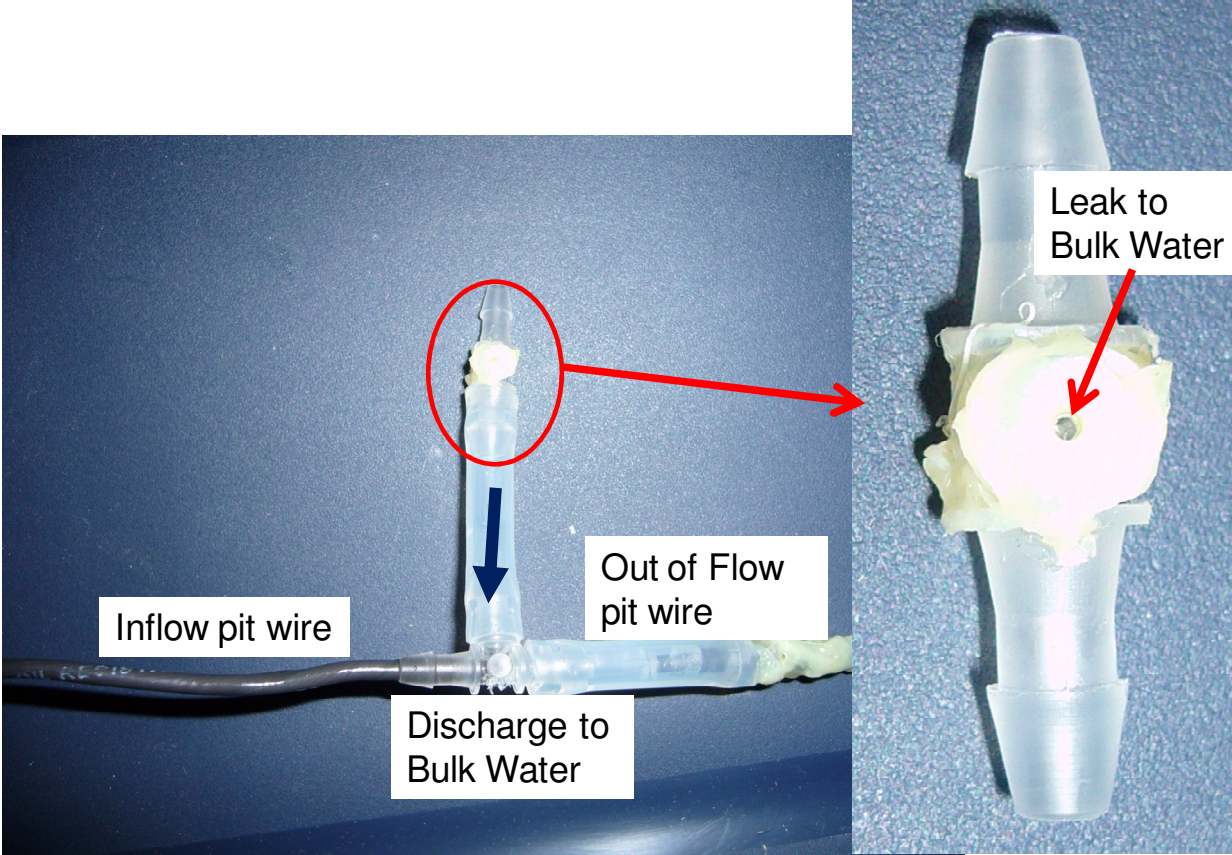


Figure A-3: Short-term Concentration Cell Testing Apparatus after Installation of Leak

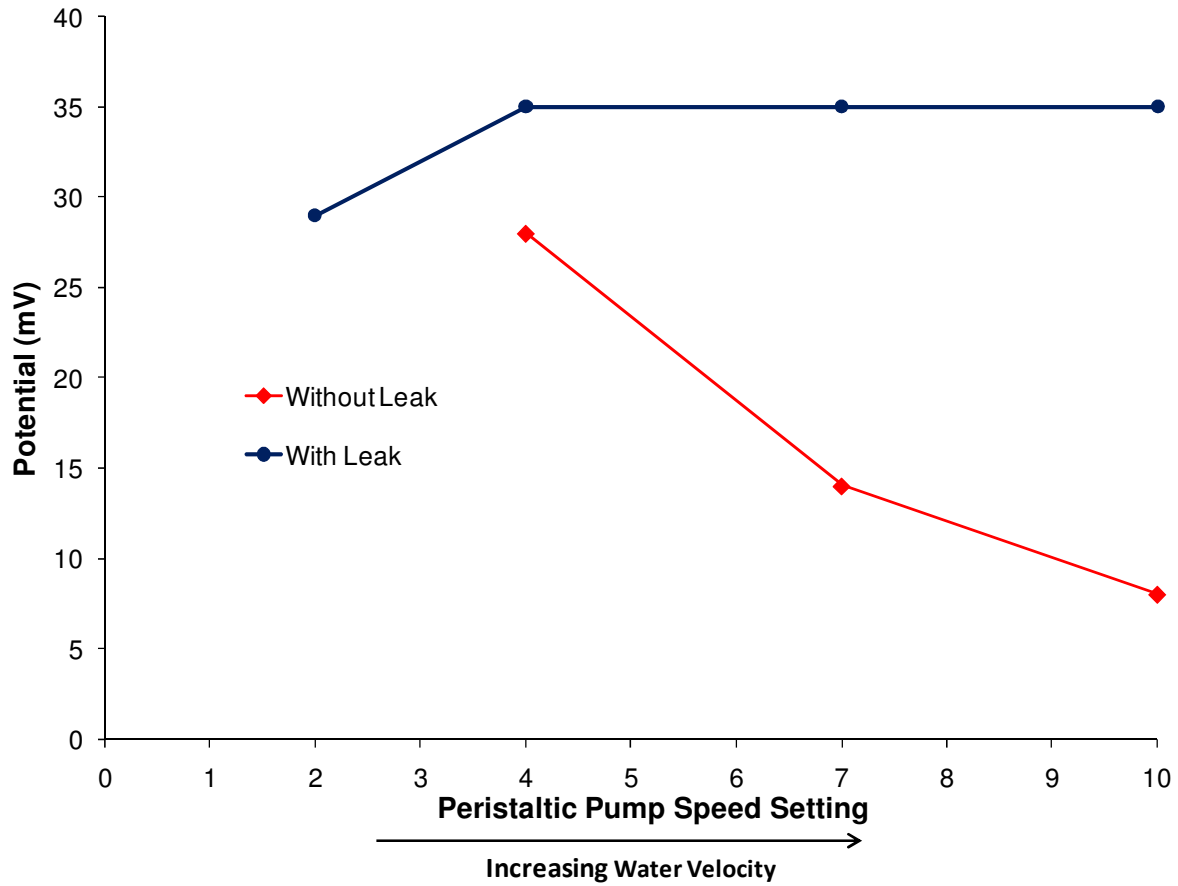


Figure A-4: Potential Measured between Insulated Copper Wire Recessed from Flow and Copper Plate Submersed in Stagnant Bulk Water in Short-term Test - Without Leak, Potential Varies with Water Velocity (Indicating Electrification) - With Leak Installed, Electrification is Eliminated to Extent Achievable

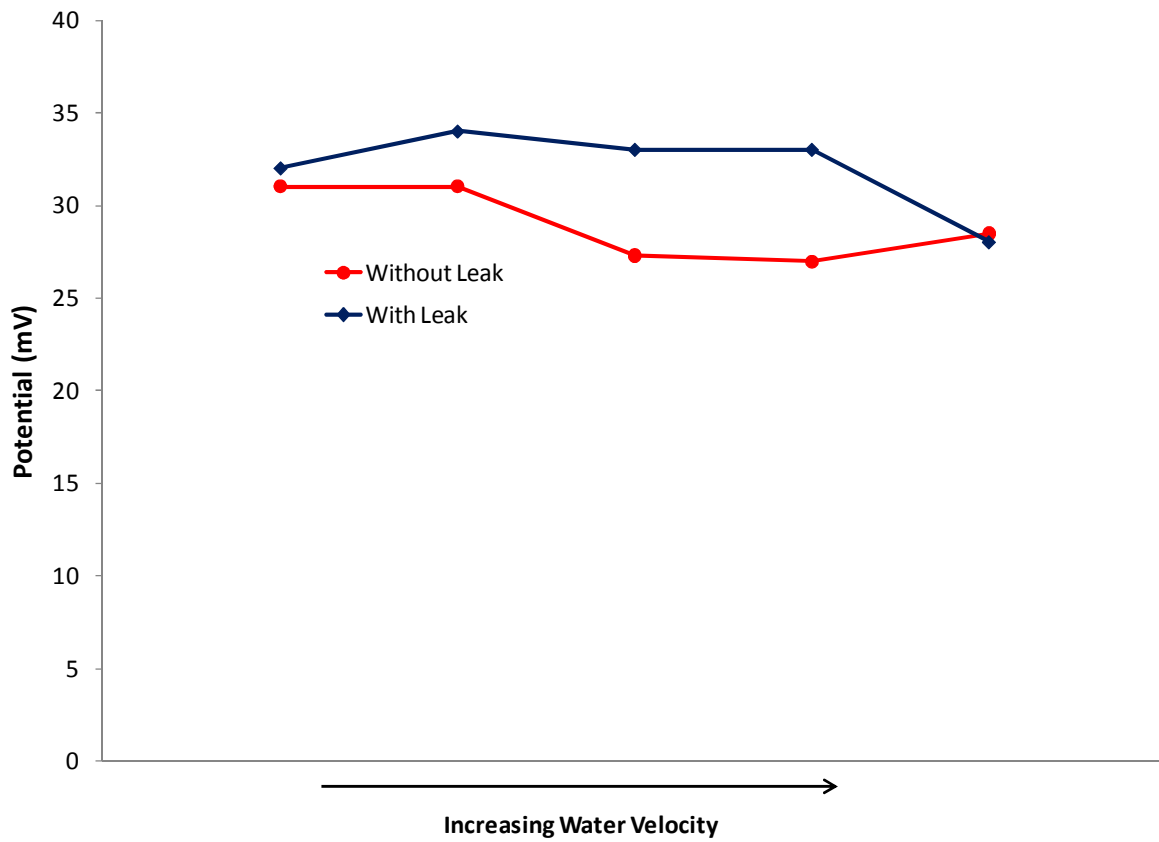


Figure A-5: Potential Measured between Insulated Copper Wire Recessed from Flow and Copper Plate Submersed in Stagnant Bulk Water in Long-term Test – Electrification Effect was Determined to be Insignificant

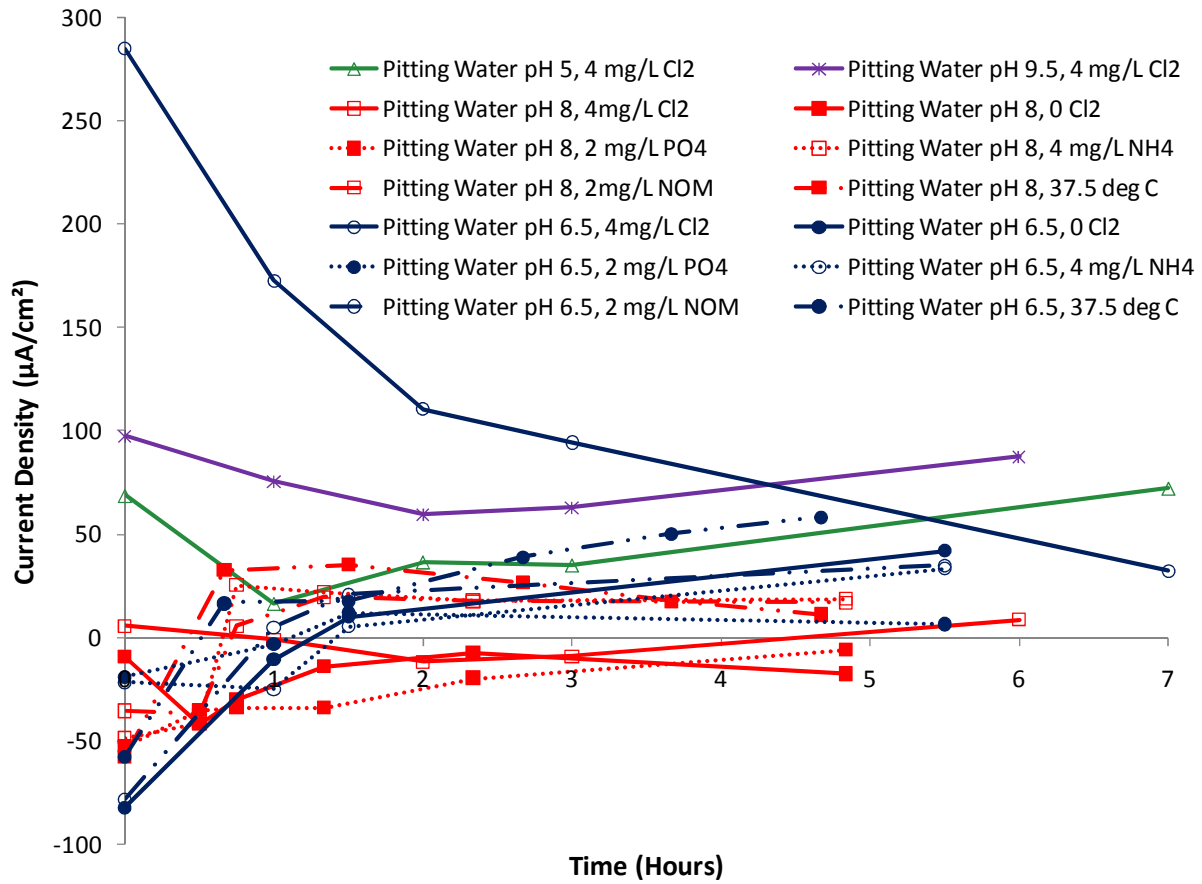


Figure A-6: Current Density between Insulated Copper Wire Subject to High Flow and Copper Plate in Stagnant Bulk Water. Note: All Tests were Performed at Room Temperature unless otherwise Stated)

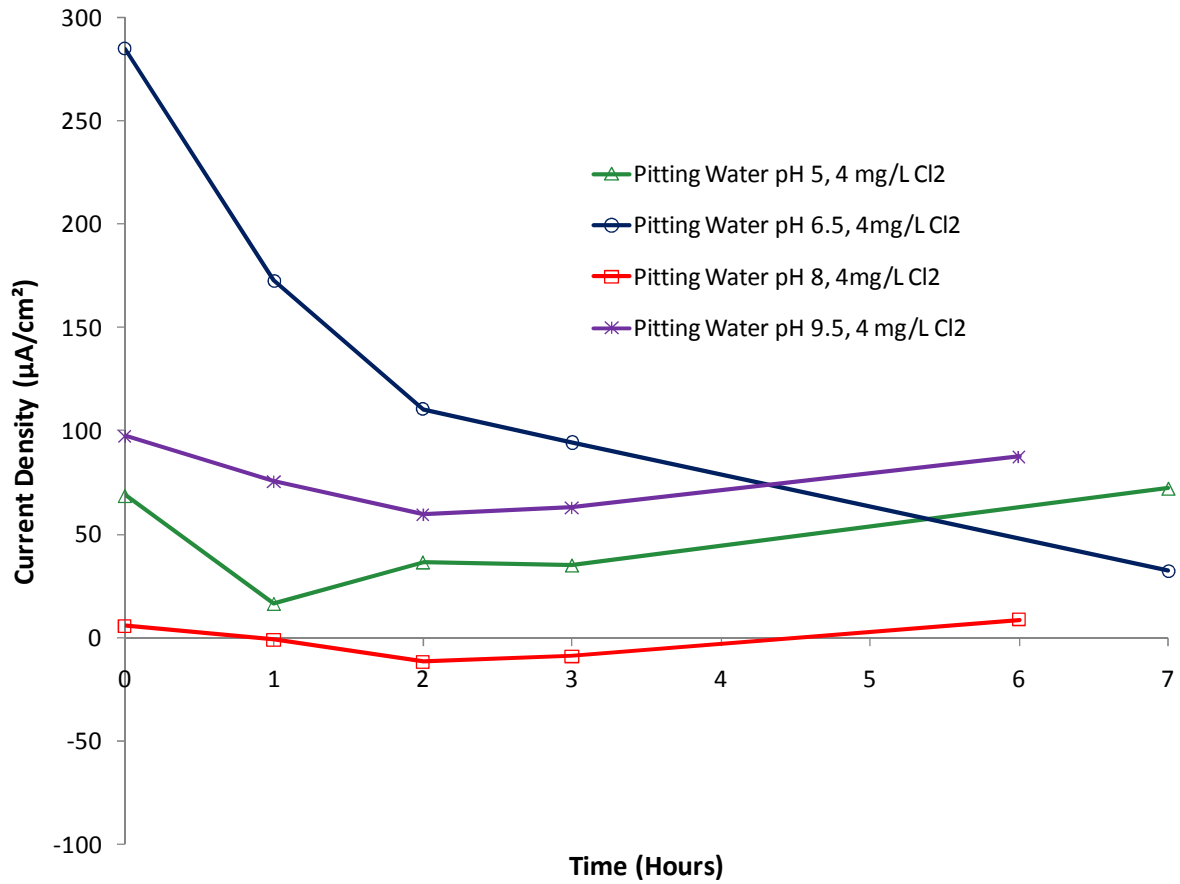


Figure A-7: Current Density between Insulated Copper Wire Subject to High Flow and Copper Plate in Stagnant Bulk Water. Note: All Tests were Performed at Room Temperature)

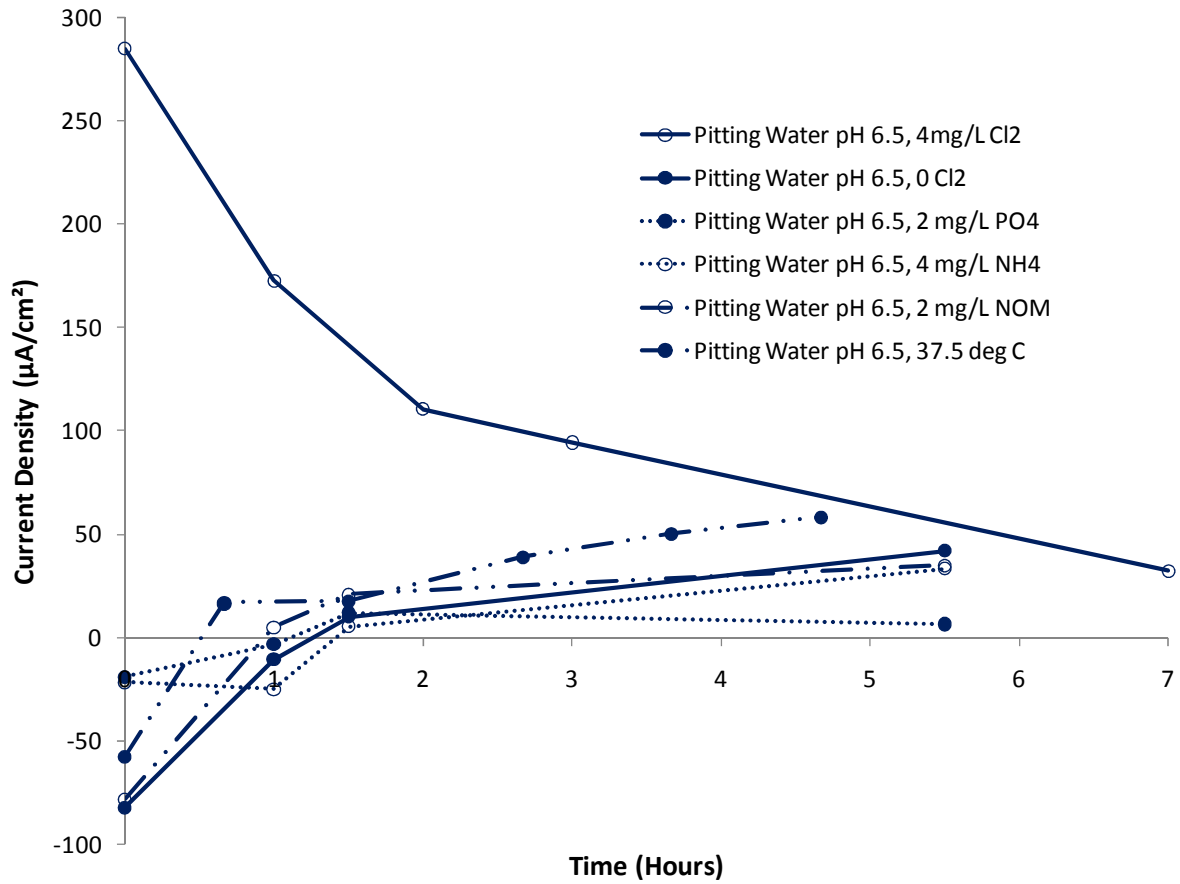


Figure A-8: Current Density between Insulated Copper Wire Subject to High Flow and Copper Plate in Stagnant Bulk Water. Note: All Tests were Performed at Room Temperature unless otherwise Stated)

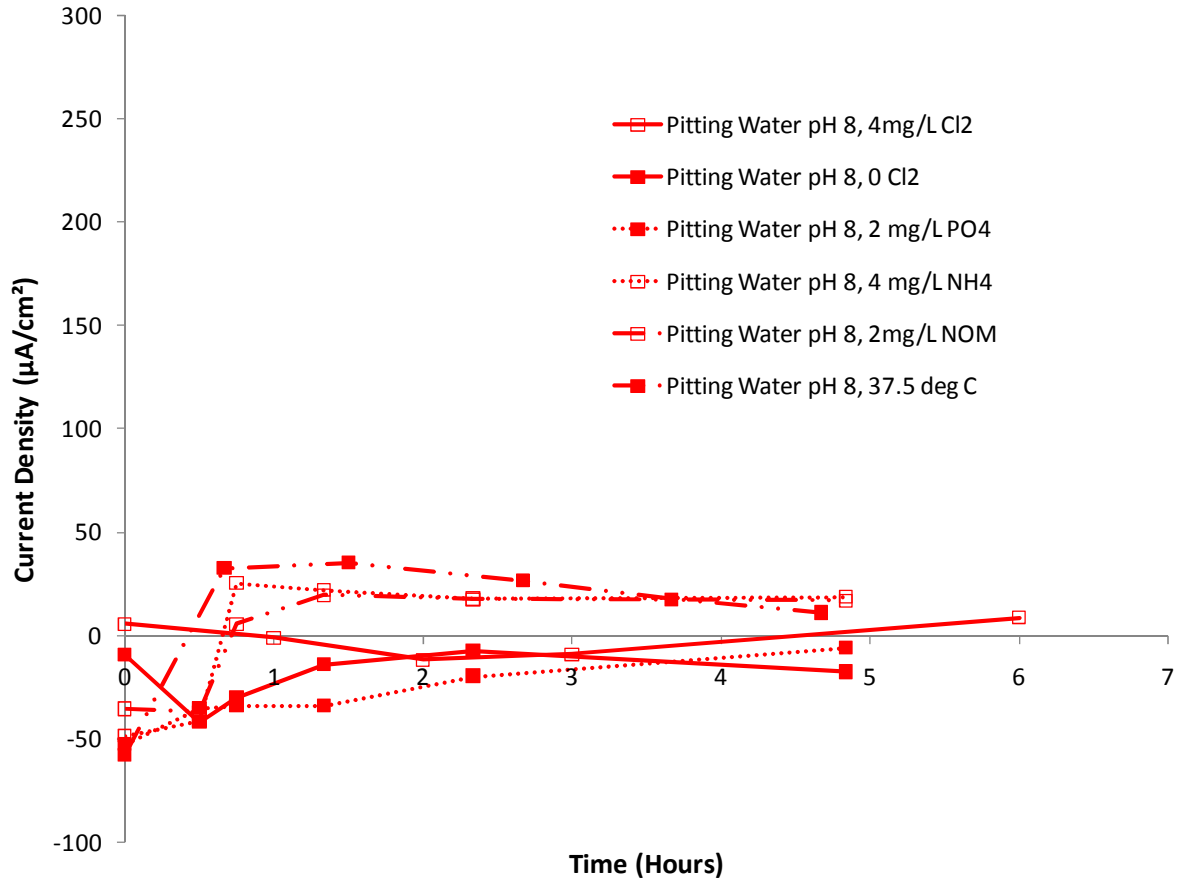


Figure A-9: Current Density between Insulated Copper Wire Subject to High Flow and Copper Plate in Stagnant Bulk Water. Note: All Tests were Performed at Room Temperature unless otherwise Stated)

APPENDIX B

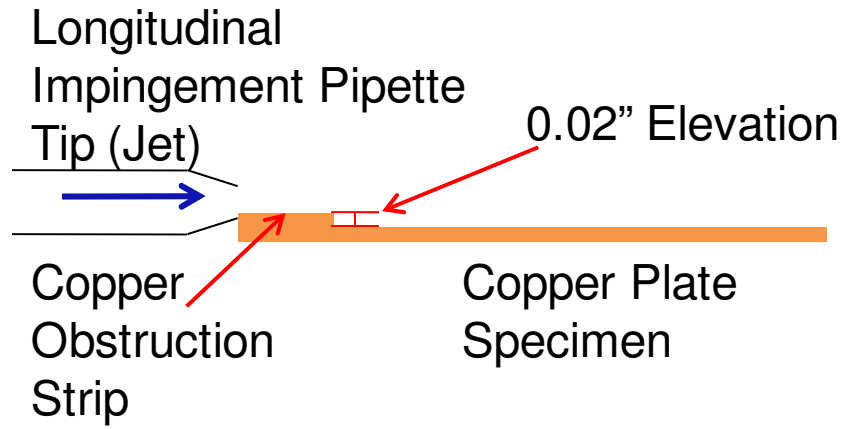


Figure B-1: Experimental Setup of Jet Copper Plate with Copper Joint Edge

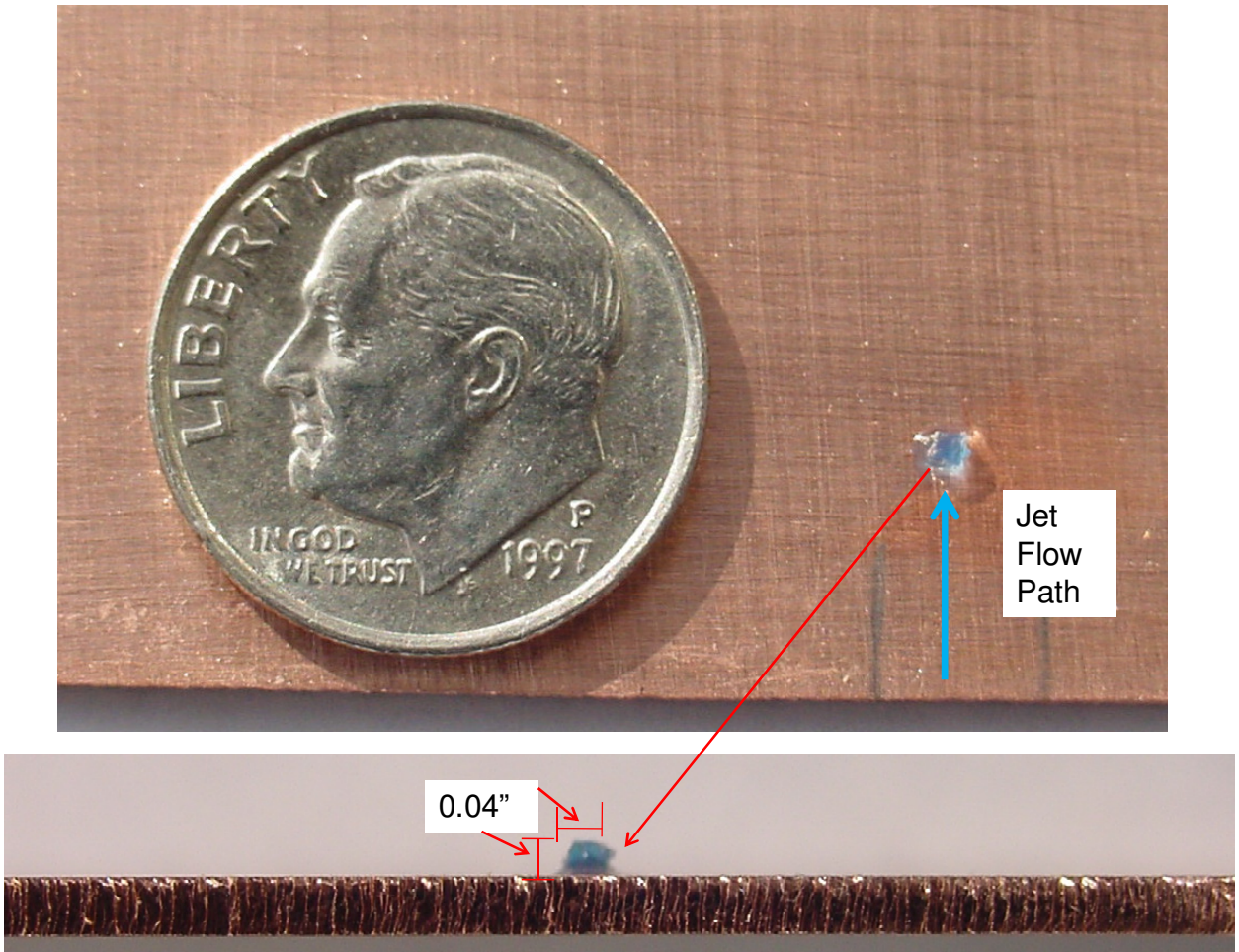
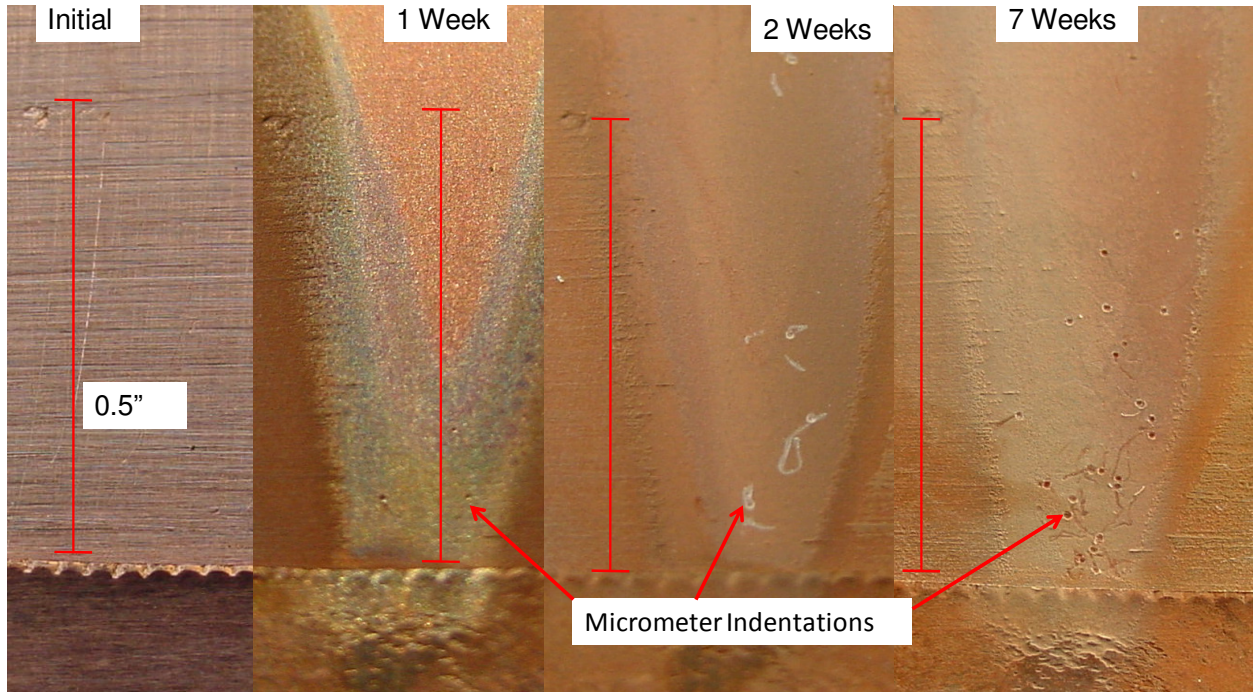


Figure B-2: Experimental Setup of Copper Plate with Plastic Surface Blockage



**Figure B-3: Damage due to Longitudinal Jet with Copper Joint Edge in Heated Salt Water
(Note: Small Divots in Undamaged Areas are Point Micrometer Indentations)**

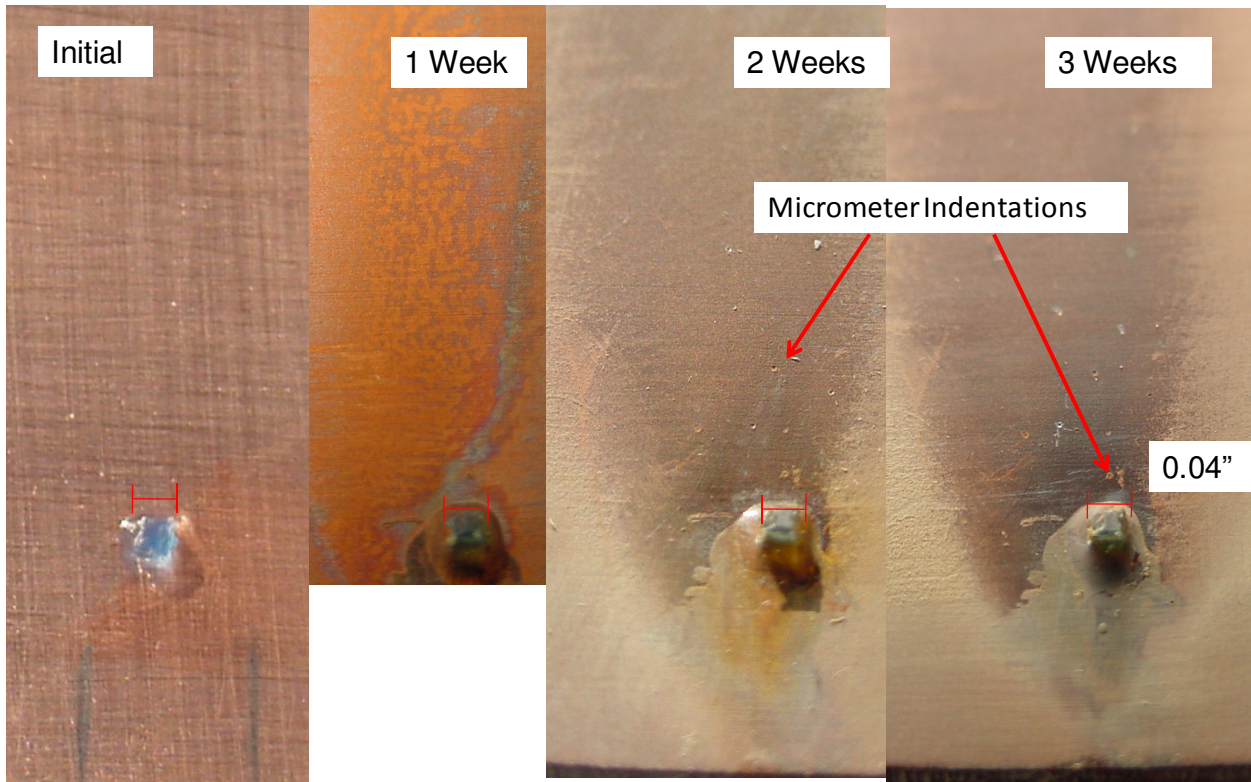


Figure B-4: Damage due to Longitudinal Jet with Plastic Surface Blockage in Heated Salt Water (Note: Small Divots in Undamaged Areas are Point Micrometer Indentations)

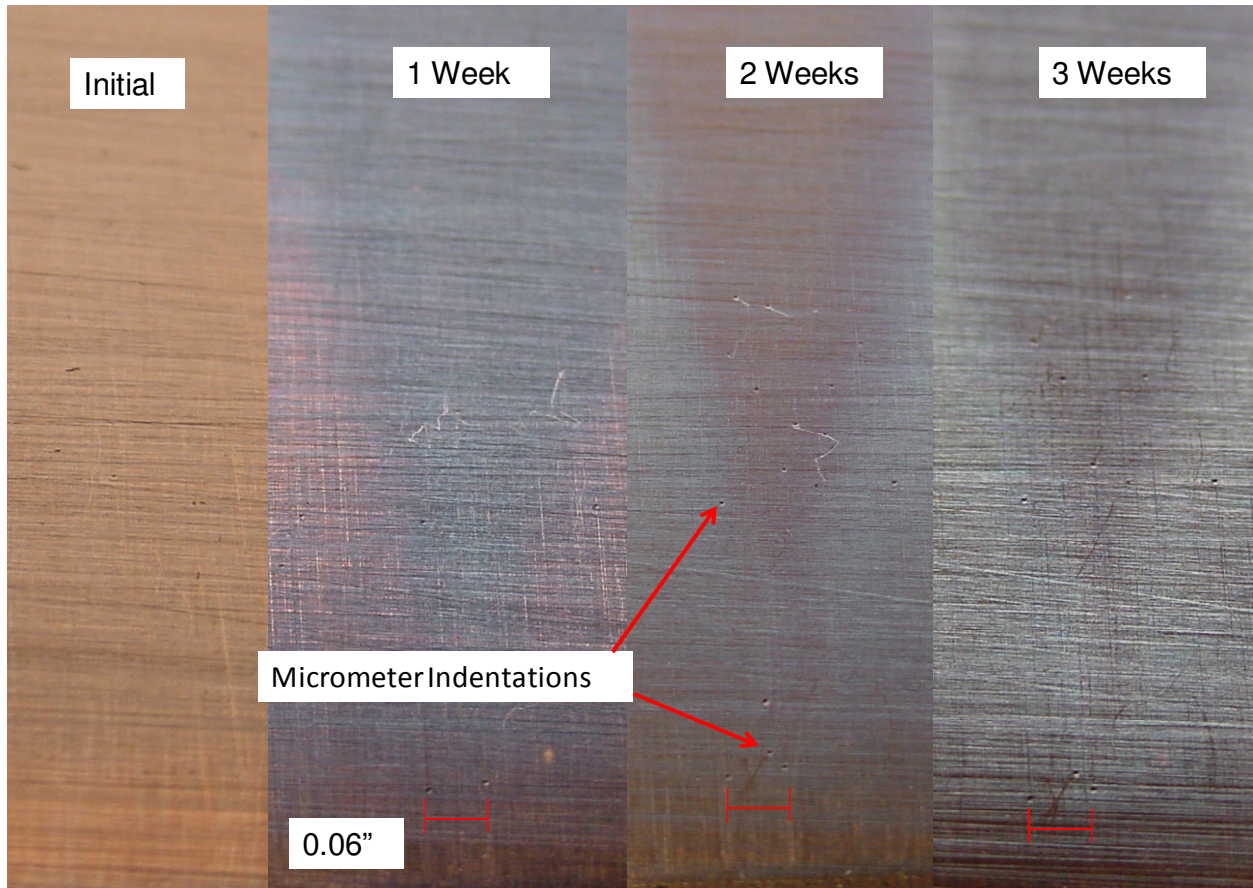


Figure B-5: Damage due to Longitudinal Jet in Heated, Water at pH 6 (Note: Small Divots in Undamaged Areas are Point Micrometer Indentations)

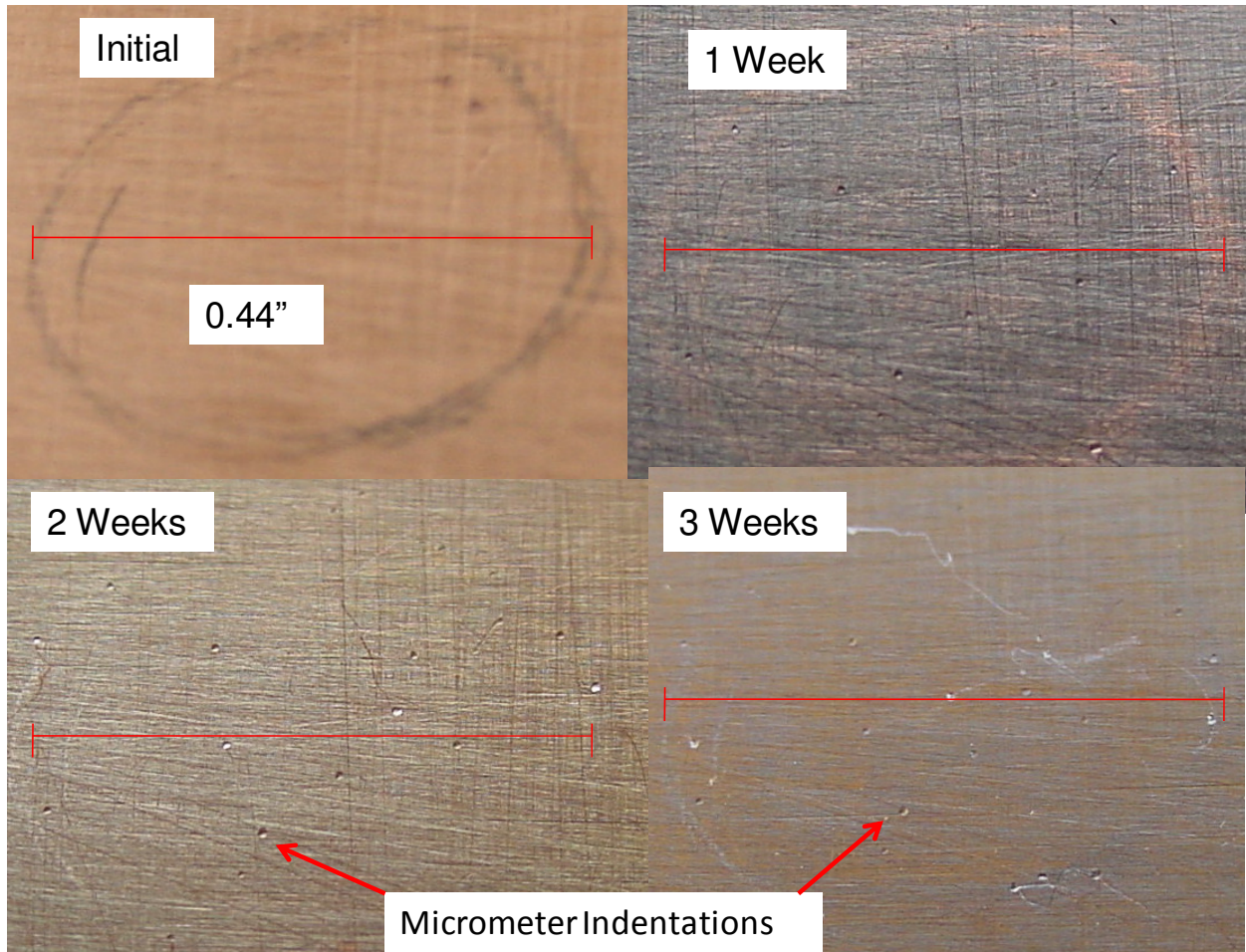


Figure B-6: Damage due to Perpendicular Jet in Heated Fresh Water at pH 6 (Note: Small Divots in Undamaged Areas are Point Micrometer Indentations)

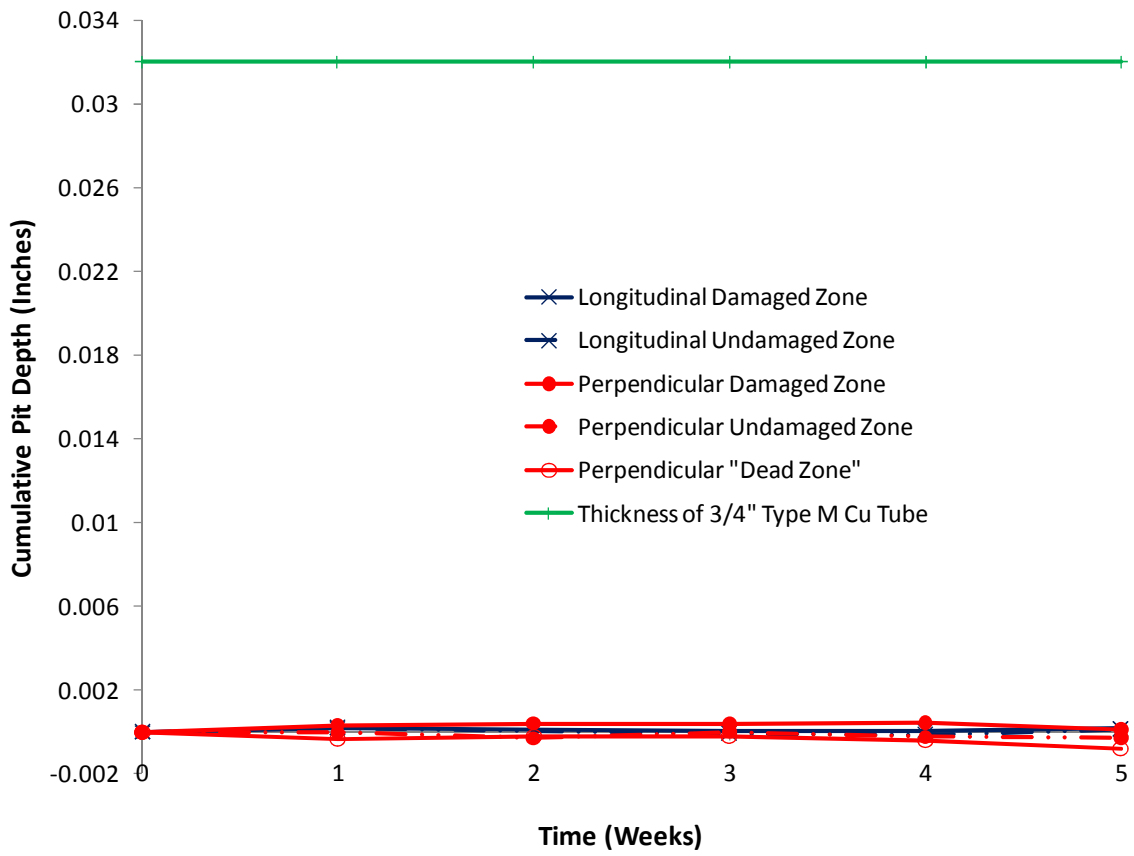


Figure B-7: Cumulative Penetration for Various Longitudinal and Perpendicular Jet Test Plates in Heated Fresh Water at pH 6

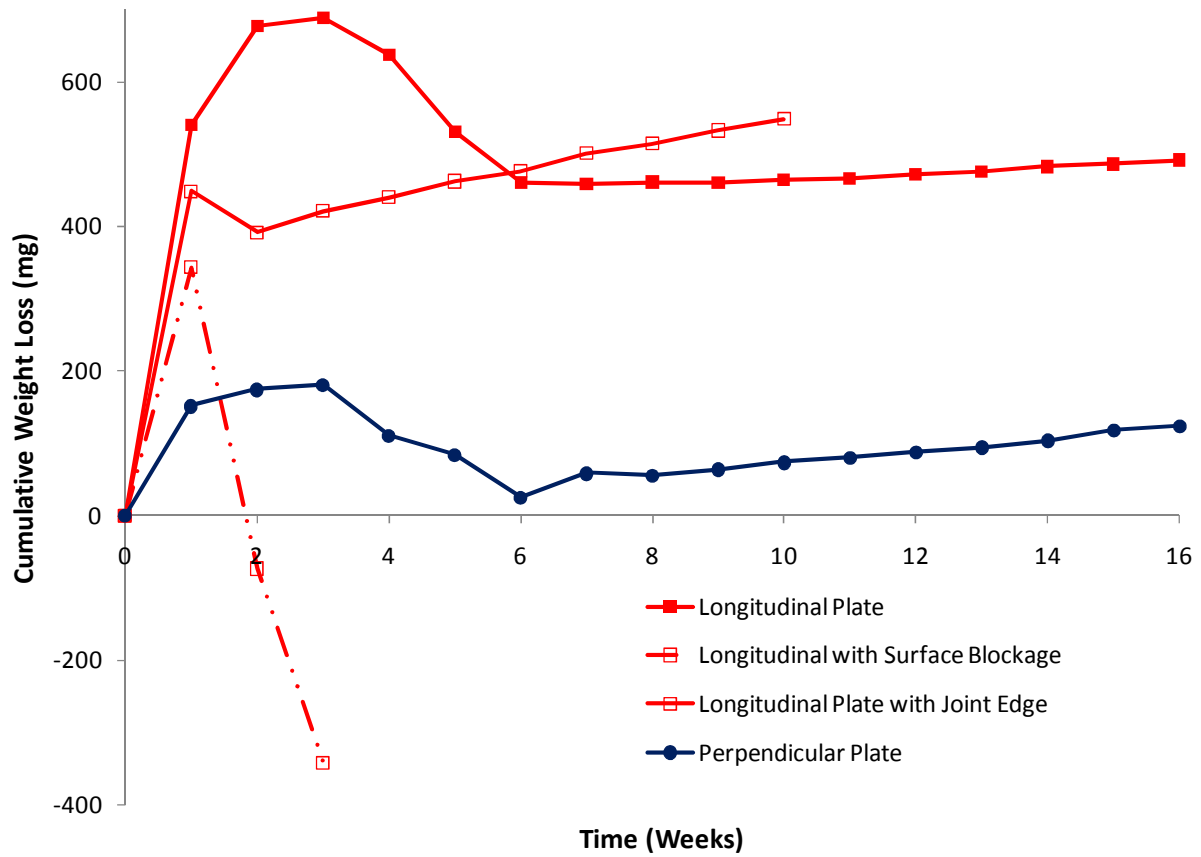


Figure B-8: Cumulative Weight Loss for Various Longitudinal and Perpendicular Jet Test Plates in Heated Salt Water

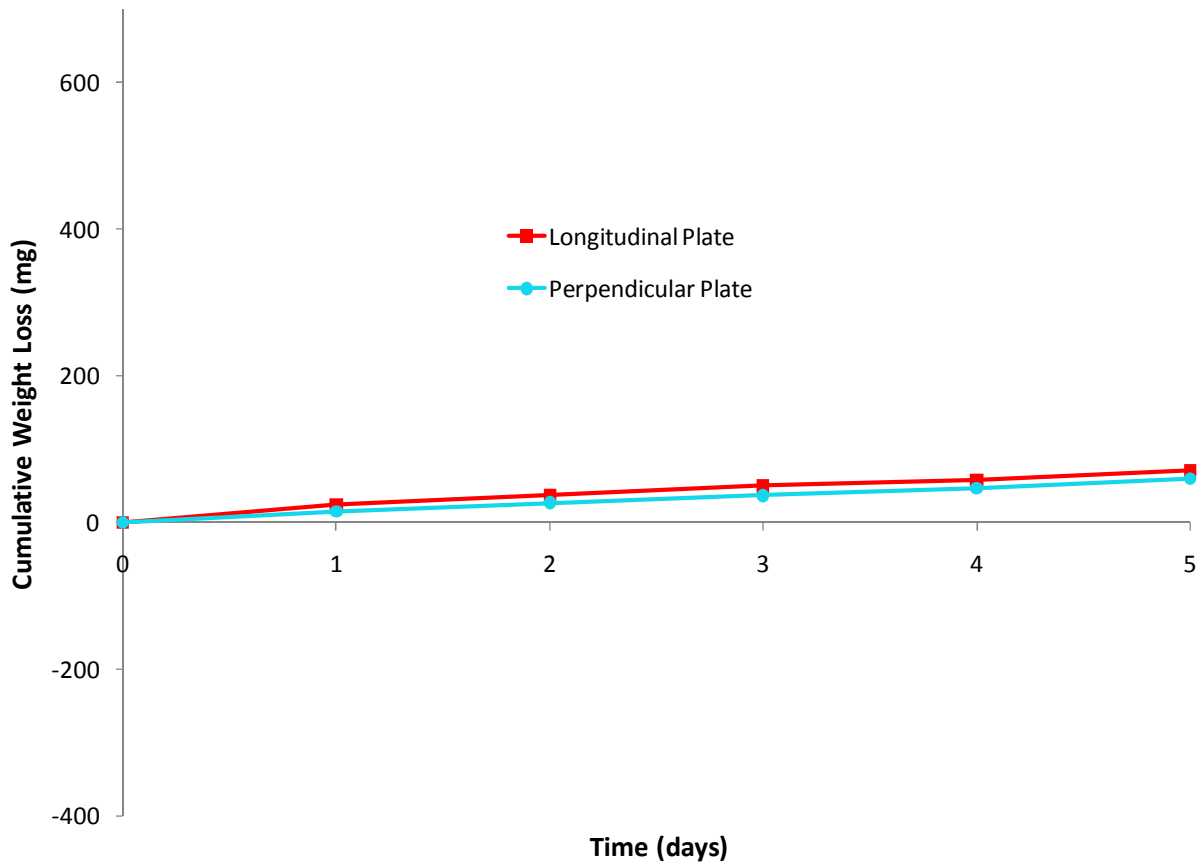


Figure B-9: Cumulative Weight Loss for Longitudinal and Perpendicular Jet Test Plates in Heated Fresh Water at pH 6

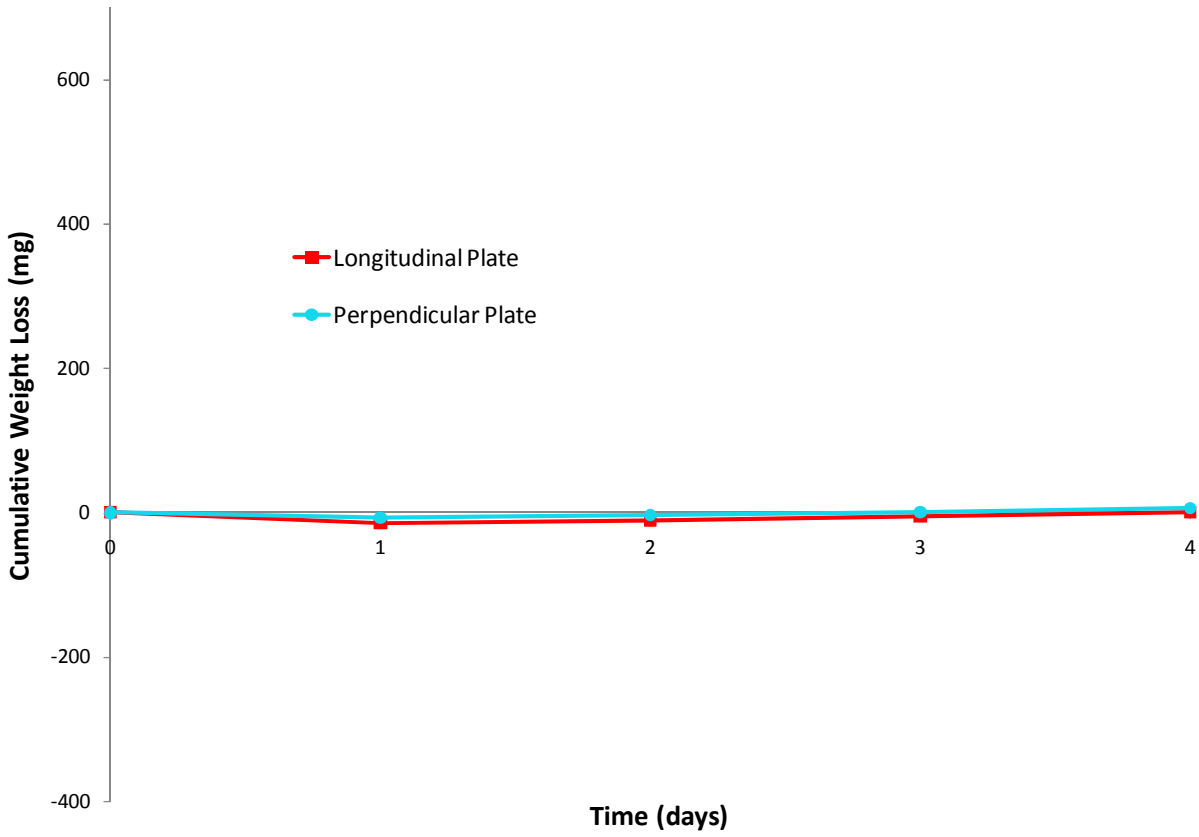


Figure B-10: Cumulative Weight Loss for Longitudinal and Perpendicular Jet Test Plates in Room Temperature Fresh Water at 4 mg/L Cl₂ at pH 8